EXCITATION-CONTRACTION COUPLING IN THE CAT MYOCARDIUM AND ITS RELATION TO ULTRASTRUCTURAL DEVELOPMENT

by

James G. Maylie

A THESIS

Presented to the Department of Physiology and the
Graduate Division of the University of Oregon Health Sciences Center
in partial fulfillment of
the requirements for the degree of

Doctor of Philosophy
February 1977

APPROVED:

[redacted]

(Professor in Charge of Thesis)

[redacted]

(Chairman, Graduate Council)

ACKNOWLEDGMENTS

I am grateful to the staff and faculty of the Department of Physiology for their help and encouragement. In particular I wish to thank Carla Baltrusch Dow for her expert technical assistance.

I am indebted to Dr. Kent Thornburg for his friendship during my thesis study. His training and advice were gratefully appreciated. This work could not have proceeded without his assistance throughout the training period.

No acknowledgment can do justice to the amount of time, guidance and assistance given to me by Dr. Job Faber. As a scientist he is not surpassed. His excellence in physics and mathematics as well as in physiology has continually inspired me. I am forever indebted to him for my beginning and hope our association will continue.

Most important I express my sincere appreciation to my wife, Judy, for withstanding the six long years of this program. Her help in the typing and the preparation of this thesis is gratefully acknowledged.

Support for my training came from a NIH training grant 5T01 GM 00538 and grants from the Oregon Heart Association.

TABLE OF CONTENTS

LIST OF ILLUSTRATIONS

LIST OF TABLES

I. INTRODUCTION

Background

Excitation-contraction (E-C) coupling was defined by Sandow (1952) as the process in muscle by which membrane depolarization (action potential) induces the contraction of intracellular myofibrils. The mechanism of E-C coupling in skeletal muscle is generally understood (Fuchs, 1974; Ebashi, 1976) in contrast to the situation in cardiac muscle.

Although there are major differences between skeletal muscle and frog and mammalian ventricular muscle (table I-1), the organization of contractile material in cardiac muscle such as in cat papillary muscle (figure I-1B) is similar to that found in skeletal muscle (figure I-1A) (Fawcett and McNutt, 1969). In both skeletal and cardiac muscle thin actin filaments extend from the Z-line in both directions and interdigitate with thick myosin filaments. The "I-band" (optically isotropic) (figure I-1) is composed of only actin filaments and the "A-band" (optically anisotropic) is the region of overlapping actin and myosin filaments. Figure I-2A shows a schematic representation of thin and thick filaments. The thick filament is an assembly of long myosin molecules with an orderly array of globular heads projecting from the myofilaments in groups of three. Actin, tropomyosin and troponin are the proteins forming the thin filament. Actin molecules are arranged in a double helix with thin continuous strands of tropomyosin attached to the actin molecules alongside each groove of the double helix (figure I-2B). Globular units of troponin are attached

TABLE I-1

Comparison of structural and functional characteristics of muscle

	Ventricular Muscle		Frog Skeletal
Structure	Frog	Mammalian	Muscle
Cellular structure	Functional syncitium	Functional syncitium	True syncitium
Cell size	2-8 μ	8-40 μ	60-120 μ
T-tubular system (diameter)	None	Located at Z-line (1000-3000 A)	Located at Z-line and A-I junction (100 A)
Basement membrane	Present on surface of fiber bundles; absent on cell surface within bundles	Present on sarcolemma and in T-tubles	Present on sarcolemma (not evident in T-tubules)
Sarcoplasmic reticulum	Little & disorganized	Moderate & well organized	Abundant & highly organized
Mitochondria	(+++)	(+++)	(++)
Function			
Action potential duration	600-1000 ms	200-600 ms	3-5 ms
Active state duration	500 ms at 25 °C	200 at 37 °C	40 ms at 0 °C
Sensitivity to extracellular calcium	(+++)	(+++)	(-)
Tetanus	(-)	(-)	(+)

Figure I-1. A. Drawing depicting the T-tubules and sarcoplasmic reticulum (SR) relation to several myofibrils of amphibian skeletal muscle. There are discrete myofibrils of uniform size, each ensheathed by SR with pairs of terminal cisternae associated at each Z-line with a slender T-tubule to form a "triad".

B. A drawing of the T-tubules and SR of mammalian cardiac muscle. Notice the large size of T-tubules, the simpler pattern of the SR, and the absence of terminal cisternae. Instead of terminal cisternae, small saccular expansions of the SR, called sarcolemmal cisternae, are in close contact with the T-tubules or with the sarcolemma at the periphery of the cell. Taken from Fawcett and McNutt, 1969.

A

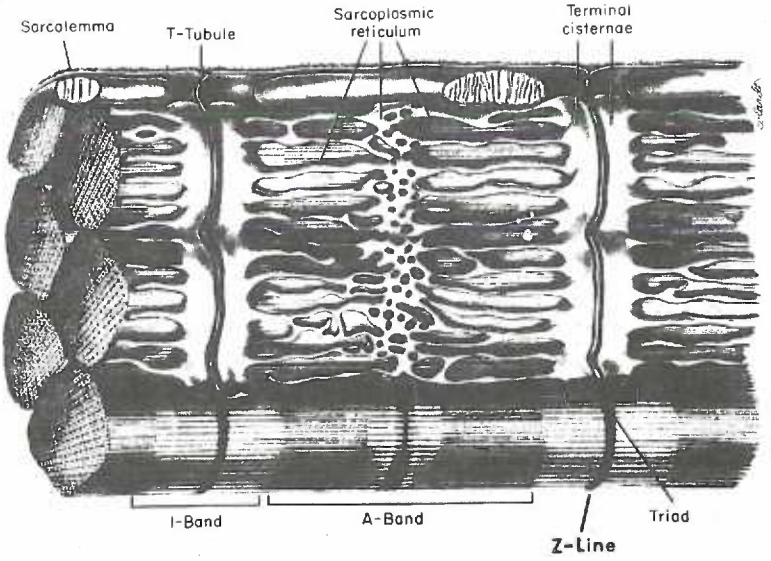
Sarcolemma
T-Tubule
Sarcoplasmic reticulum
Terminal cisternae
I-Band
A-Band
Triad
Z-Line

B

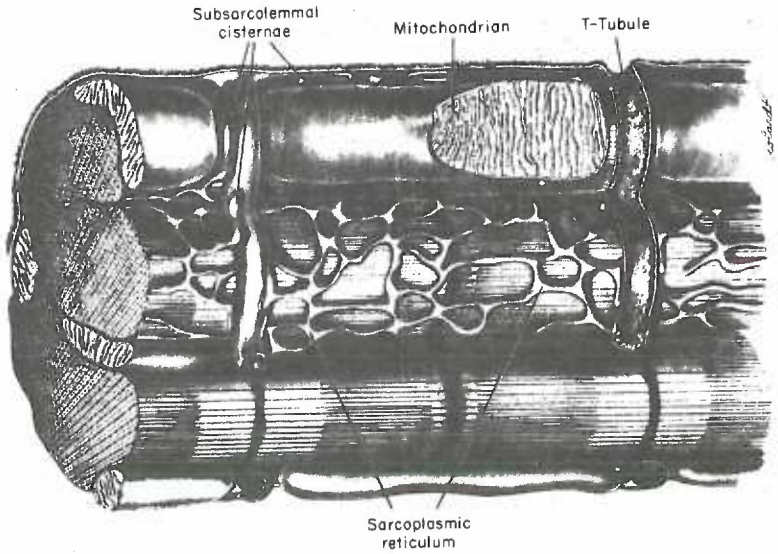
Subsarcolemmal cisternae
Mitochondrian
T-Tubule
Sarcoplasmic reticulum

Figure I-2. A. Thick and thin filaments interdigitate in an orderly array. Myosin heads of the thick filaments act as cross bridges between the thick and thin filaments.

B. Thin filaments are an assembly of actin, tropomyosin, and troponin molecules. From Murray and Weber, 1974.

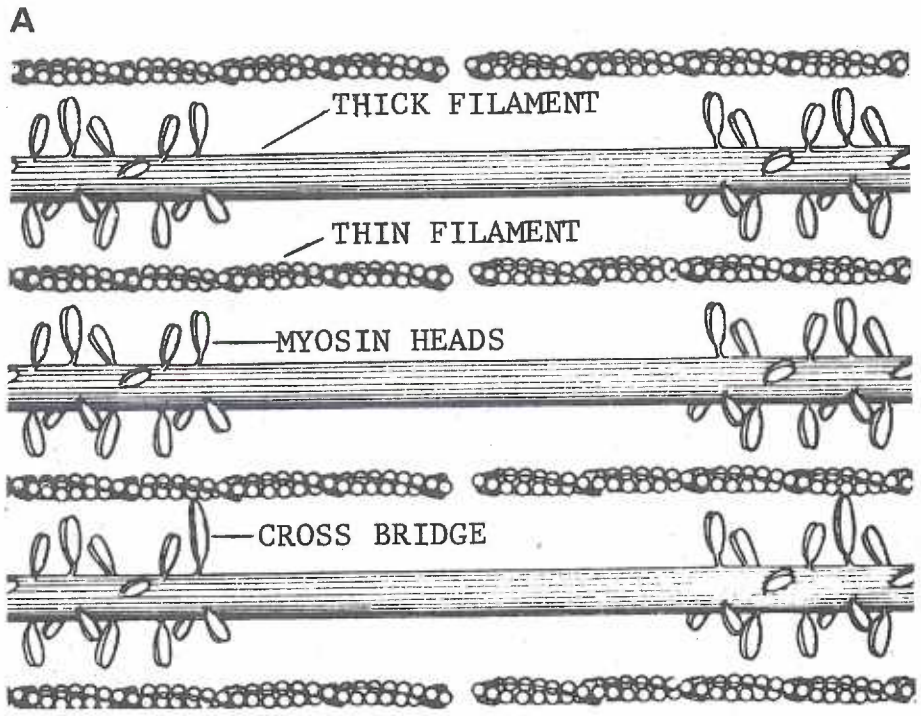
A
THICK FILAMENT
THIN FILAMENT
MYOSIN HEADS
CROSS BRIDGE

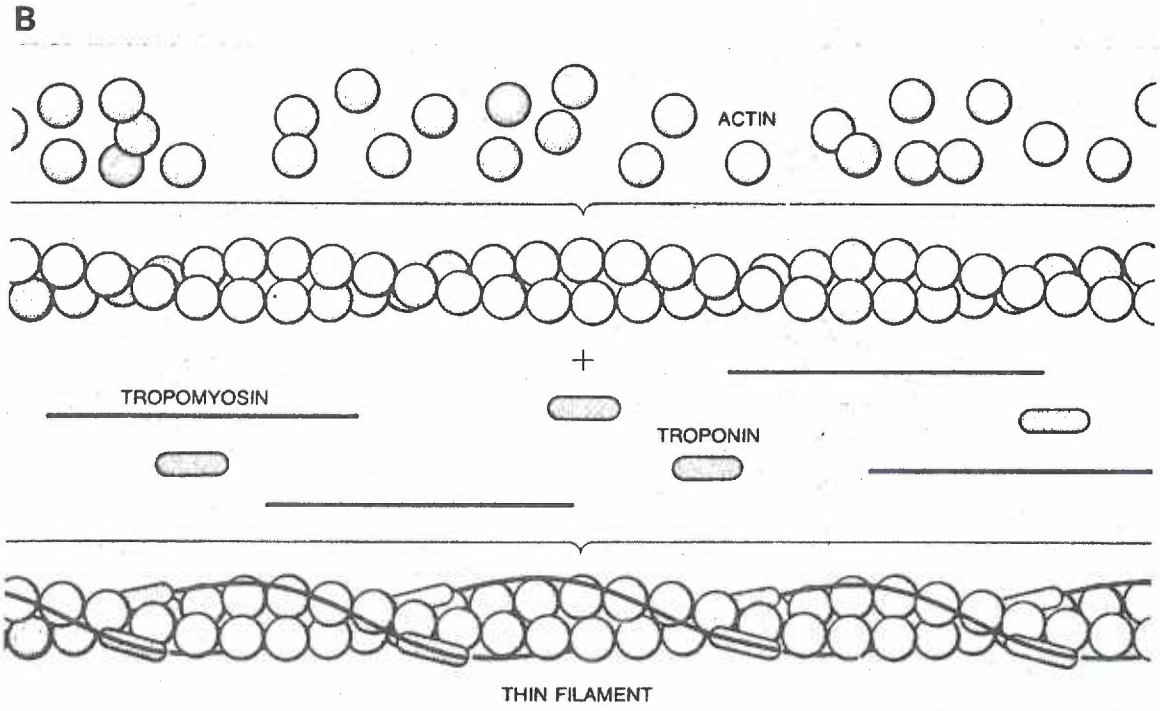
B
ACTIN
TROPOMYOSIN
TROPONIN
THIN FILAMENT

to tropomyosin every seventh actin molecule. In the presence of ATP the myosin head binds to "active sites" on the actin molecule; this is called cross-bridge formation. ATP undergoes hydrolysis to ADP, providing the energy for contraction, presumably by attracting the thin filament along the thick filaments. When a myosin head has moved as far as it can, the bridge breaks and another ATP molecule binds to the myosin head and the cycle is repeated (Murray and Weber, 1974).

Tropomyosin and troponin regulate the number of actin sites available for binding with myosin, a regulation that is modulated by the free myoplasmic calcium concentration. Calcium binds to troponin causing conformational change in the tropomyosin uncovering active sites which form cross bridges with myosin. Thus the number of available active sites and therefore the force of contraction are determined by the concentration of free calcium in the myoplasma (figure I-3).

A short description of the current concept of E-C coupling in skeletal muscle is given here by way of introduction. In the resting state myoplasmic calcium concentration is below 10^{-7}M and at that low concentration bridge formation is inhibited. Upon excitation an action potential is conducted along the sarcolemma and into the interior of the muscle fiber via transverse invaginations of the sarcolemma (T-tubules) (figure I-1). Depolarization of the T-tubular membrane causes a rapid release of calcium stored in the terminal cisternae of the sarcoplasmic reticulum (SR) (figure I-1). Consequently the myoplasmic calcium concentration rises from 10^{-7}M to about 10^{-5}M which results in bridge formation and contraction. The longitudinal SR

Figure I-3. Relative tension produced by chemically skinned frog ventricular strips as a function of the pCa. Each point is an average of 7 muscles. The normal twitch is shown as 20% of maximal tension. The experiment was carried out at room temperature; pH of the solution was 6.4. From Winegrad, 1971.

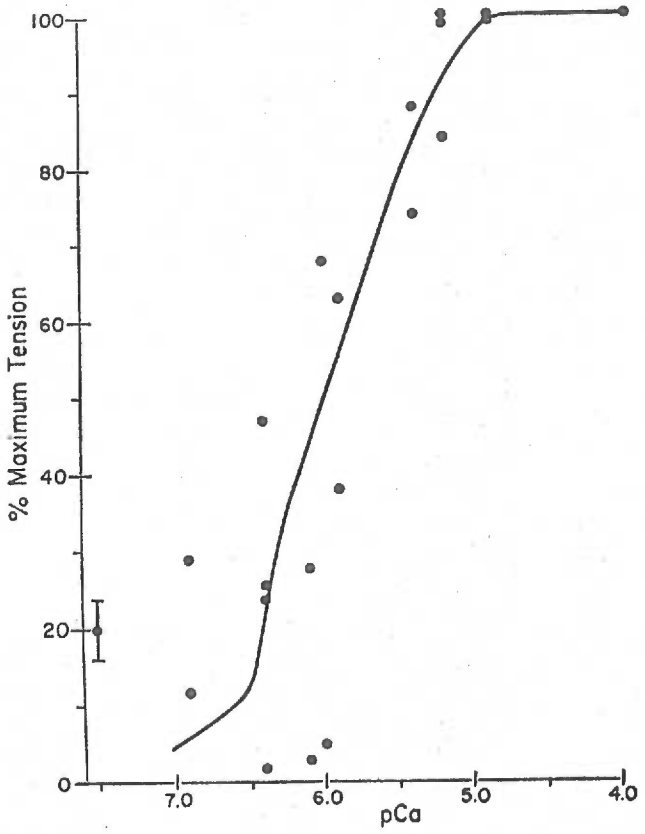
100
80
60
40
20
0
% Maximum Tension
7.0
6.0
5.0
4.0
pCa

(figure I-1) actively accumulates calcium and reduces the myoplasmic calcium concentration to 10^{-7}M. The cross-bridges then detach and muscular relaxation ensues. The sequestered calcium then travels along the longitudinal SR and is stored in the terminal cisternae where it is available for the next cycle.

Until recently, the conclusions derived from E-C coupling experiments on skeletal muscle were thought to hold also for cardiac muscle. But major ultrastructural and functional differences exist between skeletal and cardiac muscle (table I-1) suggesting that the E-C coupling theory for skeletal muscle may have to be modified before it can be applied to cardiac muscle.

Page, McCallister and Power (1971), in a quantitative ultrastructural study, measured the fractional volume of T-tubules in cardiac muscle and found it to be four times that of skeletal muscle. By contrast, they calculated the SR fractional volume in skeletal muscle to be four times that of cardiac muscle. Fawcett and McNutt (1969) observed that the number of terminal cisternae of the SR system in cardiac muscle is less than in skeletal muscle and in cardiac muscle the SR frequently makes contact with the sarcolemma, forming subsarcolemmal cisternae.

Peak twitch tension induced by electrical stimulation in skeletal muscle declines with a half-time of between one and two hours after calcium is removed from the perfusion solution. This implies that most of the calcium required for activation in skeletal muscle cycles intracellularly. However, in mammalian cardiac muscle, peak twitch tension declines with a half-time of about one minute when perfused

with Ca^{++}-free Ringer's (Langer, 1973). Thus, activation of contraction in mammalian cardiac muscle appears to be dependent on a calcium source which is in rapid equilibrium with the extracellular space. Lanthanum added to the perfusion fluid of cardiac muscle abolishes tension rapidly, without affecting the action potential (Sanborn and Langer, 1970). Using electron microscopy Langer and Frank (1972) found lanthanum localized on the superficial surface of cardiac cells and observed no lanthanum intracellularly. In skeletal muscle addition of lanthanum has very little effect upon twitch tension (Weiss, 1970). The data emphasize a major functional difference between skeletal and cardiac muscle; cardiac muscle is much more dependent upon an extracellular source of calcium than skeletal muscle.

The function of the SR and T-tubular system in E-C coupling in cardiac muscle is not well established, but much insight into this problem has been gained by comparing frog and mammalian hearts. The SR in frog ventricle was carefully examined by Page and Niedergerke (1972). They found the SR to be a loose network of fine longitudinal tubules that extend between myofibrils and surround the myofibrils at the Z-line. The SR terminated on the sarcolemma forming subsarcolemmal cisternae, connections similar to those found in mammalian heart. However, in the frog heart the fractional volume of SR was some 15 times less than in the mammalian heart. No transverse invaginations of the sarcolemma (T-tubules) were observed in the frog heart although wide T-tubules are found in the mammalian heart (table 1-1).

Radio Isotope Flux Studies in Cardiac Muscle

Reuter's group (1974), using guinea-pig hearts "loaded" with Calcium-45, found that more than 80% of calcium efflux depends on external sodium and calcium. Their data supported an exchange system where sodium influx is coupled with calcium efflux as described by the model of Bassingthwaighte et al. (1973), (figure I-4). If the permeabilities of the carrier-calcium complex (P_{Ca}) and carrier-two sodium complex (P_{Na_2}) of Bassingthwaighte's model are large compared to those of the carrier-one sodium complex (P_{Na}) and carrier only (P), the system behaves as an obligatory carrier extruding one calcium in exchange for two sodium ions, as supported by the data of Reuter and Seitz (1968) and Glitsch, Reuter and Scholz (1970). The carrier (C) is not necessarily specific for one calcium ion or two sodium ions but may shuttle with one sodium ion, NaC^{-}, or in the free state, C^{-2} (Bassingthwaighte et al., 1973; Watson and Winegrad, 1973). This sodium-calcium exchange carrier has a low affinity for lithium, potassium, magnesium or lanthanum and has a temperature coefficient (Q_{10}) between 3°C and 35°C of 1.35 (Reuter, 1974). The metabolic inhibitors cyanide and 2,4-dinitropenol do not immediately affect the calcium efflux.

Using Calcium-45 to study calcium kinetics in heart muscle, Langer (1973) defined a calcium washout curve in terms of four exponential phases. Table I-2 lists the rate constants for both dog papillary muscle and frog ventricle for which the rate constants are very similar. Phase 1 is believed to reflect washout of calcium from the extracellular space since the rate constant for the washout of sucrose ^{14}C

Figure I-4. Model of coupled sodium-calcium exchange. A negatively charged carrier, C, transports 1 Ca^{2+} ion, or 1 or 2 Na^{+} ions. P_{Ca} and P_{Na_2} are permeabilities of uncharged complexes CaC and Na_2C. P and P_{Na} are permeabilities of charged complexes C^{2-} (free carrier) and NaC^{-}. The subscripted K's are steady state binding constants. From Bassingthwaighte et al., 1973.

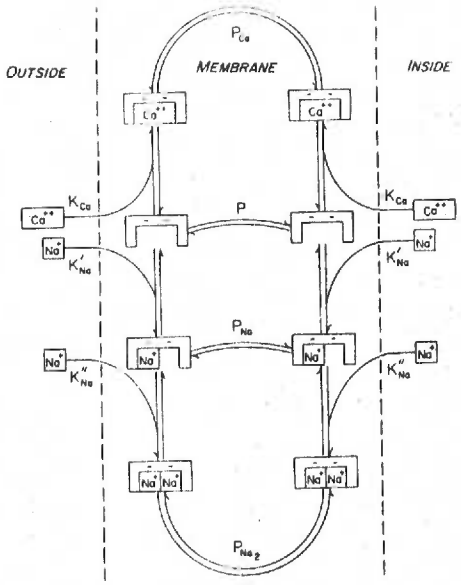
OUTSIDE
MEMBRANE
INSIDE
P_{Ca}
Ca^{++}
K_{Ca}
P
K'_{Na}
P_{Na}
K''_{Na}
P_{Na_2}
Na^+

TABLE I-2

Rate constants of calcium washout determined by curve peeling.

From Sopis and Langer, 1970.

Dog Papillary Muscle		Frog Ventricle	
Phase	λ (min^{-1})	Phase	λ (min^{-1})
0	3.5 ± 0.4	0	2.34 ± 0.06
1	0.59 ± 0.14	1	0.687 ± 0.038
2	0.116 ± 0.012	2	0.176 ± 0.008
3	0.021 ± 0.001	3	0.037 ± 0.002

is similar to that of calcium (.58 min^{-1}).

Perfusions with solutions of low sodium did not affect the rate constants. However the calcium content in phase 2 with low sodium perfusion was seven times greater in dog papillary muscle than in the frog ventricle. Langer (1968) proposed that phase 2 reflects washout from a compartment that is at least partly SR. This interpretation reconciles the larger concentration of calcium calculated from the mammalian washout curves with the ultrastructural difference between mammalian and frog heart.

Reperfusion with normal sodium concentrations required 15-20 minutes to eliminate the accumulated calcium in phase 2, but active tension declined more rapidly to control values. An earlier study by Langer (1968) showed that in an arterially perfused dog papillary muscle tension declines proportionally to the decline in calcium content in the compartment kinetically-defined as phase 2 (compartment 2). However, in arterially perfused rabbit intraventricular septum, Langer (1973) found tension to decline ($T_{\frac{1}{2}}$ = 72 ms) in proportion to the decline in calcium content of the compartment kinetically-defined as phase 1 ($T_{\frac{1}{2}}$ = 83 ms) which may represent an extracellular compartment. Langer (1973) suggested that the major source of contractile-dependent calcium during a single beat is derived from the extracellular space (compartment 1) or from sites in rapid equilibrium with it and that a second pool of cellular calcium (compartment 2) contributes very little to force development and is not in rapid equilibrium with the extracellular space. Langer's theory predicts that compartment 2 is the region of calcium sequestration upon which relaxation is

dependent. Further support for Langer's theory came from his study (Sanborn and Langer, 1970) which showed that a concentration of lanthanum in the perfusion solution as low as 40 μM can abolish force development with little effect on the action potential. As mentioned earlier lanthanum does not penetrate the cell but binds to the cell surface. Langer's main conclusion is that the calcium necessary for contraction (activator calcium) is derived from the extracellular space. He postulates a sodium-calcium exchange as the mechanism by which calcium enters cardiac cells. Consequently the internal sodium concentration must regulate the amount of calcium entering the cell. Langer suggests that an increase in rate of stimulation (heart rate) increases internal sodium which is followed by an increase in tension. The Na-K pump accommodates the buildup of sodium by an increase in NaK ATPase activity but with a time delay (sodium-pump lag hypothesis). Langer's theory does not predict how the calcium flux into the cell during an action potential is regulated nor does it deal with a calcium efflux mechanism.

In summary, Langer finds a "compartment 1" where the calcium content is linearly proportional to the calcium concentrations in the perfusion medium between 0.5 and 12 mM. This compartment exchanges with a half time of 83 ms and appears to be located in the interstitial space or at sites in rapid equilibrium with this space or both. During the washout of calcium in calcium-free solution, the efflux of calcium from "compartment 1" has a half time which is similar to the decline in the active tension of the muscle which suggested to Langer that most of the activator calcium is derived from "compartment 1". Reuter

has found that more than 80% of the calcium efflux is dependent upon extracellular sodium and appears to be passive. A proposed hypothetical carrier shuttles two sodium ions into the cell in exchange for the extrusion of one calcium ion.

Membrane Control of Development of Tension

Another method for studying the E-C coupling process in heart muscle has made extensive use of a recently developed technique allowing the membrane potential, in the working myocardium, to be maintained (clamped) at any desired value. Thus the membrane potential becomes an independent variable subject to experimental control. Two methods have been employed to make electrical contact within the myoplasma of heart cells: 1) the intracellular electrode and 2) an artificial "node" formed by insulating a segment of tissue with a sucrose gap. Either of these methods can be used to pass current into the cell or to measure the transmembrane potential. The technique used for voltage clamping depends upon the type of tissue used. Since I will be primarily presenting studies on working myocardium, I will review first the technique most commonly used for studying membrane control of tension in ventricular preparations, the "single sucrose gap".

The single sucrose gap electrically isolates a small active segment of tissue from a larger segment by a gap filled with isosmotic sucrose (figure I-5). A tissue chamber is divided into three compartments by two thin rubber membranes, each containing a small central hole through which a strand of muscle, such as a papillary muscle, is

Figure I-5. Single sucrose gap chamber. A high input impedance (10^{14} ohms) amplifier (V_m amplifier) is used to measure the membrane potential (V_m) recorded by an intracellular microelectrode in the active end of the muscle. The output of the electrode amplifier is connected to the feedback amplifier. The amplified difference between V_m and the control pulse is applied at the current injection end. Current flows intracellularly through the muscle (I_m) and crosses the membrane in the active end of the muscle until V_m equals the control pulse in the active end of the muscle.

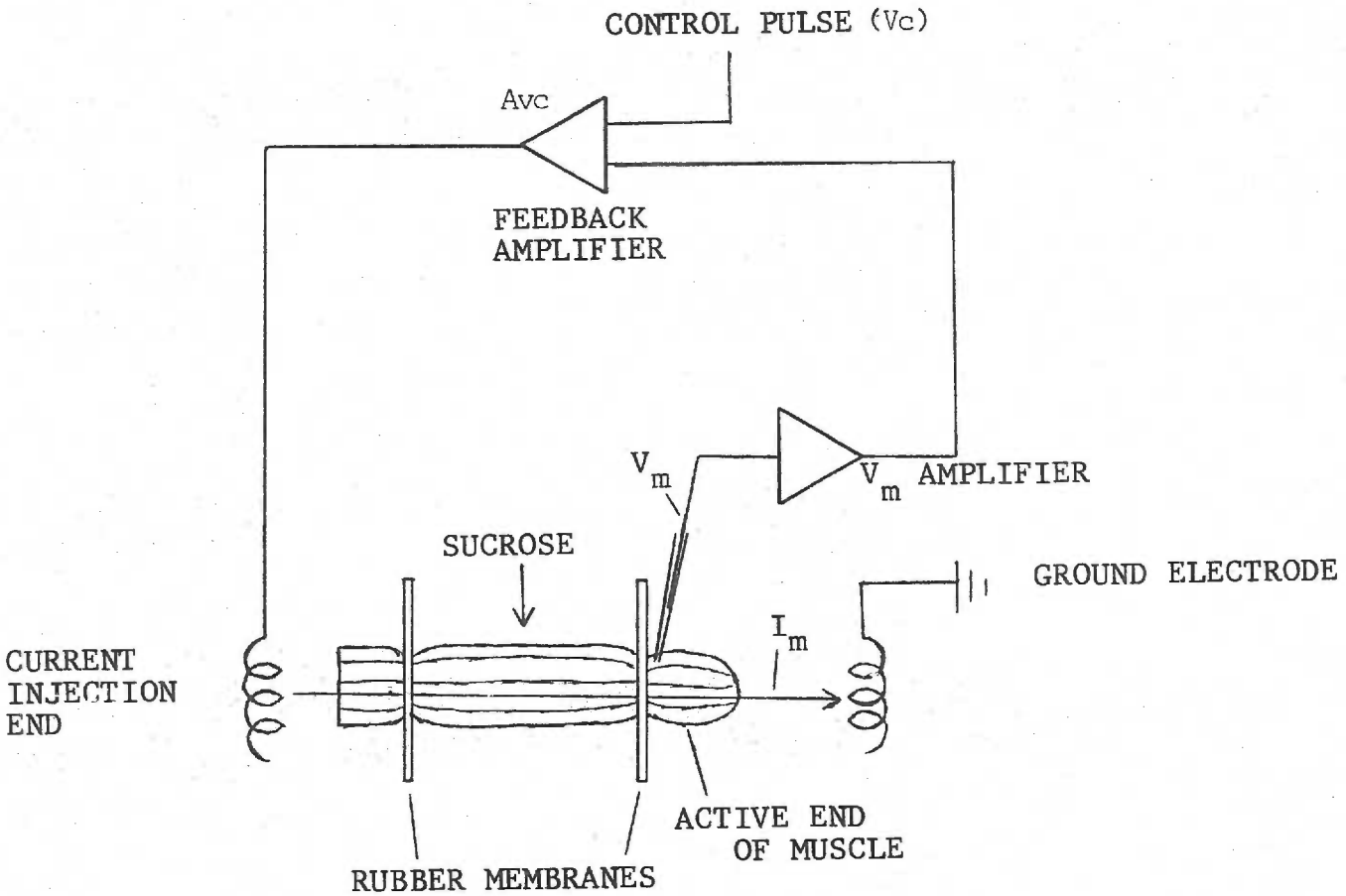
CONTROL PULSE (Vc)
Avc
FEEDBACK
AMPLIFIER
V_m
V_m AMPLIFIER
SUCROSE
GROUND ELECTRODE
I_m
CURRENT
INJECTION
END
ACTIVE END
OF MUSCLE
RUBBER MEMBRANES

pulled leaving a small segment of tissue protruding out through each rubber membrane. Tension is easily measured by attaching a tension transducer to the active segment (figure I-5). The membranes fit snuggly around the tissue so that current flow between compartments is through the small interstitial spaces within the muscle interior. The middle compartment (gap) can be perfused with isosmotic sucrose with little leakage into the adjacent compartments. The sucrose in the gap diffuses into the interstitial spaces of the muscle in the gap so that the interstitial fluid of the cells in the gap is replaced with isosmotic sucrose. When a voltage is applied "across" the gap current will flow through the gap but because of the high resistance of the sucrose solution compared to the intracellular resistance in the gap most of the current will flow intracellularly. In the active end of the preparation (right compartment, figure I-5) the current must flow across the cell membranes to the ground electrode and depolarize or hyperpolarize the membrane depending on direction of current flow. The same occurs at the other end of the muscle, but here it is of no interest. With this technique, the membrane potential (Vm) in the active end can be maintained at the desired control voltage (Vc) (figure I-5). The difference between Vm and Vc is used to drive a clamping amplifier (Avc) which will "inject" current into the left-hand side. The current will flow intracellularly through the gap and across the membrane in the active side and thus forces Vm to equal Vc. In this way the action potential can be interrupted and the membrane of muscle can be subjected to polarizations of any desired voltage and duration. Ideally the total current injected represents

only the current passing intracellularly through the gap and is thus equal to the membrane current necessary to control the membrane potential in the active segment. In practice between 20% and 50% of the total current leaks through the interstitial spaces of the muscle segment in the sucrose gap since the sucrose is inevitably contaminated with ions. A second practical limitation is the speed at which the membrane potential is clamped to a new voltage; it is not possible to force changes faster than a few ms.

Another commonly used arrangement is the double sucrose gap. Here a second gap replaces the microelectrode of the single sucrose gap (figure I-6). With the double sucrose gap the potential recorded across this second gap is closely related to the intracellular membrane potential within the active segment and is used as the comparative input of the feedback amplifier. Two problems plague the double sucrose gap arrangement since the active segment is between the two gaps. Tensions are difficult to measure accurately because an inactive segment of tissue is in series with a tension transducer. Secondly the control point in the double sucrose gap is at the end of the active segment opposite the current injection end. Consequently the whole active segment is included in the electronic feedback path which introduces instability and inhomogeneity in the control of the membrane potential. The existence of this problem has been confirmed by a roving microelectrode used to check the homogeneity of the membrane potential during a voltage clamp in the double sucrose gap (Tarr and Trank, 1974; Connor, Barr and Jakobsson, 1975). With the single sucrose gap one is able to place the recording microelectrode in the middle

Figure I-6. Double sucrose gap chamber. The membrane potential is measured as the difference between the extracellular potential in the test node and KCl compartment. The Ringer compartment is used to inject current through the muscle as in the single sucrose gap.

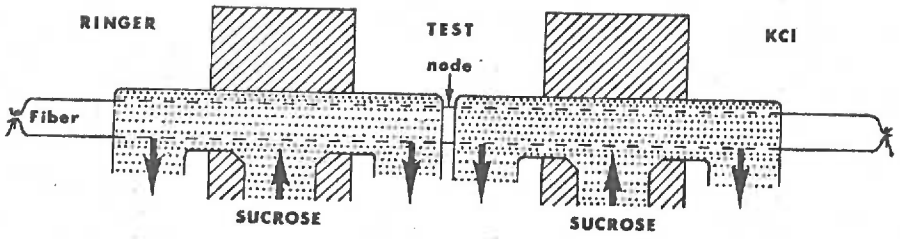
RINGER
TEST
node
KCl
Fiber
SUCROSE
SUCROSE

of the active segment or even closer to the rubber partition. This allows much better stability and control of membrane potential as confirmed with the use of a second microelectrode by New and Trautwein (1972a).

The major ultrastructural differences between the mammalian and frog hearts make it appropriate to discuss separately the voltage clamp data.

Frog Heart

During membrane depolarizations above the threshold for electrical excitation two distinct inward currents occur in atrial and ventricular preparations from the frog (Tarr, 1971; Morad and Goldman, 1973; Niedergerke and Orkand, 1966a). Immediately upon depolarization a short lasting (about 5 ms) "fast" inward current, with a voltage threshold at -65 mV, occurs that is blocked by Tetrodotoxin (TTX) and is sodium-dependent and is thus believed to be primarily carried by sodium ions. The fast inward current in the frog heart is similar to the fast inward current in squid axon. The maximum rate of depolarization (dV/dt of the upstroke of a normal action potential) and the fast inward current are linearly dependent on the extracellular sodium concentration suggesting that the initial upstroke of the frog action potential is the result of the fast inward sodium current as it is in the squid axon. A slower secondary inward current, with a voltage threshold around -40 mV, occurs following inactivation of the fast inward current. The secondary inward current is calcium and sodium sensitive, TTX insensitive, and is considerably reduced in the

presence of ionic manganese, lanthanum, cobalt and nickel (Reuter, 1973). The action potential overshoot, the rate of depolarization of the second phase, and the plateau of the action potential are dependent on calcium as well as sodium (Niedergerke and Orkand, 1966b). In summary, it is believed that the early rapid phase of depolarization is due to a large inward sodium current, whereas the slow secondary depolarization and plateau of the action potential results from a much smaller "secondary" inward current carried by calcium as well as sodium ions.

Frog Ventricle

Using a single sucrose gap Morad and Orkand (1971) found that the duration of depolarization, at a given membrane potential above the electrical threshold for tension development, was linearly related to the time to reach peak tension up to about 2 sec (normal action potential duration equal to 800 ms at 22°C). For durations greater than 2 sec the developed tension reached a plateau and relaxed only after the membrane was repolarized. Depolarizations longer than 80 ms were required to produce tension. Premature termination of a normal action potential gave similar results to short duration depolarizations (Morad and Orkand, 1971). The time course of tension development was always monophasic with no indication of a phasic or twitch-like component of tension superimposed on the tonic tension. After alterations in the duration or level of depolarization, tension develops its new equilibrium value within the

first altered beat and resumption of the original action potential produces the control level of tension in the first and succeeding beats (Morad and Goldman, 1973).

For any given duration of depolarization, contractility was found to be related to the level of depolarization. Figure I-7 from Morad and Orkand (1971) shows the tension-voltage relation to be fairly linear above +5 mV. Increasing external calcium from 0.2 to 1.0 mM rotated the tension-voltage curve upward as expected. However, no relation between the secondary inward current and tension was observed in the frog ventricle and peak tension continued to increase in the range of the calculated Nernst potential for calcium (+104 to +95 mV), where the electrochemical gradient for calcium is zero.

Voltage clamp studies reveal differences between frog atrial and ventricular preparations. The atrial preparations, in a double sucrose gap, develop a phasic tension to short depolarizations (250 ms) that appears to be dependent on the secondary inward current (Einwächter, Haas and Kern, 1972; Leoty and Raymond, 1972; Vassort and Rougier, 1972). For depolarizations longer than 300 ms, tension development is biphasic (figure I-8) and tension is maintained for the duration of depolarization (tonic tension). This is unlike frog ventricular preparations which in a single sucrose gap show only a tonic tension, regardless of the duration of depolarization.

It is possible that this difference, the phasic component of tension, is artifactual. Recent studies have tested the adequacy of the double sucrose gap (Tarr and Trank, 1974; Connor et al., 1975). Using a roving microelectrode to measure intracellular potentials

Figure I-7. Relation between membrane potential and tonic tension at two calcium concentrations in frog ventricle with the single sucrose gap. Clamp duration was 1.2 sec and bath temperature was 22°C. From Morad and Orkand, 1971.

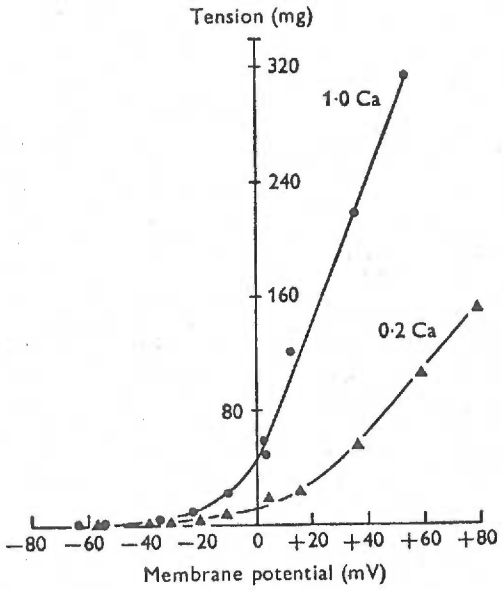
Tension (mg)
320
240
160
80
1·0 Ca
0·2 Ca
−80 −60 −40 −20 0 +20 +40 +60 +80
Membrane potential (mV)

Figure I-8. Separation of the phasic and tonic component of contraction in frog atria with a double sucrose gap. Full and interrupted lines show the time course of contraction as measured with pulses of 2 sec and 200 ms in duration, respectively. The dash-dot curves represent the difference between the experimental values and was assumed to represent the time course of the tonic tension by Einwächter et al. (1972). Amplitude of depolarization from the holding potential (-70 mV) was +40 mV in 'a' and +100 mV in 'b'. Bath temperature was 5°C. From Einwächter et al., 1972.

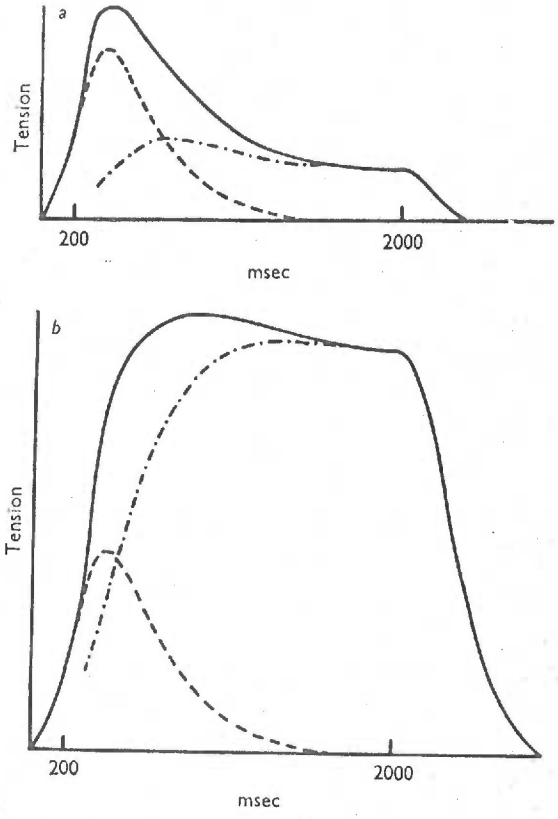
a
Tension
200
2000
msec
b
Tension
200
2000
msec

Tarr and Trank (1974) found that the voltage control of an impaled cell was lost during both the fast and slow excitatory inward currents. They argued that the loss of the spatial control of voltage during the excitatory inward currents raises serious doubts as to the adequacy of the double sucrose gap technique. Thus it is possible that the phasic component of tension observed in frog atrial tissue is due to a loss of voltage control, which results in the generation of an action potential, in a high percentage of the cells in the active preparation. The fact that time to peak tension of the phasic component is independent of clamp duration between 40 and 250 ms suggests the phasic tension might be the result of such uncontrolled action potentials generated within the active segment (Einwächter et al., 1972). The single sucrose gap technique has been tested for spatial control of membrane voltage with an independent roving microelectrode. Control of the potential was usually within 5% of the control signal at various locations on the preparation (Morad and Orkand, 1971). Consequently in Morad and Orkand's work (1971) there was better control of membrane voltage than in other studies.

Mammalian Ventricle

In the mammalian heart it appears that the action potential upstroke and plateau are the result of two different components of current (Reuter, 1973) as in the frog heart. The initial upstroke of the action potential is altered by variations in external sodium and reduced when TTX is added. The action potential plateau is not affected by TTX but is decreased by a low external calcium concentration

or addition of ionic lanthanum, manganese or nickel to the bath solution. Results obtained from voltage clamp studies on ventricular preparations in a single sucrose gap lead to similar conclusions. In preparations where the homogeneity of the voltage clamp was checked with a roving microelectrode and found to be within 5% of the control signal, two active inward currents have been observed (figure I-13) (Trautwein, 1973). The initial fast inward current is believed to be carried by sodium ions because it is very sensitive to TTX and alterations of external sodium concentration and has a reversal potential* that follows the extracellular sodium concentration in accordance with the Nernst equation. Following inactivation of the fast inward current (3-5 ms) a secondary slow inward current is activated that decays exponentially with a time constant as high as 200 ms (New and Trautwein, 1972a). The secondary inward current is reduced by ionic lanthanum, manganese and nickel present in the external media and also by a decrease in the external calcium concentration. However the reversal potential of the secondary inward current does not follow the extracellular calcium concentration as predicted by the Nernst equation unless calcium flows into a hypothetical small intracellular compartment, separate from the myofilament space, with an internal calcium concentration well above that of the myoplasma (New and Trautwein 1972b). As in the frog heart, it appears that the initial

* The reversal potential for a current component is the potential at which the current changes direction from inward to outward or vice versa. This is equivalent to saying the electrochemical gradient is zero at the reversal potential. The reversal potential on a current-voltage plot would then be the potential where the curve crosses the zero current axis.

upstroke of the action potential is the result of a rapid inward sodium current and the plateau of the action potential is the result of a more slowly decaying, secondary inward current, carried predominantly by calcium.

The control of tension by the membrane potential has been studied with the single sucrose gap technique. Alterations in membrane depolarization or duration of depolarization do not produce an immediate change in steady state tension in the first altered beat as in the frog heart. Tension gradually changes to a new steady state value in 5 to 8 beats even though the secondary inward current changes to its new value on the first altered beat (Beeler and Reuter, 1970b).

Prolongation of the action potential with membrane depolarizations at the plateau level is illustrated in figure I-9. An initial phasic component of tension (phasic tension) develops followed by a period of incomplete relaxation and maintained tension (tonic tension) which completely relaxes only upon repolarization. The development of tonic tension has been observed in cat and sheep myocardium (Morad, Mascher and Brody, 1968; New and Trautwein, 1972b; Wood, Heppner and Weidmann, 1969).

Premature termination of the action potential so that its duration is less than 100 ms results in a phasic tension that outlasts the clamp duration. Increasing the duration of depolarization from 100 ms up to 200 ms increases the phasic tension (figure I-10) but for durations longer than 200 ms tension does not increase further (Beeler and Reuter, 1970b; Morad and Trautwein, 1968). Time to peak tension depends upon the duration of depolarization between 100 and

Figure I-9. Superimposed tension tracings elicited by a normal action potential and a step depolarization in the mammalian ventricle at 24°C. A biphasic tension response to the step depolarization is clearly apparent. The initial twitch-like contraction (phasic tension) seems to have a similar time course and magnitude as the normal twitch contraction while the tonic component is maintained for the duration of depolarization. From Morad and Goldman, 1973.

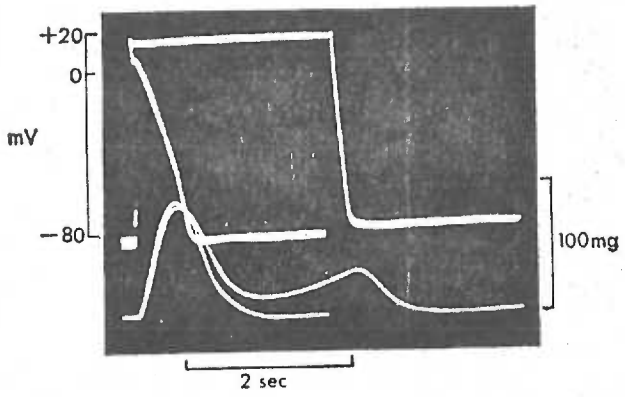
+20
0
mV
−80
100mg
2 sec

Figure I-10. Premature termination of ventricular action potentials in the mammalian heart (with a single sucrose gap). The amplitude of the contraction elicited by the first shortened beat as a percent of the control contraction is plotted on the ordinate versus the duration of the shortened action potential on the abscissa. Bath temperature ranged between 26 and 28°C. From Morad and Trautwein, 1968.

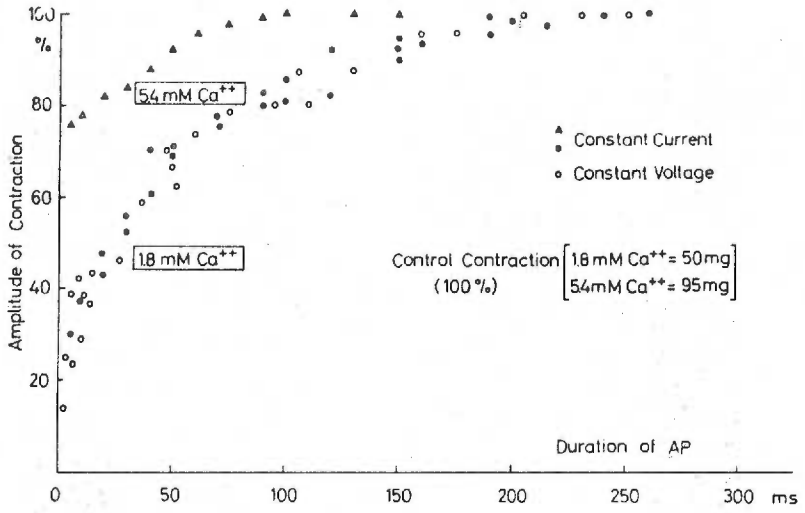
100
%
80
60
40
20
Amplitude of Contraction
5.4 mM Ca++
1.8 mM Ca++
Constant Current
Constant Voltage
Control Contraction
(100 %)
1.8 mM Ca++ = 50mg
5.4mM Ca++ = 95mg
Duration of AP
0
50
100
150
200
250
300 ms

200 ms but for longer durations time to peak tension is not affected by the duration of depolarization (figure I-11).

The phasic tension is voltage dependent and has a voltage threshold at around -35 mV, similar to the voltage threshold of the secondary inward current (New and Trautwein, 1972b). The voltage-tension relation of the phasic contraction elicited by the eighth voltage clamp beat shows an S-shaped relation with a plateau at around +5 mV (figure I-12). Peak tension is constant for membrane depolarizations between +5 mV and +50 mV and thereafter peak tension declines with membrane depolarizations greater than +50 mV (Beeler and Reuter, 1970b; New and Trautwein, 1972b). The peak of the secondary inward current measured as the difference between the steady state outward current (a, figure I-13) and the peak of the inward deflection (b, figure I-13) has a voltage threshold at -35 mV. The secondary inward current is maximal for depolarizations between -5 and +5 mV and declines to almost zero at about +60 mV (Beeler and Reuter, 1970a; New and Trautwein, 1972b). For depolarization greater than +10 mV, contractility does not appear to depend on the secondary inward current. For example, at +60 mV, where the secondary inward current is nearly zero, peak tension of the eighth altered contraction is still about 75% of the maximum tension obtained (Beeler and Reuter, 1970b; New and Trautwein, 1972b). Morad and Goldman (1973) studied the contraction developed by the first voltage clamp beat and found a similar tension-voltage relation for depolarizations up to +10 mV. But for depolarizations greater than +10 mV peak tension of the first altered contraction decreased and by +50 mV peak tension was 35%

Figure I-11. Relation between action potential duration and time to peak tension in the mammalian heart (with a single sucrose gap). Time to peak tension of the contraction elicited by the first shortened action potential as a percent of time to peak tension of the control contraction (270 ms) is plotted on the ordinate versus the duration of the shortened action potential (abscissa). From Morad and Trautwein, 1968.

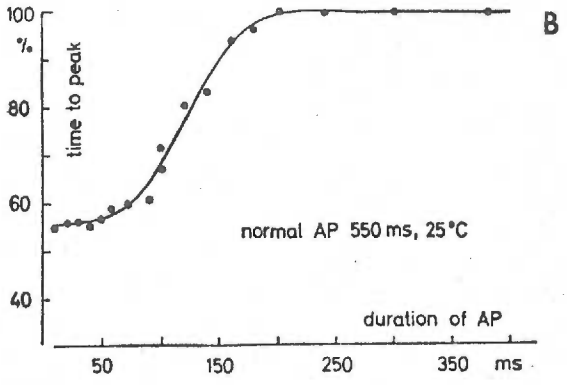
100
%
80
60
40
time to peak
B
normal AP 550 ms, 25 °C
duration of AP
50
150
250
350
ms

Figure I-12. Tension-voltage relation in the mammalian heart. Steady state peak tension normalized by the maximum steady state peak tension is plotted on the ordinate versus the membrane potential. The voltage clamp pulse duration was 350 ms and the bath temperature was 37°C. From New and Trautwein, 1972b.

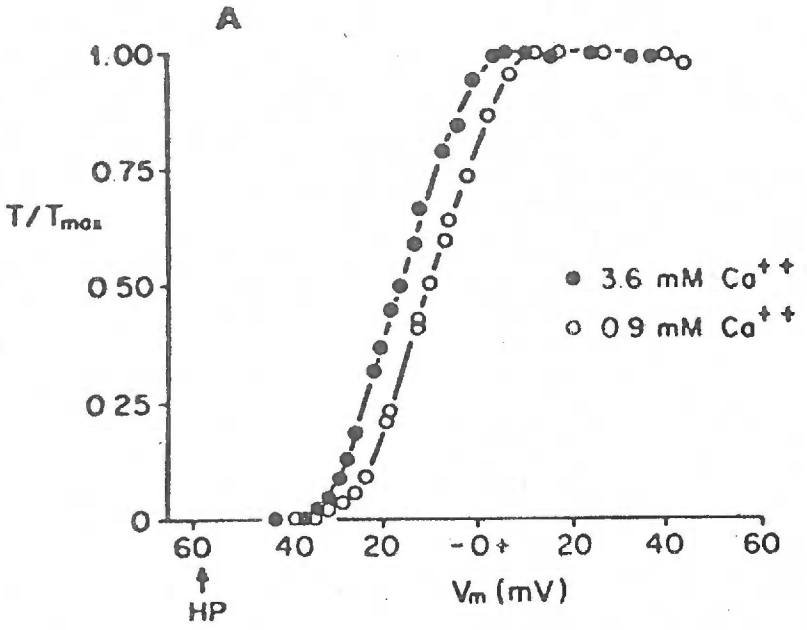
A
1.00
0.75
T/T max
0.50
0.25
0
60
40
20
-0+
20
40
60
HP
Vm (mV)
3.6 mM Ca++
0.9 mM Ca++
8

Figure I-13. Demonstration of the fast inward sodium current (I_{Na}) followed by the secondary inward current (I_{Ca}) during a voltage clamp depolarization from -55 mV to -5 mV for 300 ms in the mammalian heart (with a single sucrose gap). The current recorded (I) in response to the voltage step (V) shows the way in which the secondary inward current was estimated (a-b). From McDonald, Nawrath and Trautwein, 1975.

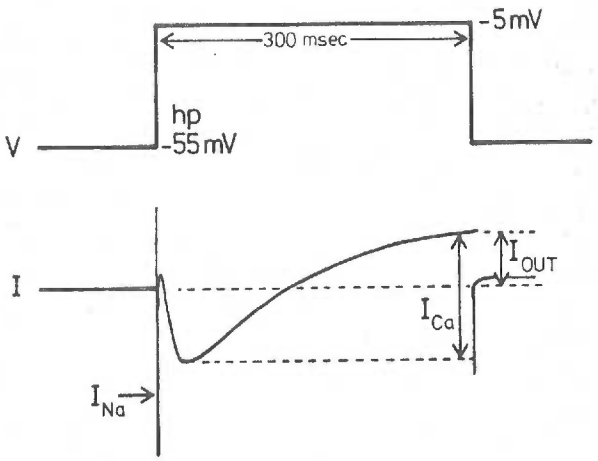
-5mV
300 msec
hp
-55mV
V
I
I_{OUT}
I_{Ca}
I_{Na}

of maximum tension developed (figure I-14).

The tension-voltage relation of the tonic tension was studied with 2 sec depolarizations (Morad and Goldman, 1973). The threshold for the tonic tension is about -30 mV. Peak tonic tension progressively increases as a function of the membrane potential (figure I-14) with no maximum observed up to +80 mV (Morad and Goldman, 1973). It appears that the tonic tension is dependent on the bath temperature, for the tonic tension developed at 35°C (New and Trautwein, 1972b) is smaller than the tonic tension developed at 25°C (Morad and Goldman, 1973). Thus two components of tension are observed for long clamp pulses, suggestive of two sources of activator calcium.

Calcium antagonists such as lanthanum, manganese or low extracellular calcium, significantly reduce or abolish, both the secondary inward current and phasic tension (Leoty, 1974; Reuter, 1973). The effect of lanthanum is of particular interest for the ion does not appear to cross the membrane but is found to bind to the superficial basement membrane (Langer, 1973). This suggests that a superficial store of calcium is necessary for the secondary inward current and excitation-contraction coupling in the mammalian heart. Unfortunately, to my knowledge no one has studied the effects of these ionic blockers on the development of tonic tension.

Decreasing extracellular sodium increases twitch tension and shifts the tension-voltage curve, along the voltage axis, to more negative potentials. The resting level of tension increases and the rate of relaxation is slowed. The peak of the tension-voltage curve is shifted from +5 mV in normal Tyrode to about -10 mV in low

Figure I-14. Relation between tension and membrane potential of the first voltage clamp pulse in the mammalian ventricle. Peak tension of the phasic and tonic components of contraction elicited by the first voltage clamp pulse is plotted on the ordinate versus the membrane potential on the abscissa. Pulse duration was 2.5 sec and the bath temperature was 24°C. From Morad and Goldman, 1973.

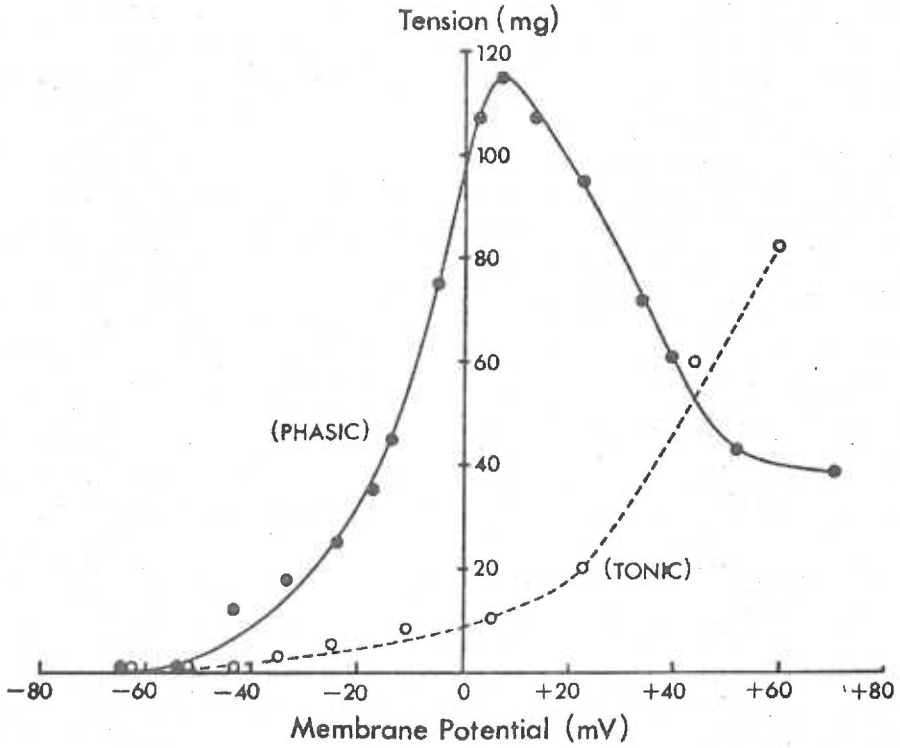
Tension (mg)
120
100
80
60
40
20
(PHASIC)
(TONIC)
−80
−60
−40
−20
0
+20
+40
+60
+80
Membrane Potential (mV)

sodium (12 mM) (Beeler and Reuter, 1970b; New and Trautwein, 1972b; Leoty, 1974). The plateau of the tension-voltage curve is absent so that peak tension declines at depolarizations more positive than -10 mV. In low sodium solution the secondary inward current is little affected and the peak of the secondary inward current-voltage curve strongly correlated with the tension-voltage curve (New and Trautwein, 1972b). In contrast to the frog heart the tonic component of tension is reduced in the mammalian heart with a reduction of external sodium (Morad and Goldman, 1973). More important is the observation that in low sodium solution the treppe response of phasic tension to alterations in membrane depolarization or duration of depolarization is abolished (Beeler and Reuter, 1970b; New and Trautwein, 1972b; Leoty, 1974). The reality of the biphasic response (a phasic and a tonic component) is attested by the observation that the two components can be individually changed in magnitude.

The mechanism involved in the control of the tonic tension is not associated with the secondary inward current, for peak tonic tension continues to increase with membrane depolarizations greater than +80 mV which is above the reversal potential for the secondary inward current in 1.8 mM calcium. Vassort (1973) gave evidence suggesting that the tonic tension in the frog heart is dependent on intracellular sodium. He argued in favor of a sodium-calcium exchange such that calcium inflow is coupled with sodium outflow. However at +120 mV where the tonic tension is still increasing the transport of calcium in and sodium out would be against the electrochemical gradient for each ion which makes this exchange unlikely, unless it

is energy dependent. Morad suggested that calcium influx is coupled with potassium efflux since the potassium electrochemical gradient continues to increase for potentials positive to -80 mV. This is a highly attractive explanation although at present there is no additional evidence for it.

The mechanism for the release of activator calcium has attracted much interest in the past 8 years. The correlation between the phasic tension-voltage curve and the secondary inward current-voltage curve for the first voltage clamp pulse suggests that the secondary inward current acts as a signal for the graded release of calcium. The secondary inward current, believed to be carried predominantly by calcium, has a reversal potential at around +80 mV in 3.6 mM $CaCl_2$ and +40 mV in 0.9 mM $CaCl_2$ (New and Trautwein, 1972b). If it is assumed that the reversal potential represents the Nernst equilibrium potential for calcium, then the myoplasmic calcium concentration during systole would be 8.6×10^{-6}M and 4.4×10^{-5}M respectively. This increase in myoplasmic calcium concentration (with decreasing external calcium concentration) is not consistent with a decrease in tension associated with the decrease in external calcium. Consequently the secondary inward current cannot be represented by a simple Nernst model. From Winegrad's study (1971), it is known that a myoplasmic calcium concentration greater than 10^{-7}M is necessary to produce tension and that maximum tension is produced at around 2×10^{-5}M (figure I-3). Normal twitch tension is about 20% of the maximum possible tension which suggests that myoplasmic calcium concentration increases from below 10^{-7}M to 4×10^{-7}M during an action potential.

This led Bassingthwaigthe and Reuter (1972) to suggest that the secondary inward current flows into a subsarcolemmal space such as the SR cisternae. Thus it is attractive to postulate that the secondary inward current triggers a graded release of calcium stored in the SR cisternae. Support for a calcium-induced release of internally stored calcium comes from the studies on skinned mammalian cardiac cells (Fabiato and Fabiato, 1975). Cyclic contractions are induced in skinned cardiac cells when the EGTA buffered free calcium concentration is increased to above $10^{-7.65}$M. Further increase in the calcium concentration increases the force of cyclic contraction with a maximum at $10^{-7.4}$M. Tonic contractures are induced with further increases in the buffered calcium concentration. A sigmoid relation is observed for the tonic tension versus the calcium concentration with a maximum at 10^{-5}M. The cyclic contractions at $10^{-7.4}$M calcium are equal in magnitude to the tonic tension observed at $10^{-6.1}$M calcium. These results suggest that a small calcium current intermittently triggers a graded release of internally stored calcium from the SR. Furthermore studies on skinned frog heart cells show no cyclic contractions but only contractures reinforcing a hypothesis that the SR found in the mammalian heart is necessary for intracellular release of calcium (Fabiato and Fabiato, 1975).

Current Model of the E-C Coupling Mechanism in Mammalian Heart

The voltage clamp data indicate major differences between the E-C coupling mechanisms of the frog and mammalian ventricle. a) In the frog ventricle alteration of tension development as a result of

external manipulation of the action potential is produced within the first altered action potential with no further change during the succeeding altered action potentials. Similarly there is no tension staircase during paired pulse stimulation in the frog heart. The mammalian heart exhibits a tension staircase in response to external manipulation of the action potential and requires 6 to 8 beats before contractility reaches a new steady state. Potentiation, in the mammalian heart, produced either by paired pulse stimulation, increased stimulation rate, or current injection via a sucrose gap builds up and decays with identical beat dependent kinetics (Woods et al., 1969). b) Tension development in the frog ventricle is monophasic (tonic) and is directly related to the duration and degree of depolarization. Tension development in the mammalian heart is biphasic with a twitch-like component for short duration depolarizations followed by development of a tonic component for longer durations of depolarization. Repetitive stimulation with identical membrane depolarizations produces a tension staircase. c) A plot of peak tension versus membrane potential for the first clamp of the staircase has a bell-shaped curve similar to the plot of the slow inward current versus voltage. The shape of the tension-voltage curve for steady state depolarizations deviates from the current-voltage curve at about -10 mV.

These data strongly suggest that activator calcium is derived functionally from two different sources in the mammalian heart. However in the frog ventricle it appears that activator calcium is derived from only one source. Considering the ultrastructural differences between the frog and mammalian heart and the results

described above Morad and Goldman (1973) postulated an E-C coupling scheme with the following characteristics.

(1.) The well organized SR acts not only to sequester calcium (longitudinal SR) from the myoplasma during each cycle but also to store (SR cisternae) a releasable quantity of calcium. The sarcolemma and T-tubules may be involved in the transport of calcium both inward and outward and may contribute to the second source of activator calcium.

(2.) The release of activator calcium and its availability is controlled by the action potential through two separate mechanisms. The initial 100 ms of the action potential triggers a release of activator calcium stored inside the SR cisternae. Continued depolarization releases additional activator calcium into the myoplasma by transport across the sarcolemma from an extracellular source. Release continues for the duration of depolarization and is not a simple influx under the influence of the electrochemical gradient for calcium.

(3.) The sum of activator calcium from these two sources minus the calcium sequestered by the longitudinal SR or extruded by the sarcolemma (sodium-calcium exchange) determines the strength of contraction.

(4.) A fraction of the calcium sequestered by the longitudinal SR is returned to the SR cisternae after some delay.

The events leading to a normal contraction in the mammalian heart are postulated as follows: The action potential propagates along the surface of the membrane and down the T-tubular system.

The initial depolarization phase of the action potential initiates a secondary inward current carried in part by calcium ions which triggers a release of intracellularly stored calcium from terminal SR cisternae. The plateau of the action potential initiates a further influx of calcium ions across the sarcolemma into the myoplasma. There is a competition for the removal of myoplasmic calcium, the longitudinal SR actively sequestering calcium from the myoplasma and the sarcolemma sequestering calcium from the myoplasma possibly by a sodium-calcium exchange. The balance between the amount of calcium released and sequestered at any instant determines the myoplasmic calcium concentration and hence the force of contraction. A fraction of the calcium sequestered by the longitudinal SR is recycled back to the SR cisternae for the next beat; the remainder is eliminated by a sodium-calcium exchange. An increase in the rate of SR sequestration or in the rate or duration of calcium influx during the plateau phase of the action potential will lead to an increase in internally stored calcium which will result in an altered inotropic state and require 6 to 8 beats to attain a new steady state. This sequence is essentially that proposed by Morad and Goldman (1973) and Reuter (1974) for the E-C coupling relation in the mammalian heart.

Purpose of Study

The proposed role of the SR in the E-C coupling process in the mammalian heart described above was formulated on the basis of the structural-functional differences between the frog and mammalian ventricle. Thus in the mammalian myocardium, the tension staircase

associated with post-extrasystolic potentiation, altered rate of stimulation or altered action potential configuration with a sucrose gap are the direct result of the capacity of the SR to sequester calcium and recycle a fraction of the sequestered calcium for subsequent beats. This hypothesis is reinforced by studies on the frog heart which demonstrate a lack of both the tension staircase and a well-organized SR. However the frog heart cells also lack T-tubules and have a diameter of 3-5 μ in comparison to 10-40 μ of mammalian ventricular cells. Furthermore the basement membrane found in the T-tubules and on the external sarcolemma of mammalian heart cells is lacking on the cell surfaces of frog heart (Staley and Benson, 1968). Thus the functional differences between the frog and mammalian heart cells could also be associated with some of the other ultrastructural differences besides the relative amounts of SR. Langer has proposed that the basement membrane is the main compartment for the storage of activator calcium and that the SR acts to maintain the myoplasmic calcium concentration below 10^{-7}M. Langer's hypothesis suggests that the lack of basement membrane in frog heart cells is the reason for a lack of a tension staircase. However Fabiato's work on skinned frog and mammalian heart cells argues against this.

The purpose of this thesis is to study the E-C coupling mechanism in a mammalian heart that lacks T-tubules and a well organized network of SR. It has been observed in neonatal kitten hearts that T-tubules and SR begin to appear only after the first week of life (Orkand, 1964). Schiebler and Wolf (1966) observed in the rat heart that the SR develops in the first few days after birth

and that the T-tubules begin to form 2 to 3 weeks after birth. Similar findings have been reported for neonatal dog hearts (Legato, 1976). Thus the neonatal hearts from cat, dog and rat have ultrastructural features in common with the frog heart. The neonatal heart is therefore a good preparation to test the hypothesis that the functional differences between the frog and mammalian heart are due to differences in the relative amounts of SR.

This study is organized in three sections; each contains an Introduction, Methods, and Results as well as a Discussion of the validity of the results. The three sections are followed by a general discussion of the relation between the experimental findings and their meaning in the context of cardiac physiology. The three sections are:

Section II: A short ultrastructural study to confirm the findings of Orkand (1964) that the neonatal cat heart lacks T-tubules and a developed network of SR.

Section III: An examination of post-extrasystolic potentiation and frequency potentiation in the hearts of neonatal and adult cats.

Section IV: An investigation of the relation between contractility and membrane potential in hearts of neonatal and adult cats.

II. ULTRASTRUCTURAL EXAMINATION OF NEONATAL CAT HEART

Methods

Papillary muscles from the right ventricle of cats, of ages ranging from 1 day to adult, were used for an electron microscopy study. The cats were anesthetized with halothane or ether and the thorax was opened and the pulmonary artery and aorta were quickly clamped. A perfusion tube was inserted into the aorta between the left ventricle and the clamp. After cutting the right atrium to allow for escape of fluid, cold fixative was injected through the perfusion tube (from a bottle about 150 cm above the cat) into the aorta. Within seconds the coronary arteries were clear with fixative. After 2 min when the heart had hardened, a papillary muscle was quickly removed from the right ventricle and placed in fresh fixative. The muscle was sliced longitudinally into thin strands ranging from 0.5 to 1 mm in diameter and these segments were transferred to a vial containing fresh fixative. Two fixatives were used: 2.5% glutaraldehyde buffered with 0.1 M sodium phosphate (pH = 7.4) or 2.5% glutaraldehyde and 2% formaldehyde buffered with 0.1 M sodium phosphate (pH = 7.4).

The segments of muscle were initially fixed in one of the fixatives for 60 to 90 min at 0°C and rinsed in 0.1 M sodium phosphate overnight at 0°C. The next day the segments were post-fixed in 2% osmium tetroxide buffered in 0.1 M sodium phosphate for 90 to 120 min at 0°C. After rinsing in 0.1 M sodium phosphate the segments were dehydrated in graded alcohol solutions and embedded in low viscosity plastic (Spurr, 1969).

In some of the cats, horseradish peroxidase (Type II, Sigma Chemical Company, St. Louis or Worthington, Freehold, New Jersey) was used as an extracellular marker (Graham and Karnovsky, 1966). Fifty to 75 mg of horseradish peroxidase (HRP) in 0.9% saline was slowly perfused into the femoral vein of the neonatal cats (0.3 g of HRP was used for adult cats). Five minutes were allowed for equilibration after which the thorax was opened and the heart was fixed by perfusion with glutaraldehyde-formaldehyde fixative as described previously. The segments were fixed for 60 to 90 min and rinsed overnight in 0.1 M sodium phosphate at 0°C. After a rinse in 0.05 M Tris-HCl, the sections were incubated for 8 to 10 min at room temperature in a saturated solution of 3',3'-diaminobenzidine (free base) (Sigma Chemical Company) or 0.05% 3',3'-diaminobenzidine tetrahydrochloride (Sigma Chemical Company). Both were buffered in a solution of 0.05 M Tris-HCl (pH = 7.6) containing 0.01% H_2O_2. The sections were washed three times in distilled water and processed for electron microscopy as described previously.

Thin longitudinal sections were cut with a glass or diamond knife on a LKB Ultrotome ultramicrotome and stained with saturated aqueous uranyl acetate or lead citrate or both (Venable and Coggeshall, 1965). The sections were examined with a JEOL JEM-100S or a Siemens Elmiskop I electron microscope.

Results

1. Ultrastructure of adult cat heart.

Fawcett and McNutt (1969) described the ultrastructure of the right ventricular papillary muscle of the adult cat. Consequently only two adult cats were studied, mainly to verify that with my technique similar structures were observed. Figure II-1 shows a low magnification micrograph of an adult papillary muscle perfused with HRP. The diameter of the adult heart cells ranged between 10 and 30 μ. Sarcomeres and mitochondria are packed tightly within the cells and HRP fills the extracellular spaces and the T-tubules (figures II-1 and II-2). Occasionally a longitudinal T-tubule was observed (figure II-3) as previously described by Forssmann and Girardier (1970) on rat papillary muscle. A basement membrane (basal lamina) coats the plasma membrane of the cell surface and T-tubules (figure II-4).

The sarcoplasmic reticulum (SR) consists of a longitudinal network that surrounds the sarcomeres (figures II-2 and II-4). At the I-band region extensions of the SR (SR saccules) are closely apposed to the sarcoplasmic surface of the T-tubule (figures II-2, II-3 and II-4). SR saccules were also observed along the sarcolemma of the cell surface (figure II-4). HRP was not observed in the SR saccules or the SR network. The ultrastructural arrangement in the two adult cat hearts was similar to the arrangement of the adult cat hearts described by Fawcett and McNutt (1969).

2. Ultrastructure of the neonatal cat myocardium.

Figure II-5 shows a low magnification micrograph of a neonatal papillary muscle. The diameters of neonatal heart cells range between 3 and 8 μ. The cellular organelles are loosely packed with myofibrils

running longitudinally only at the cell periphery. Nuclei and mitochondria are centrally located within the cell. Comparison with the adult heart (figure II-1) clearly shows the much lower concentration of myofilaments in the neonatal heart.

In 1 to 2 day old neonates, T-tubules were not observed and perfusion with HRP supported the observation that T-tubules had not yet developed in the neonates (figure II-6). Small tubules occasionally observed at the Z-line were also not filled with HRP. As in the adult, figures II-5, II-7 and II-8 show that a basement membrane coats the sarcolemma of each cell.

Small saccules were frequently observed adjacent to the sarcolemma in all the neonatal hearts studied (figures II-7 and II-8). These saccules are similar to the saccules apposed to the T-tubules and the sarcolemma of adult heart cells. Furthermore loose networks of SR-like membranes were occasionally observed (figures II-3 and II-4). The SR in the neonatal cat heart was more organized than the loose network of individual tubules that make up the SR in the frog heart (Page and Niedergerke, 1972). The occurrence of the SR networks in the neonate were very sparse in comparison to adult hearts. Figures II-7 and II-8 were chosen only to demonstrate that SR is present, and the figures are not representative in the sense that 90% of the micrographs taken (about 100) fail to show networks of SR. Numerous observations of neonatal sections in the electron microscope confirm this. Thus it appears that the neonatal cat heart has at least a rudimentary network of SR with peripheral couplings apposed to the sarcolemma. The difference in SR content between the neonate and

the adult was not quantified but it appears that the density of saccules in the neonate is significantly less than in the adult.

Discussion

Like the frog heart (Staley and Benson, 1968), 1 to 2 day old neonatal cat hearts lack transverse tubules which are prominent in adult cat hearts. Orkand (1964) also observed that neonatal cat hearts lack T-tubules. However, she further said that the neonatal cat heart lacks SR and she did not observe saccules apposed to the sarcolemma. Contrary to the results reported by Orkand (1964), I found saccules apposed to the sarcolemma and infrequent networks of SR in 1 day old neonatal cat hearts.

Page and Niedergerke (1972) reported that the SR in the frog heart is composed of small individual tubules with a single longitudinal tubule between sarcomeres and a transverse tubule surrounding the sarcomere at the Z-line. These tubules are continuous with each other but they are not continuous with the extracellular space as demonstrated by the extracellular markers, HRP and ferritin (Page and Niedergerke, 1972). Saccules of SR terminate on the sarcolemma and are associated with an average of 75% of the sarcomeres of the superficial myofibrils in the frog.

The centrally located SR in the neonatal cat heart when present at all forms small networks in comparison to the individual tubular structure of the SR in the frog heart. But the SR saccules in the neonatal cat and frog hearts do not appear to be different. Though the amount of SR in the neonatal cat heart was not quantified,

I am convinced by numerous micrographs and EM observations on 5 neonatal cats that the SR in the neonatal cat heart is more developed than in the frog heart and the quantity of SR is greater in the neonatal cat heart than in the frog heart. However, the cat heart at birth has not yet fully developed the characteristic T-tubules and SR of the adult cat heart and the density of SR saccules in the neonate appears to be less than in the adult cat heart.

Figure II-1. Electron micrograph of an adult cat heart perfused with HRP. Note the clear capillary (Cap) and the HRP within the T-tubules (TT) and the extracellular spaces between cells. Parts of 3 cardiac cells are easily distinguishable. The 2 upper cells are joined end to end by an intercalated disk (InD). Rows of mitochondria (Mt) divide the contractile material into myofibril-like units (Mf). The nucleus (NcL) is found off centered and packed between myofibrils. Lipid droplets (Lp) are found between the ends of the mitochondria. The horizontal calibration bar is 4 μ.

Figure II-2. Electron micrograph of an adult papillary muscle showing a close-up of the T-tubules (TT) and extracellular spaces (E) filled with HRP. The flattened saccules of the SR (asterisks) associated with the T-tubules and with the sarcolemma are not filled with HRP. Part of an SR network is also found free of HRP. Lipid droplets (Lp) and mitochondria (Mt) are packed tightly between the myofilaments. The horizontal calibration bar is 1 μ.

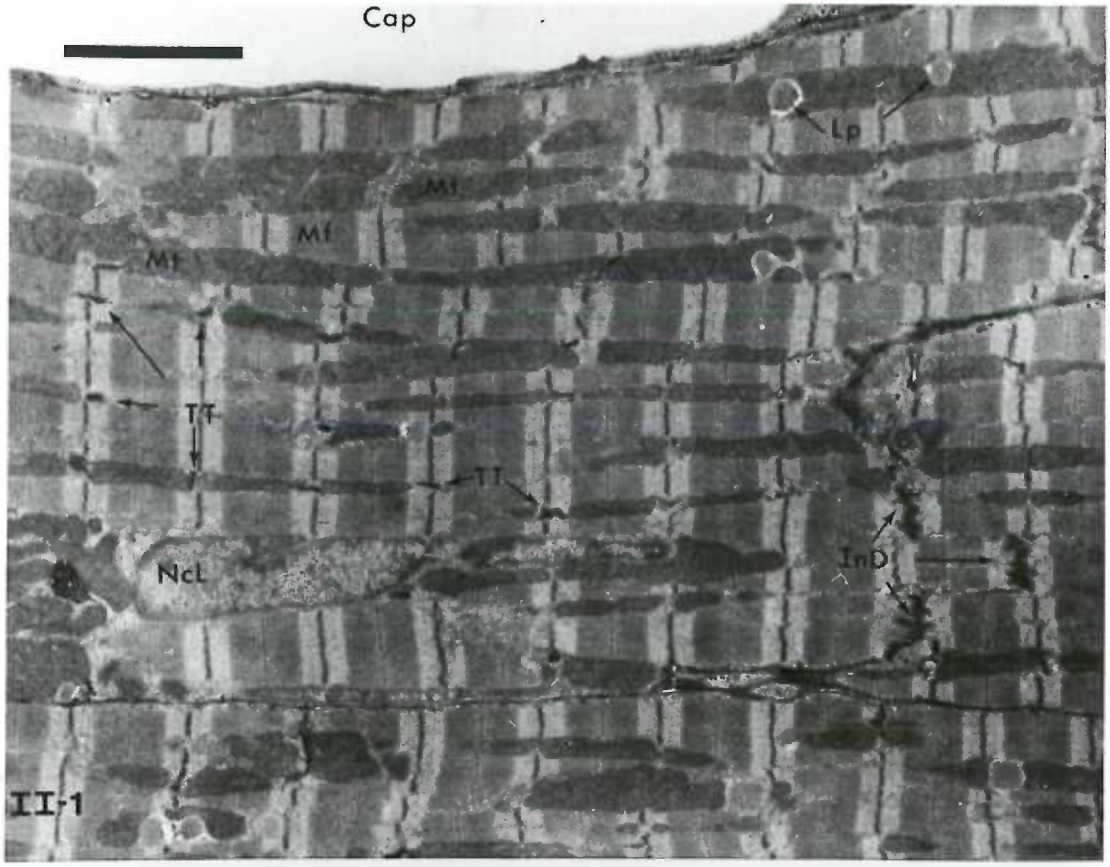

II-1

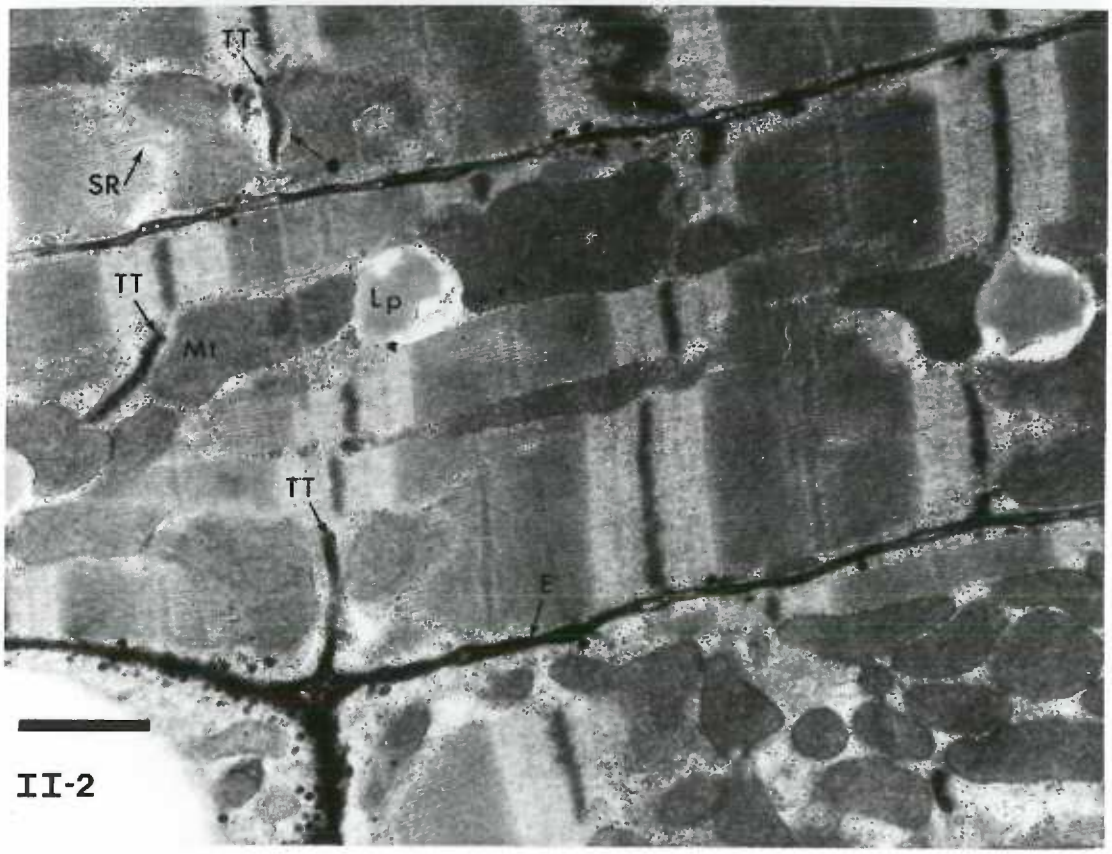

II-2

Figure II-3. Electron micrograph of an adult papillary muscle showing a longitudinal T-tubule (LTT) filled with HRP. SR saccules (asterisks) are apposed to the T-tubules (TT). Other abbreviations are: nucleus (NcL), mitochondria (Mt) and sarcolemma (SL). The horizontal calibration bar is 1 μ.

Figure II-4. Electron micrograph of an adult papillary muscle. Longitudinal portions of the SR (SR) are seen over the center of the A-band and at the Z-band. SR saccules (asterisks) are clearly associated with T-tubules (TT) and the sarcolemma (SL). The T-tubules are filled with HRP and a basal lamina (BL) coats the sarcolemma. Other abbreviations are: nucleus (NcL) and mitochondria (Mt). The horizontal calibration bar is 1 μ.

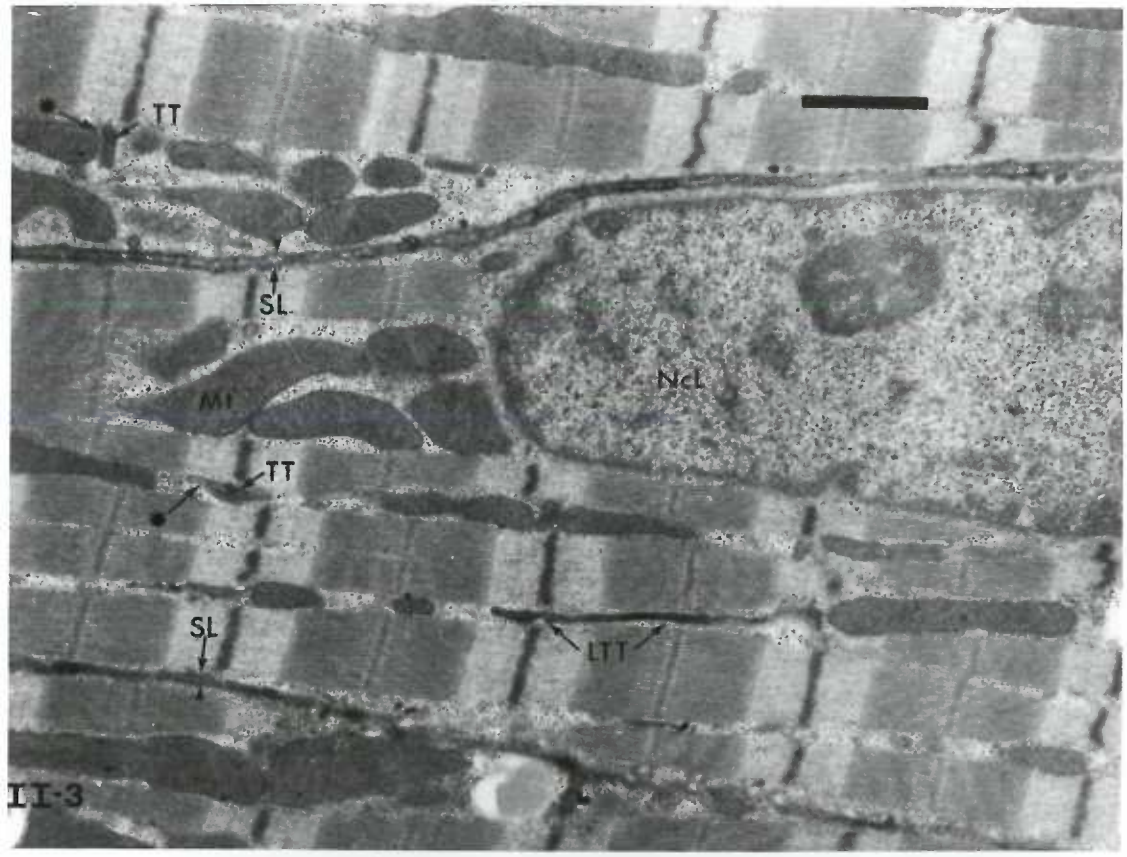
TT
SL
NcL
Mt
TT
SL
LTT
II-3

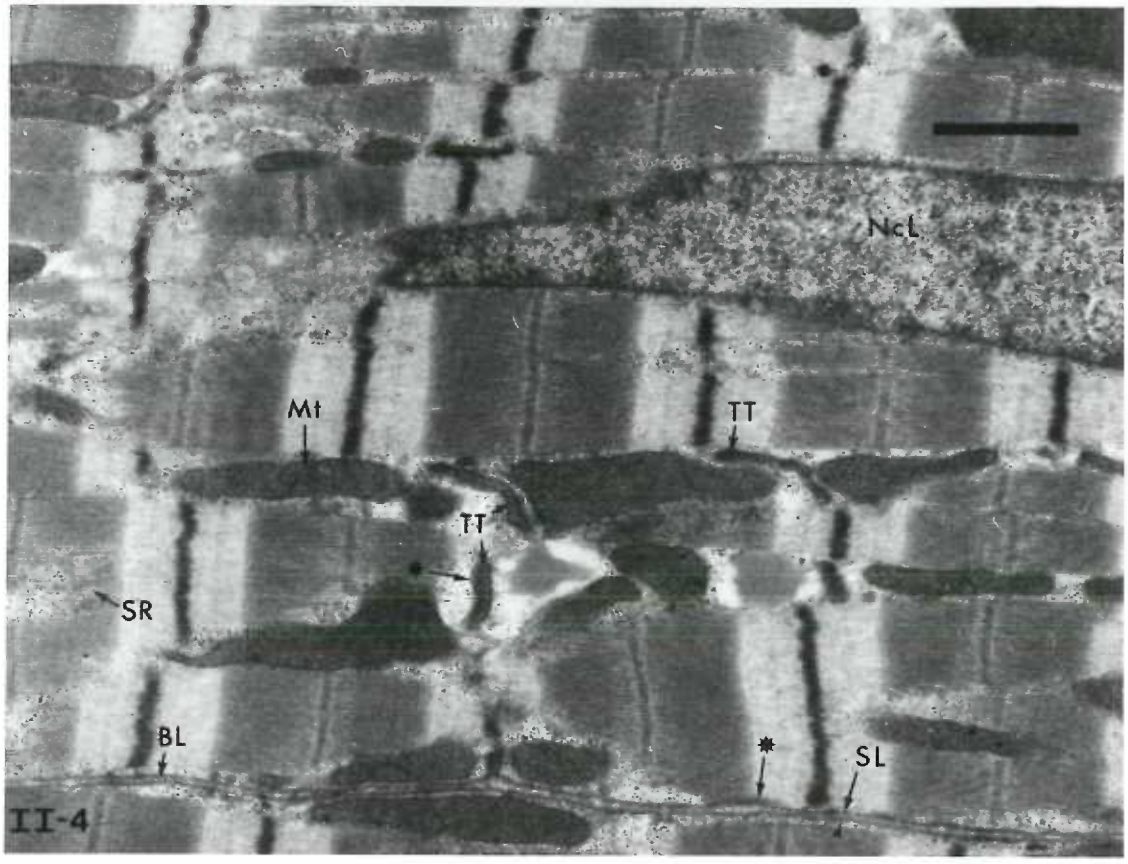
NcL
Mt
TT
TT
SR
BL
SL
II-4

Figure II-5. Electron micrograph showing parts of 7 cardiac cells adjacent to a capillary (Cap) in a 2 day old kitten heart. The cells are seen separated by a sarcolemma (SL) coated with a basal lamina (BL). The density of contractile material in the cells is low in comparison with the adult heart (figure II-1). A single layer of myofibrils (Mf) appears to coat the edge of each cell and the sarcomeres are in register. The nucleus (NcL) is centered within the cell and the mitochondria (Mt) do not divide the contractile material into myofibril-like units as in the adult heart. Instead many mitochondria and glycogen particles (GL) occupy the center of the cell. Parts of an intercalated disk (InD) can be seen separating the ends of the cells. The horizontal calibration bar is 4 μ.

Figure II-6. Electron micrograph of a 1 day old neonatal heart perfused with HRP. The HRP clearly fills the extracellular space to delineate the cell boundaries as a dark border. The general arrangement of the cells is described in figure II-5. Pinocytotic vesicles (PV) associated with the sarcolemma are filled with HRP. No structures filled with HRP are observed within the center of the cells indicating that the T-tubules have not yet developed. The horizontal calibration bar is 4 μ.

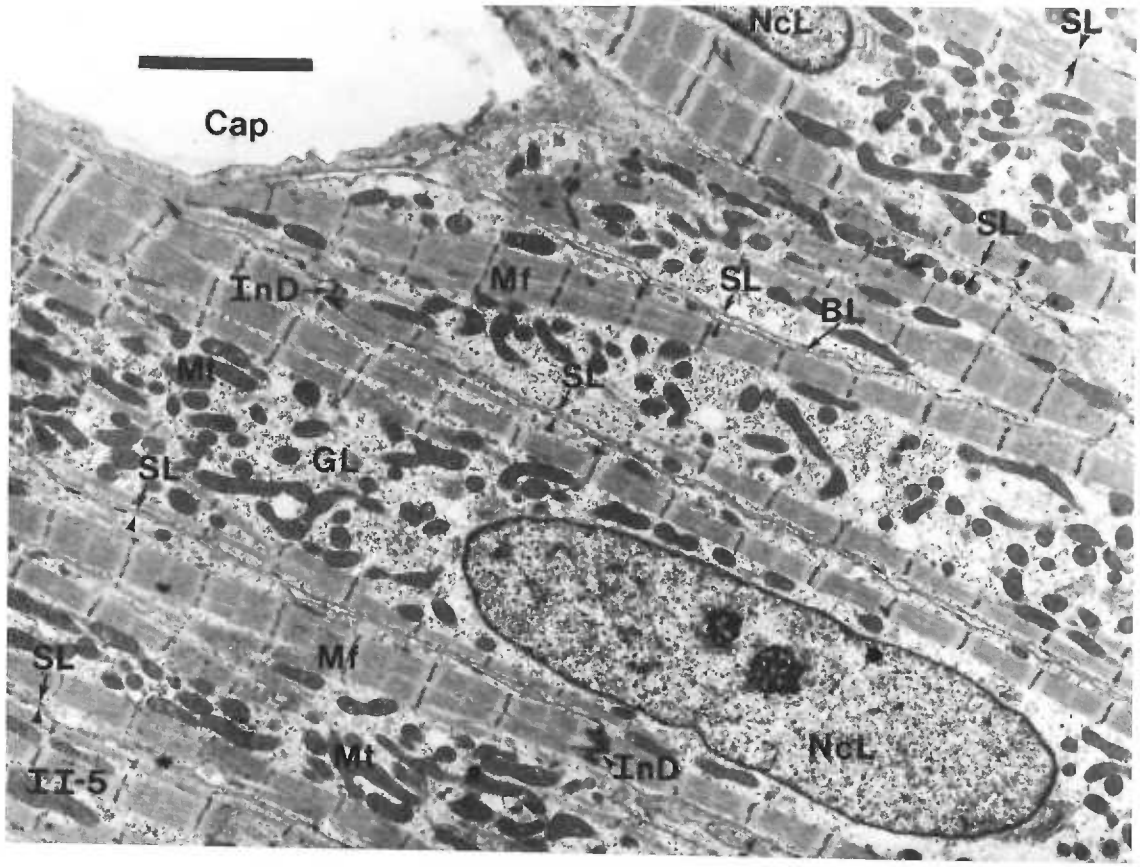
Cap
NcL
SL
SL
InD
Mf
SL
BL
Mf
SL
SL
GL
SL
Mf
Mf
InD
NcL
II-5

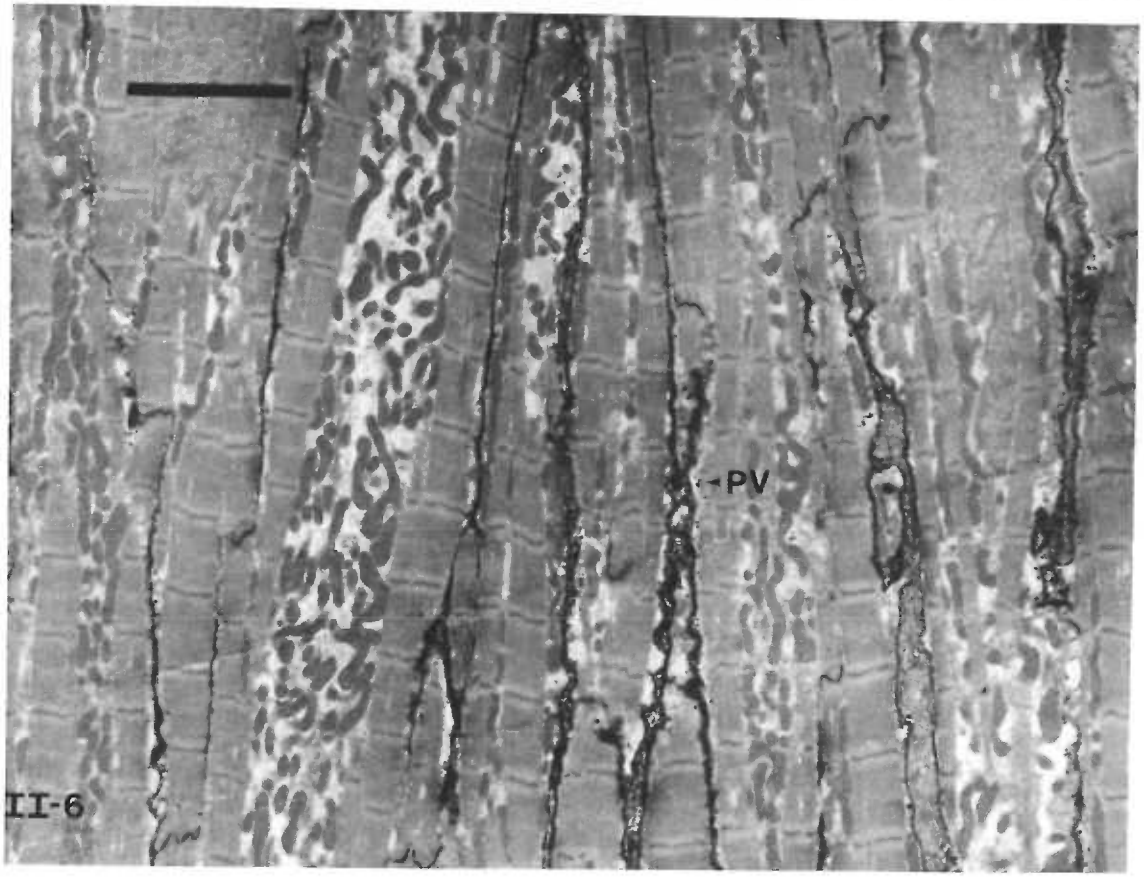
PV
II-6

Figure II-7. Electron micrograph of a 2 day old kitten heart. Flattened saccules (asterisks), suggestive of SR saccules, are found apposed to the sarcolemma (SL). Internal membrane structures (SR) resembling a network of SR is observed overlapping 2 sarcomeres. A basal lamina (BL) coats the sarcolemma of each cell. Other abbreviations are: nucleus (NcL) and mitochondria (Mt). The horizontal calibration bar is 1 μ.

Figure II-8. Electron micrograph of a 2 day old neonate further demonstrating saccules (asterisks) apposed to the sarcolemma (SL). Part of an SR network (SR) with a transverse component at the Z-line overlaps one of the sarcomeres. Part of an intercalated disk (InD) separates 2 cells. The basal lamina (BL) is further observed in the extracellular space of each cell. Numerous mitochondria (Mt) fill the center of the cell with a single layer of myofibrils (Mf) adjacent to the sarcolemma. The horizontal calibration bar is 1 μ.

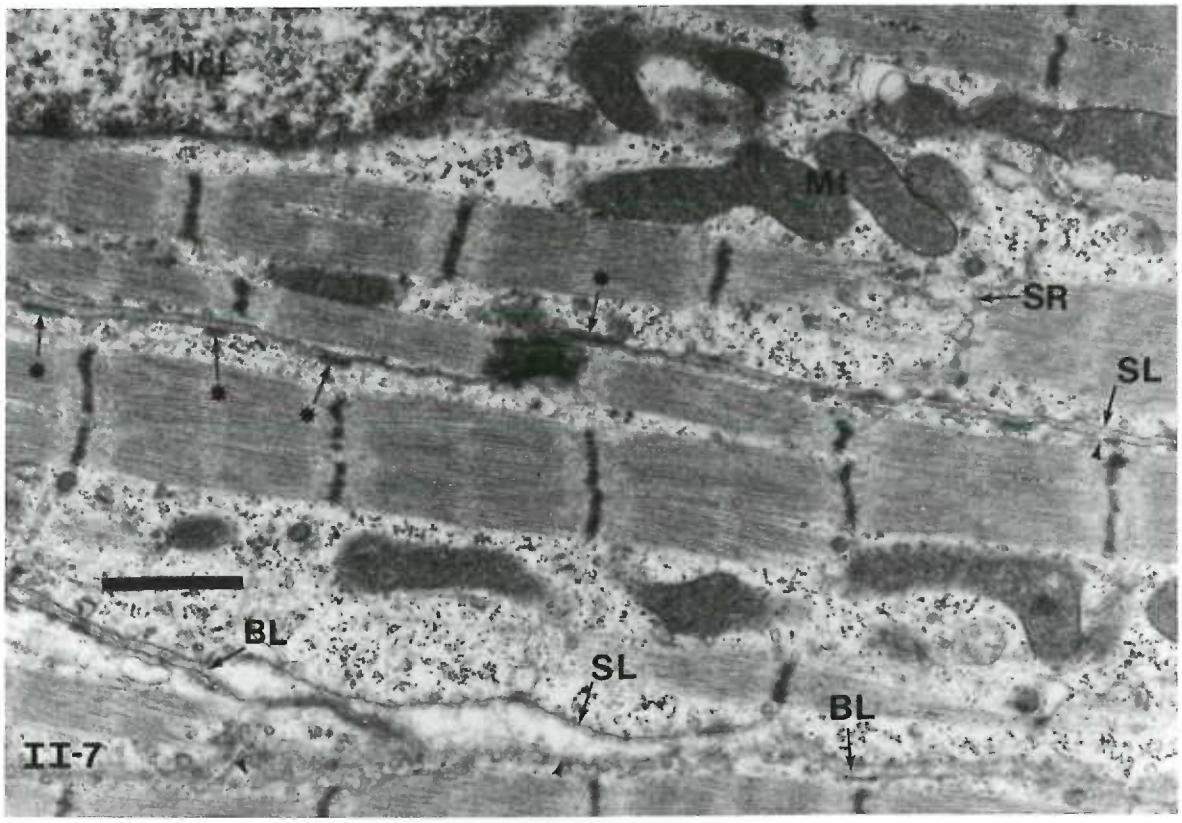
Mf
SR
SL
BL
SL
BL
II-7

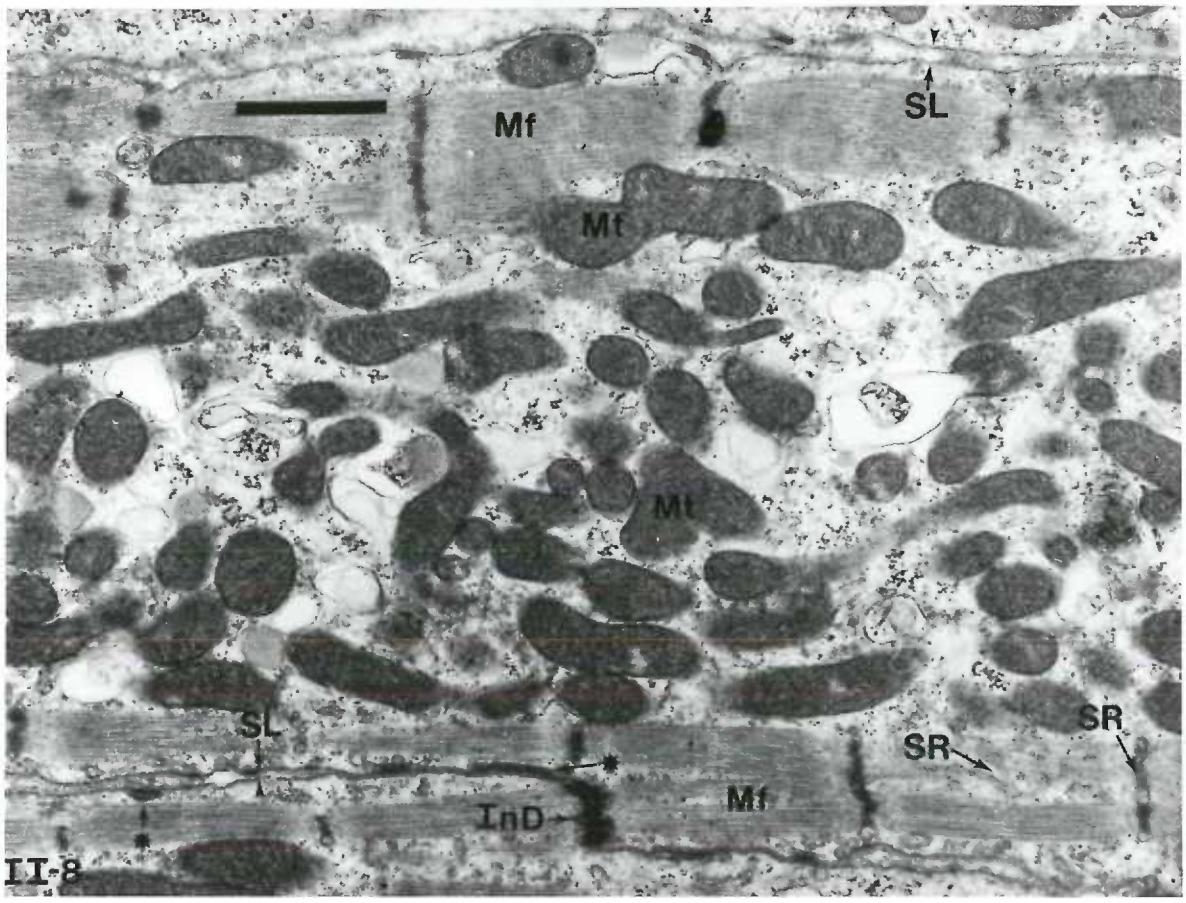
SL
Mf
Mf
Mf
SL
SR
SR
InD
Mf
II-8

III. AN EXAMINATION OF POST-EXTRASYSTOLIC AND FREQUENCY POTENTIATION IN THE HEARTS OF NEONATAL AND ADULT CATS

Introduction

When a quiescent myocardium of either frog or mammal is made to contract at regular intervals by external stimulation , one observes that the first beat is relatively weak and that subsequent beats become stronger until a steady state is reached. However, the force-frequency relationships in the frog and mammalian heart are different from each other. Bowditch (1871) discovered the tension staircase resulting from an increased stimulation rate in the frog heart. An increased stimulation rate in the mammalian heart also produces a tension staircase (McWilliam, 1888). However, an increase in the stimulation rate in the mammalian heart results in an initial rapid increase in peak tension for 10 to 20 beats followed by a slow increase in peak tension for the next 100 beats (Page et al., 1976) whereas an increased stimulation rate in the frog heart produces only a slow rise in peak tension for about 100 beats (Chapman and Niedergerke, 1970).

Woodworth (1902) showed in the mammalian heart that an early extrasystole* results in potentiation of the following beat. But the frog heart lacks post-extrasystolic potentiation (Edmands, Greenspan and Fisch, 1968). Potentiation in the mammalian heart following an early extrasystole or a temporary increase in stimulation

* In this paper an extrasystole refers to a beat due to the application of an extra stimulus between two beats in a train of regular stimuli. Cardiologists define an extrasystole as an ectopic beat, dependent upon and coupled to the preceding beat (Marriott, 1972).

rate decays back to control tension in 8 to 10 beats with identical beat dependent kinetics (Wood, Heppner and Weidmann, 1969).

Ultrastructurally the frog heart lacks T-tubules and has only a loose network of fine tubules for SR (Page and Niedergerke, 1972). The adult mammalian heart has large T-tubules and an abundant SR (Fawcett and McNutt, 1969). The plexiform SR of the mammalian heart forms specialized contacts, saccules or cisternae, with the T-tubules and the peripheral sarcolemma.

The lack of both post-extrasystolic potentiation and the fast component of the frequency staircase in the frog heart suggests a functional role for the T-tubules and the increased organization of the SR in the mammalian heart. The neonatal kitten heart lacks T-tubules and the SR is not as abundant as in the hearts of adult cats. In this section, I will show that the function of the neonatal cat heart is intermediate between the frog heart and the adult mammalian heart. Data on post-extrasystolic potentiation, rate staircase, and decay of potentiation in beating and non-beating neonatal and adult cat hearts will be presented.

Methods

Preparation, muscle chamber and mounting of preparation.

Neonatal and adult cats were anesthetized with ether or halothane. The thorax was opened and the heart quickly excised and placed in cold Tyrode solution oxygenated with 98% O_2, 2% CO_2. The right ventricle was opened and a 5-0 silk thread was tied

around the chorda tendineae of a papillary muscle, 0.5 to 0.9 mm in diameter and 2 to 4 mm in length. The muscle was carefully dissected away from the wall of the right ventricle. A stub of wall was left attached to the papillary muscle which was transferred to a chamber perfused with oxygenated (98% O_2 and 2% CO_2) Tyrode solution at 37°C.

The chamber was made out of plexiglass^R and lexan^R (figure III-1). A 3 mm longitudinal groove was milled in a plexiglass block. The block was transversely cut into two blocks and a 0.5 mm lexan wall was glued onto one end of one of the blocks. A 1 mm diameter hole was drilled through the center of the lexan wall. The other block was hollowed out around the groove and sealed so that water from a thermostatically controlled tank could be circulated to control the temperature of the block. The two blocks were held together on an optical bench.

The silk thread and tendinous end of the papillary muscle were pulled through the hole of the lexan wall until the stub of the papillary muscle wedged in the hole which fixed that end of the muscle. The silk thread was attached to a force transducer mounted on a micrometer and the muscle was slightly stretched. A rectangular current pulse of 1 to 5 ms duration was applied between two silver-silver chloride electrodes, one located next to the stub of the papillary muscle and the other bent in the form of a half cylinder that surrounded the tendinous end of the papillary muscle. The stimulus current was adjusted to 1.5 times that necessary to initiate tension at a basal stimulation interval of 3.2 sec. An

Figure III-1. Transverse view of the tissue chamber from the top. The solutions were supplied to the chamber with thin polyethylene tubing and withdrawn by cotton wicks.

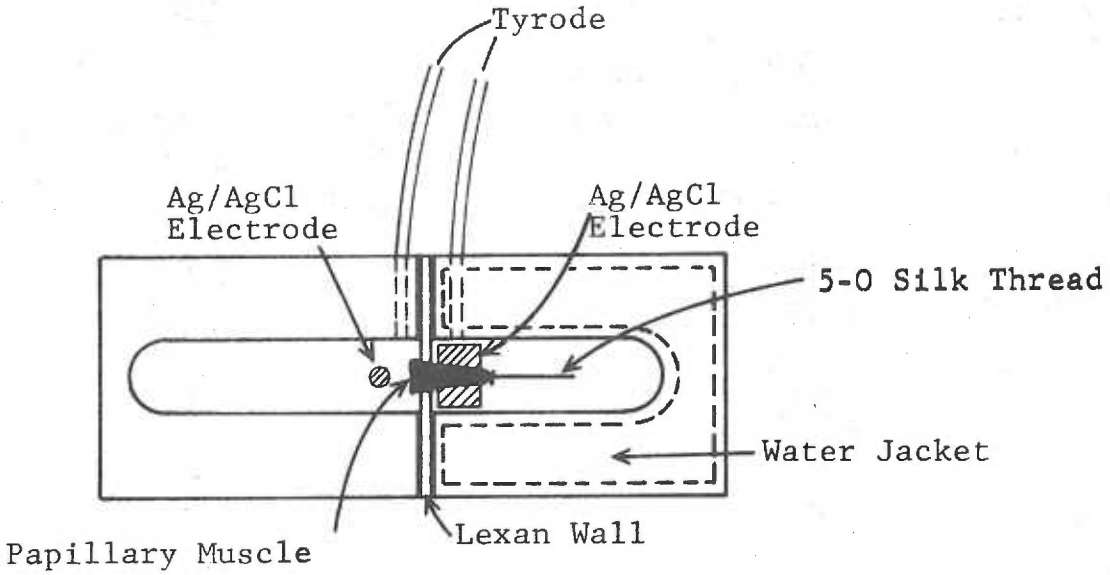
Tyrode
Ag/AgCl
Electrode
Ag/AgCl
Electrode
5-0 Silk Thread
Water Jacket
Lexan Wall
Papillary Muscle

initial period of 30 to 60 min was allowed for recovery from the damage sustained during dissection and handling before the experiment was started.

Tension transducer.

The force transducer used was a Grass FT03 strain gauge transducer. The strain gauges of the transducer formed the four arms of a Wheatstone bridge and the output voltage was amplified by means of an instrumentation amplifier (Analog device). The tension signal output of the instrumentation amplifier was displayed on a Tektronix 5103 storage oscilloscope and photographed with a Polaroid camera. The tension signal was also recorded on paper by a Grass polygraph. The tension transducer and amplifier were calibrated so 50 mV output (amplifier output) equalled 100 mg. The tension transducer had a natural frequency of 65 Hz with a compliance of 8 mg/μ. The voltage output was linearly related to force from 5 mg up to 10 gm. The voltage output was filtered by a constant time delay filter with the upper cutoff frequency set at 10 Hz. All frequencies below 10 Hz had a constant time delay of 40 ms.

Stimulation.

Tektronix 160 series pulse generators were used to produce a series of pulses of adjustable duration, magnitude and frequency. Flip-flop and analog switches were used to gate the pulses. This arrangement made it possible to switch frequencies from high to low or vice versa. It also permitted the insertion of an extrasystole

in a normal train of pulses and the administration of a test stimulus with a variable interval after the extrasystole.

Solutions.

The bath solution had the following composition (mM): NaCl, 137; KCl, 3; $NaHCO_3$, 12; $MgCl_2$, 1; NaH_2PO_4, 0.4; Glucose, 5. The concentration of $CaCl_2$ was either 1.8 or 3.6 mM. The solution was equilibrated with 98% O_2 and 2% CO_2. The pH was 7.4. All chemicals were analytical reagents.

Results

1. Post-extrasystolic potentiation.

The muscle was stimulated at 19 beats/min. When contractility reached a steady state a single extra stimulus was applied closely after a normal contraction to generate an extrasystole. The contraction of the first regular stimulus following the extrasystole was potentiated* (post-extrasystolic potentiation). This potentiation varied depending upon the interval between the extra stimulus and the preceding regular stimulus and thus the interval was adjusted (between 300 and 500 ms) to produce maximum post-extrasystolic potentiation.

It became evident after only a few experiments that post-extrasystolic potentiation was much stronger in hearts of the adult

* Potentiation is defined as the increase in tension of the potentiated beat above control tension as a percent of control tension, $100 \cdot (T_p - T_{control})/T_{control}$.

cat than of the newborn kitten. Figure III-2 gives two typical examples and also includes the result obtained on a frog heart for the purpose of comparison. In the one frog studied post-extrasystolic potentiation ranged between 0 and 5%. Post-extrasystolic potentiation in the neonate (3.6 mM $CaCl_2$ and 19 beats/min) ranged between 27 and 64% with a mean of 38% ($\pm$3.6%, S.E. of mean, N=11) whereas post-extrasystolic potentiation in the adult under the same conditions ranged between 79 and 121% with a mean of 96% ($\pm$4.2%, S.E. of mean, N=11). Table III-1 summarizes the data from experiments performed in 3.6 and 1.8 mM $CaCl_2$ at a rate of 19 beats/min. Post-extrasystolic potentiation was significantly less in the neonatal than in the adult heart at both calcium concentrations ($P<<0.01$). However, potentiation decreased in the neonate ($P<0.025$) and increased in the adult ($P<0.05$) when the calcium concentration was lowered to 1.8 mM.

2. Frequency potentiation.

An increased rate of stimulation was associated with an increase in peak tension in both neonates and adults (frequency staircase) (figure III-3). The transient change in peak tension from one steady state to another following an increased stimulation rate was composed of two components in neonates and adults. With an increase in stimulation from 19 to 60 beats/min, peak tension rapidly increased for the first 5 to 8 beats followed by a slow rise in peak tension until a new steady state was reached some 50 to 100 beats later (figure III-3). The presence of the two components was more evident in the neonate than in the adult (figure III-3). The increase

Figure III-2. Post-extrasystolic potentiation in frog, neonatal cat and adult cat hearts. The vertical arrows mark the extrasystole. Post-extrasystolic potentiation is between 0 and 5% in the frog and no staircase is observed (stimulation rate = 30 beats/min). Post-extrasystolic potentiation is much greater in the adult than in the neonatal cat but both show a descending staircase as peak tension decays back to the control tension (stimulation rate = 19 beats/min).

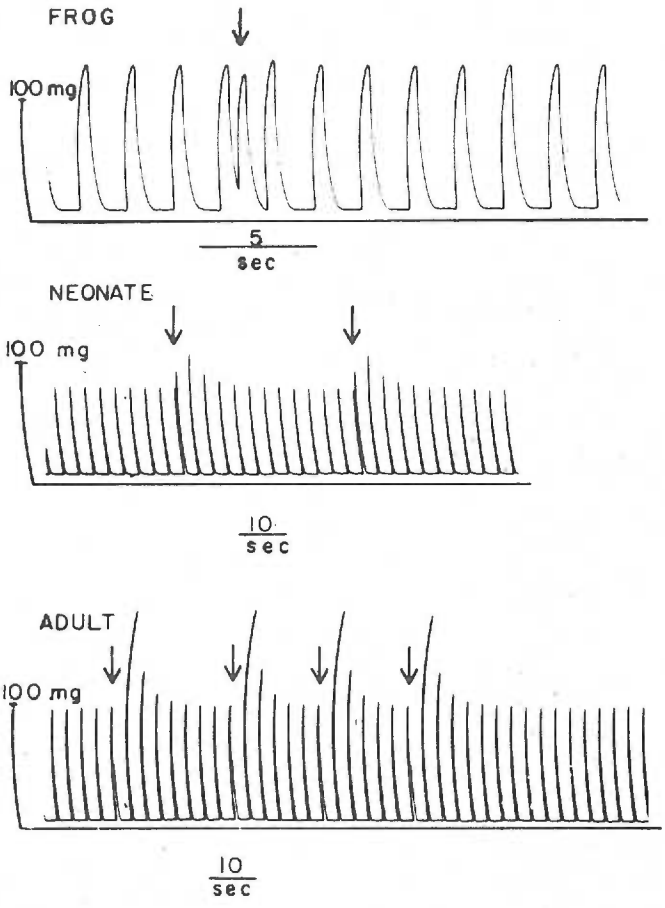
FROG
100 mg
5
sec
NEONATE
100 mg
10
sec
ADULT
100 mg
10
sec

TABLE III-1

Post-extrasystolic potentiation (%) in the adult and neonatal cat (mean ± S.E. of mean, N=number of experiments). Stimulation rate is 19 beats/min.

External calcium concentration (mM)	Neonate %	Adult %
3.6	+38 ± 3.6 (N=11)	+96 ± 4 (N=11)
1.8	+19 ± 5 (N=3)	+128 ± 19 (N=4)

Figure III-3. Ascending frequency staircase in neonatal and adult cat hearts. Rate increase is from 19 to 60 beats/min. Peak tension increases rapidly for 6 to 8 beats followed by a slow increase to a steady state peak tension at 60 beats/min. The slow increase in peak tension in the neonate makes a relatively greater contribution to the potentiation than in the adult.

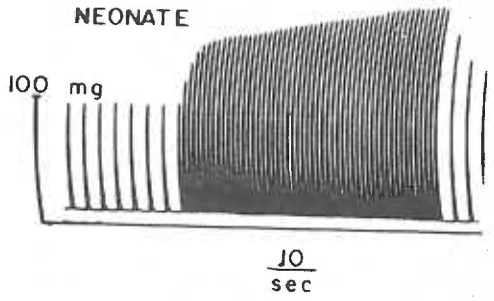
NEONATE
100 mg
10
sec

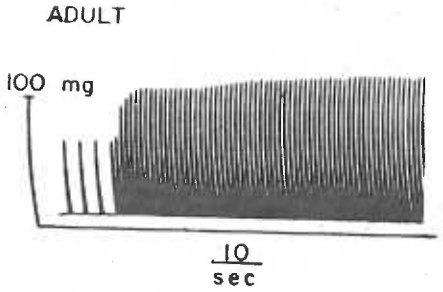
ADULT
100 mg
10
sec

in peak tension associated with the fast and slow component as a percent of the total potentiation is summarized in table III-2. The increase in peak tension associated with the fast component was taken as the difference between the extrapolation of the slow rise in tension of the slow component to zero time and the control tension at zero time. Zero time is the beginning of the frequency staircase. The fast component of a frequency staircase in the neonate produced only 50% of the total potentiation in comparison to 95% in the adult.

3. Post-extrasystolic potentiation superimposed on a frequency staircase.

That the rate inotropism consists of a fast and a slow component is also demonstrated in figure III-4. An extrasystole was generated during the fast and slow components of a frequency staircase. In neonatal and adult hearts the beat after an extrasystole generated during the slow component was potentiated but the potentiated state decayed back to the envelope of peak tension that would have existed had no extrasystole been generated. The slow component of the frequency staircase was not affected by the extrasystole suggesting independence between the fast and the slow components. I observed this phenomenon in all 8 neonatal and 5 adult cat hearts in which the experiment was tried.

4. Beat dependent kinetics.

As demonstrated in figure III-2 the first beat following an extrasystole in the adult was markedly potentiated. This potentiated state decayed over the next 6 to 8 beats. Similarly, following a

TABLE III-2

Potentiation by the fast and slow components as a percent of final potentiation in a frequency staircase (mean ± S.E. of mean)

	Neonate (N=9)	Adult (N=13)
Fast	50.1% ± 4	94.7% ± 3
Slow	49.9% ± 4	5.3% ± 3

Figure III-4. Early extrasystoles applied during a frequency staircase in a neonatal and adult cat heart. Rate increase is from 19 to 60 beats/min. Arrows mark the extrasystole. It is noteworthy that in the neonate tension, after the first extrasystole, declines even though post-extrasystolic potentiation is well below the ultimate frequency potentiation.

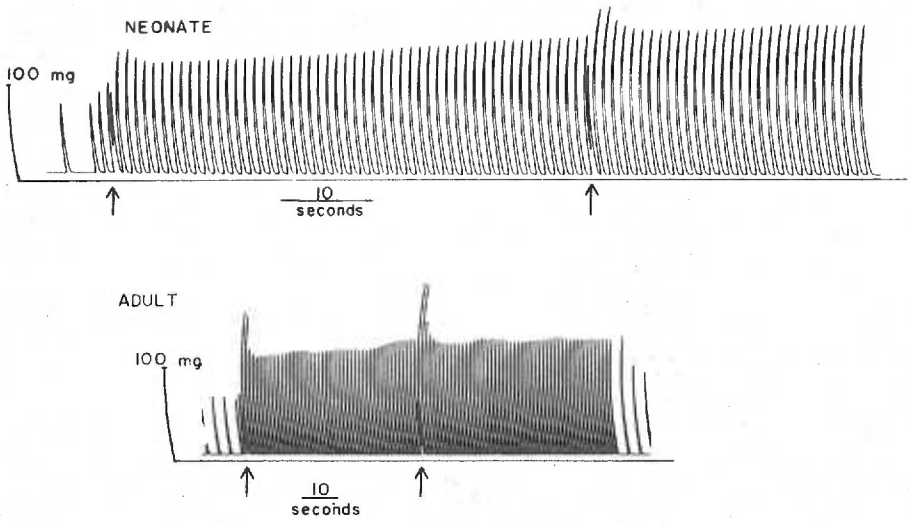
NEONATE
100 mg
10
seconds
ADULT
100 mg
10
seconds

decrease in stimulation rate from 60 to 19 cpm, peak tension decayed quickly for 6 to 8 beats and decayed at a slower rate over the next 50 beats. Thus following an inotropic procedure a fraction of the potentiated state decayed with each beat until steady state tension was reached. A plot of the natural logarithm (ln) of the tension above control levels as a percent of maximum increase (percent potentiation) versus the beat number following an inotropic procedure is shown in figure III-5. This figure illustrates that the percent potentiation decays as a single exponential indicating that the fractional decay per beat is a constant, which was also observed by Morad and Goldman (1973). This procedure was carried out for data obtained from 8 neonatal and 5 adult cats. A regression line was fitted by a least squares method to the ln of the percent potentiation versus the beat number following the inotropic stimulus. The slope of the regression line represents the exponential beat constant which is the same as the fractional decay rate per beat, figure III-6. Table III-3 lists the exponential beat constants and their standard errors obtained for the decay of potentiation following either an extrasystole or a decreased rate from 60 to 19 beats/min. The four beat constants in table III-3 are not significantly different from each other ($0.4 \leq P \leq 0.2$). This suggests that mechanisms with identical kinetics are involved in both the fast component of the frequency staircase and decay of post-extrasystolic potentiation in both the neonate and the adult.

Figure III-5. The ln of post-extrasystolic potentiation as a percent of maximum potentiation in a neonatal cat heart is plotted on the ordinate versus the beat number following the extrasystole on the abscissa. The solid line is a least squares fit to the experimental points (+). Stimulation rate is 19 beats/min.

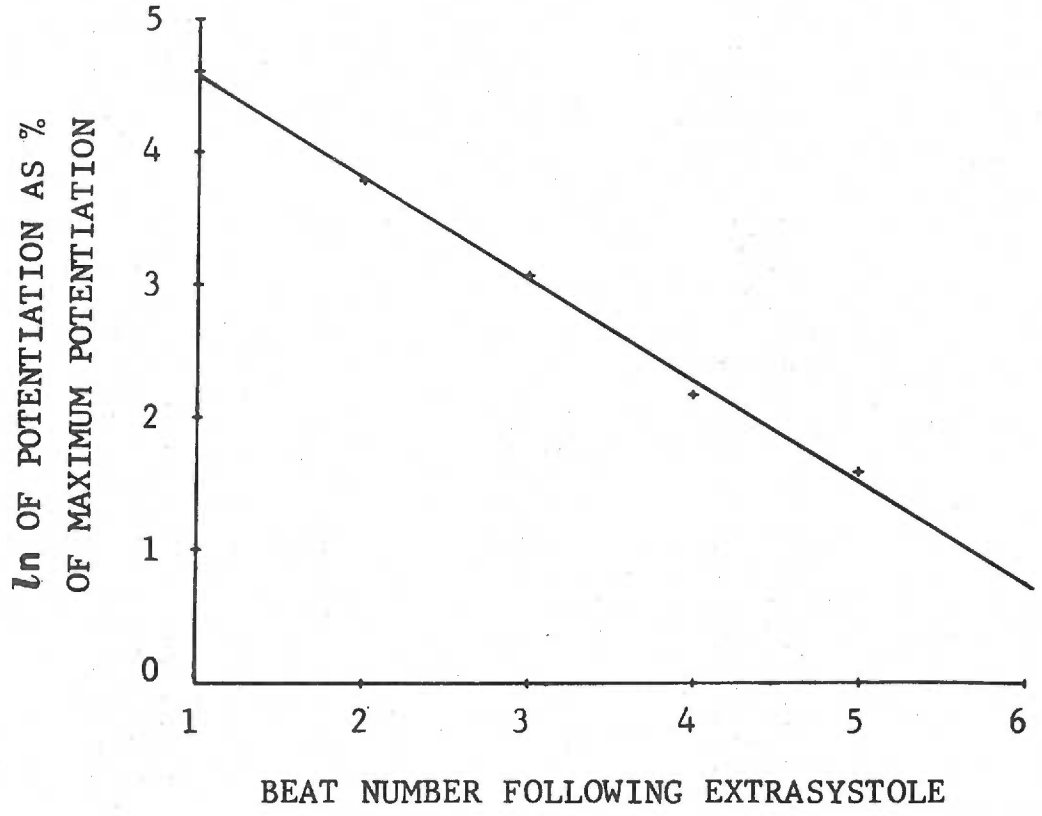
ln OF POTENTIATION AS %
OF MAXIMUM POTENTIATION
5
4
3
2
1
0
1
2
3
4
5
6
BEAT NUMBER FOLLOWING EXTRASYSTOLE

Figure III-6. Beat dependent decay of potentiation after an extrasystole or a temporary increase in stimulation rate from 19 to 60 beats/min in the neonatal and adult cat hearts. Potentiation as a percent of maximum potentiation is plotted on the ordinate versus the beat number following the inotropic procedure on the abscissa. Regression analysis was performed on the ln of the percent potentiation versus the beat number. The fast component of the frequency staircase was obtained by subtracting the extrapolated decrease of peak tension due to the slow component from the total decrease in peak tension, a procedure similar to the one used in figure III-3. This correction was small. The solid curve represents an exponential least squares fit to the experimental points (+). The dotted curves are the 95% confidence limits of the means. The exponential beat constants and the standard errors are listed in table III-3.

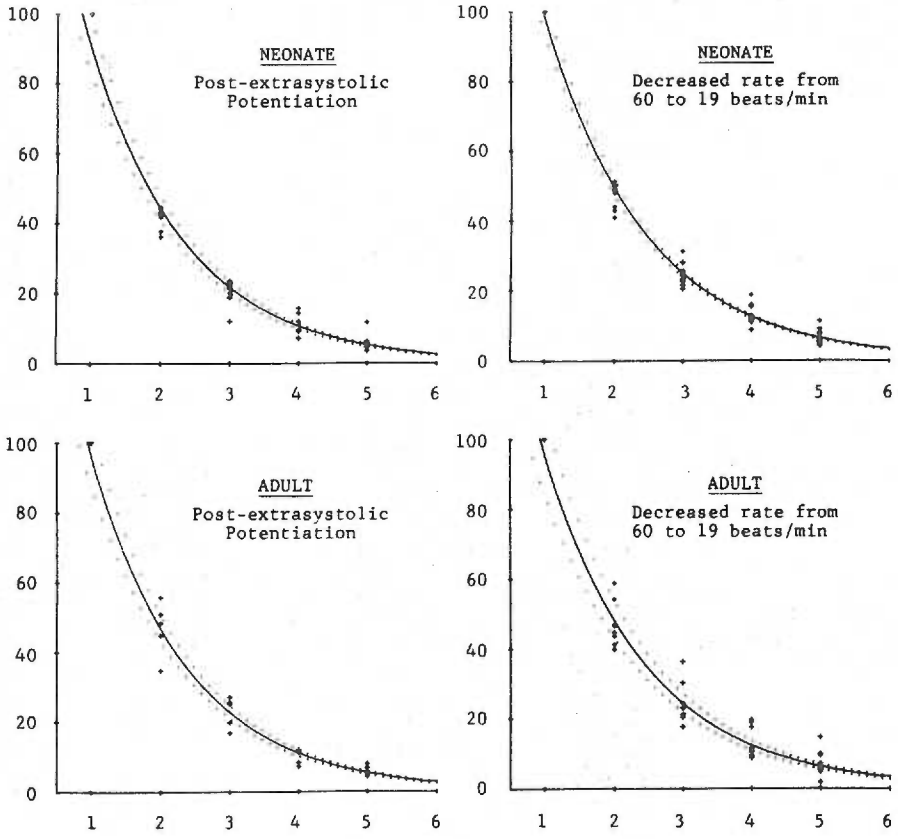
NEONATE
Post-extrasystolic
Potentiation
NEONATE
Decreased rate from
60 to 19 beats/min
ADULT
Post-extrasystolic
Potentiation
ADULT
Decreased rate from
60 to 19 beats/min
100
80
60
40
20
0
1
2
3
4
5
6

TABLE III-3

Exponential beat constant for decay of potentiation (beat number^{-1} ± S.E., N=number of experiments, and r=correlation coefficient)

Inotropic procedure	Neonate	Adult
Post-extrasystolic potentiation	-0.715 ± 0.026 (N=8, r=0.99)	-0.725 ± 0.027 (N=5, r=0.99)
Frequency staircase 60 to 19 beats/min	-0.686 ± 0.016 (N=10, r=0.99)	-0.685 ± 0.037 (N=8, r=0.97)

5. Decay of potentiated state in non-stimulated preparations.

A test stimulus was applied after increasing periods of rest following a regular train of contractions. Figure III-7 shows the results of an experiment on a 2 day neonate. Plotted is the peak tension of the test contraction as a percent of the preceding control contraction versus the rest interval. As the rest interval was increased from 0.25 sec, peak tension of the test contraction increased up to a maximum at about 0.4 sec (figure III-7A). For intervals longer than 0.4 sec peak tensions decayed towards a steady state level, the "rested state tension" (figure III-7B). The term rested state tension defines the state of contractility when the rest interval is long enough that peak tension of the test stimulus is not affected by the previous contractions (Blinks and Koch-Weser, 1961). A least squares procedure (curve peeling with linear regression analysis) was used to fit a sum of two exponentials to the buildup and decay of peak tension as a function of the rest interval. The solid curves in figure III-7 represent such a fit. The time constants for the buildup and decay of peak tension were not significantly affected (as determined by paired t test) by the extracellular calcium concentration ($0.4 \leq \underline{P} \leq 0.2$), stimulation rate ($1.0 \leq \underline{P} \leq 0.5$), or whether an extrasystole was generated before the test stimulus or not ($1.0 \leq \underline{P} \leq 0.5$) and thus the data were pooled. The time constants of the buildup and decay of peak tension are listed in table III-4. In the adult the buildup and decay of peak tension following a control beat was slower than in the neonate (figure III-8). Maximum peak

TABLE III-4

Time constant (sec) of the build up and decay of peak tension (mean ± S.E. of mean, N=number of experiments).

Phase	Neonate	Adult
Buildup	0.046 ± 0.004 (N=16)	0.272 ± 0.022 (N=12)
Decay	28.6 ± 2 (N=13)	68.0 ± 13.1 (N=10)

Figure III-7. Time course of peak tension following a control beat in a 2 day neonate at 60 beats/min. Peak tension of the test contraction as a percent of the preceding control contraction is plotted on the ordinate versus the rest interval (sec) between the control beat and test stimulus on the abscissa. Note difference between the time scales of the upper (A) and lower (B) graphs. Experimental points are denoted by pluses (+). The curve drawn from a least squares fit of a sum of two exponentials plus a constant is

$$T_{test}/T_{control} = -626.3e^{-27.2t} + 0.9e^{-0.054t} + 0.15$$

in which $T_{test}/T_{control}$ is the ratio of peak tension of test stimulus to control beat and 't' the rest interval (sec). The first exponential represents the buildup of peak tension (A) and the second the decay of peak tension (B). This equation is not valid for $T_{test}/T_{control} < 0$.

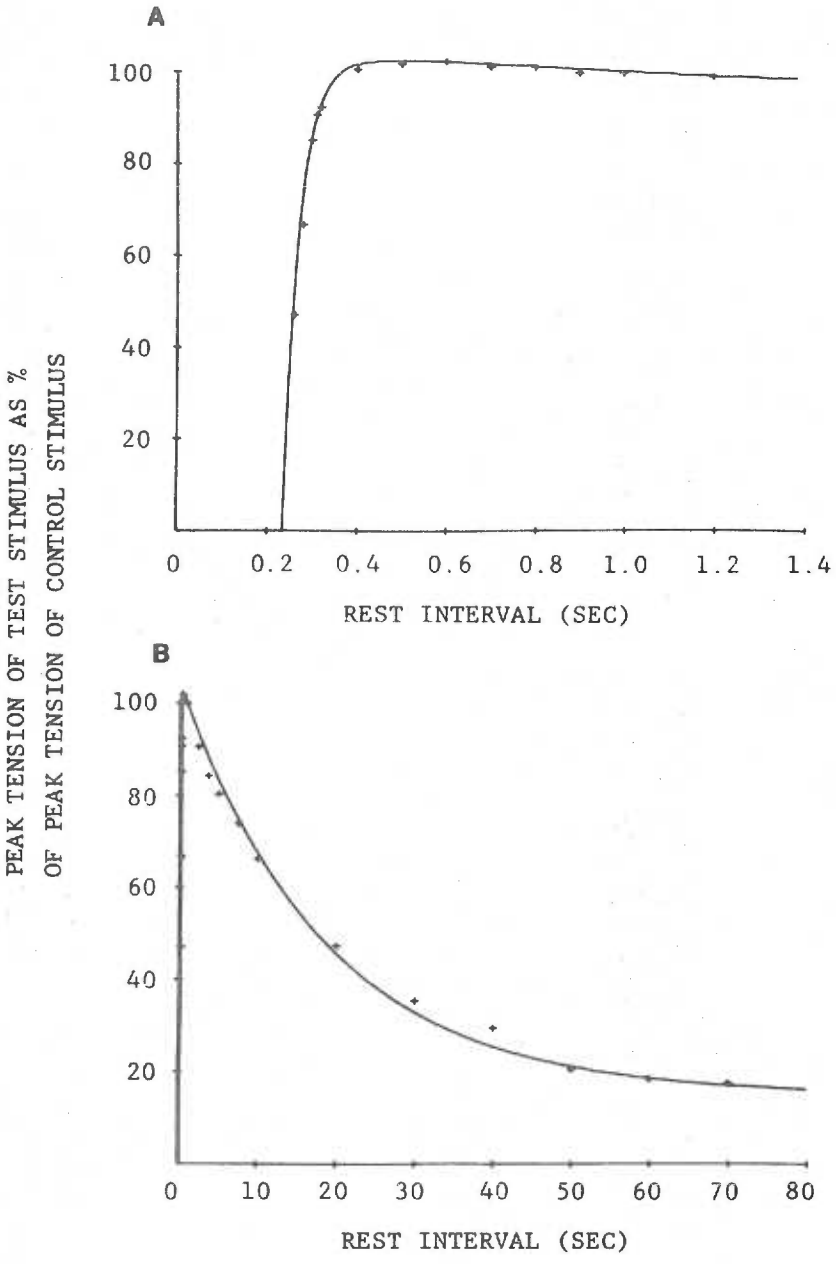
A
100
80
60
40
20
0
0.2
0.4
0.6
0.8
1.0
1.2
1.4
REST INTERVAL (SEC)
B
100
80
60
40
20
0
10
20
30
40
50
60
70
80
REST INTERVAL (SEC)
PEAK TENSION OF TEST STIMULUS AS %
OF PEAK TENSION OF CONTROL STIMULUS

Figure III-8. Time course of peak tension following a control beat in an adult cat at 19 beats/min. Peak tension of the test contraction as a percent of the preceding control contraction is plotted on the ordinate versus the rest interval (sec) between the control beat and test stimulus on the abscissa. Note the difference between the time scales of the upper (A) and lower (B) graphs. Experimental points are denoted by pluses (+). The curve drawn from a least squares fit of a sum of two exponentials plus a constant is

$$T_{test}/T_{control} = -1.64e^{-2.856t} + 0.9e^{-0.0159t} + 0.15$$

in which $T_{test}/T_{control}$ is the ratio of peak tension of the test stimulus to control beat and 't' the rest interval (sec). The first exponential represents the buildup of peak tension (A) and the second the decay of peak tension (B). This equation is not valid for $T_{test}/T_{control} < 0$.

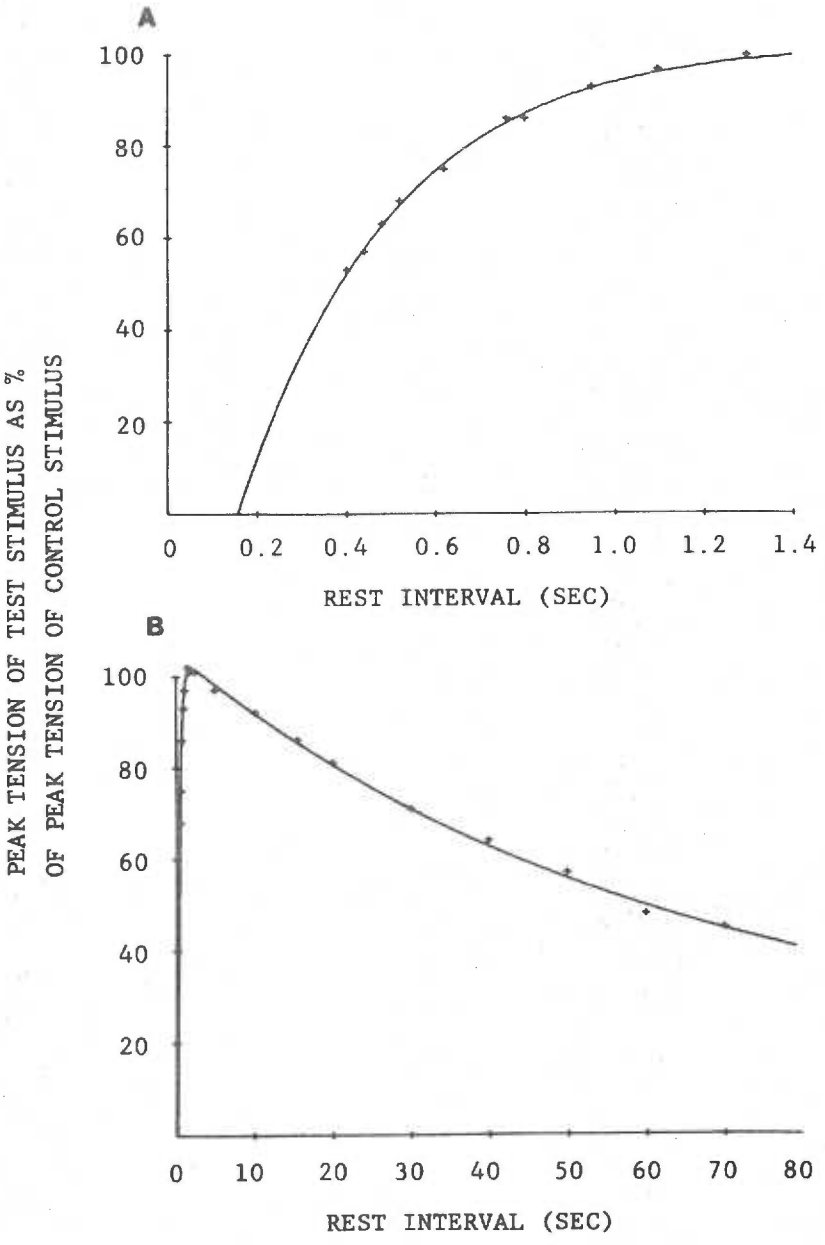
A
100
80
60
40
20
0
0.2
0.4
0.6
0.8
1.0
1.2
1.4
REST INTERVAL (SEC)
B
100
80
60
40
20
0
10
20
30
40
50
60
70
80
REST INTERVAL (SEC)
PEAK TENSION OF TEST STIMULUS AS %
OF PEAK TENSION OF CONTROL STIMULUS

tension was achieved between 1 and 1.5 sec (figure III-8A) and a rested state contraction occurred only at intervals longer than 4 min. As in the neonate the time constants were not significantly affected (as determined by paired t test) by the external calcium concentration ($0.2 \leq \underline{P} \leq 0.1$), stimulation rate ($1.0 \leq \underline{P} \leq 0.5$), or the presence or absence of an extrasystole ($0.5 \leq \underline{P} \leq 0.4$) and thus the data were pooled. The time constants of the buildup and decay of peak tension are listed in table III-4. The differences between the neonate and the adult time constants are significant ($\underline{P} < 0.01$).

Discussion

A current model for excitation-contraction coupling is based on the presumed existence of an internal compartment for the release, sequestration and storage of calcium (Morad and Goldman, 1973; Bassingthwaighte and Reuter, 1972). According to this model the action potential triggers a release of calcium stored in the lateral sacs of the SR cisternae (Morad and Goldman, 1973). During relaxation and diastole the sarcolemma and longitudinal components of the SR sequester myoplasmic calcium to return and maintain the myoplasmic calcium concentration below activation levels, 10^{-7}M (Winegrad, 1971). A part of the fraction of the calcium sequestered by the longitudinal SR is transferred to the SR cisternae where it becomes available for release again. The fraction of calcium sequestered by the sarcolemma is extruded from the cell.

Post-extrasystolic potentiation is 2 to 3 times greater in the adult than in the neonatal cat heart. Post-extrasystolic

potentiation decays exponentially with identical beat constants in the neonate and adult. About 50% of the remaining potentiation is lost with each beat. Thus the neonate is capable of storing a fraction of the sequestered calcium. That the fractional depletion of the store per beat is the same for both neonate and adult is compatible with the argument that the kinetics of the SR are not affected by age and that only the amount of SR per cell or its capacity for calcium are affected by age. This argument is consistent with the relatively smaller amounts of SR in the neonatal heart. Post-extrasystolic potentiation in the frog heart ranges between 0 and 5% above control tension and no staircase is observed. Thus the frog heart is not capable of storing calcium from an extrasystole. This suggests that the loose network of SR in the frog does not store and release calcium during an action potential.

The negative tension staircase associated with a decrease in stimulation rate occurs with two time components in the neonatal and adult cat heart. The fast time component of a frequency staircase (first 6 to 8 beats) has similar beat dependent kinetics as the decay of post-extrasystolic potentiation suggesting the same mechanism mediates both inotropic effects. The slow component (50 to 100 beats) of a frequency staircase is independent from the fast component and more predominant in the neonate. The proportion of potentiation due to the slow component is greater in the neonate than in the adult.

One possible explanation of the slow component of the frequency staircase is the effect of the increased stimulation rate on the myoplasmic sodium concentration. If the transfer of calcium ions

across the sarcolemma is modulated by the sodium concentration gradient as proposed by Reuter (1974) and Langer (1974), then an increase in the stimulation rate will increase the myoplasmic sodium concentration and thus affect the flux of calcium ions across the sarcolemma. A change in the myoplasmic sodium concentration will also influence the rate of the Na-K pump which may take some time to reach a new steady state (sodium-pump lag hypothesis of Langer, 1974). Thus in the neonatal cat and frog heart in which the majority of the myofibrils are adjacent to the sarcolemma, this argument may be of greater importance than in the adult in which only a small portion of myofibrils are adjacent to the sarcolemma.

The rate of recovery of contraction from a previous beat is about 6 times faster in the neonate (time constant = 46 ms) than in the adult (time constant = 272 ms). About 0.4 sec from the beginning of the previous beat is required for complete recovery of contraction in the neonate compared to 1 to 1.5 sec in the adult. Gettes and Reuter (1974) observed a time constant of recovery of the action potential plateau in guinea-pig and sheep hearts of about 45 ms. Analyses of the time constant of recovery of contraction were not included. Bass (1975 a, b) observed in adult cat papillary muscles that the recovery of contraction between 0.9 and 1.5 sec after a previous beat was independent of the recovery of the action potential. It is tempting to suggest the time constant for the recovery of contraction in the adult heart represents time taken for the transfer of calcium from the sequestration site to the storage and release site and is independent of changes in the action potential. The

smaller time constant of recovery of contraction in the neonatal cat heart suggests that either recirculation of internal calcium is faster in the neonate than in the adult or recirculation of calcium makes a relatively much smaller contribution. Thus the recovery of contraction may depend on the recovery of the ability to generate an action potential with a good plateau in the neonate. More information concerning the recovery of both contraction and action potential generation is needed to profitably speculate on the mechanism controlling the recovery of contraction in the neonate and adult cat heart.

For long periods of rest following a previous beat peak tension decays about two times faster in the neonate (time constant = 29 sec) than in the adult (time constant = 68 sec). Edman and Johannson (1976) reported a similar decay time constant (62 sec) in adult rabbit papillary muscle. The decay of contraction may represent a loss of calcium from an internal releasable store. The faster decay of peak tension in the neonate may be explained by assuming that a greater portion of internally stored calcium is closer to the sarcolemma and thus will exchange faster with external sodium (Glitsch, Reuter and Scholz, 1970). But a slight decrease in the action potential area has been observed with a reduction in stimulation rate from 30 to 6 beats/min in rabbit papillary muscle (Gibbs, Johnson and Tille, 1963). Thus a decrease in action potential plateau may be responsible for part of the decay in peak tension following a long rest period.

IV. MEMBRANE CONTROL OF CONTRACTILITY

Introduction

A recent review by Morad and Goldman (1973) compared the excitation-contraction (E-C) coupling mechanisms of the frog and mammalian heart. The direct control of contractility by the membrane potential (Morad and Orkand, 1971) correlated with the loose tubular structure of the sarcoplasmic reticulum (SR) and absence of T-tubules in the frog heart (Page and Niedergerke, 1972). Morad and Goldman (1973) suggested that activator calcium was derived from the surface membrane to account for the dependency of contractility on the duration or magnitude of depolarization in the frog myocardium. Consistent with this hypothesis was the observation that the frog heart lacks a tension staircase in response to successive voltage clamp depolarizations or paired pulse stimulation (Antoni, Jacob and Kaufmann, 1969; Edmands et al., 1968).

By contrast, the mammalian heart develops a phasic tension followed by a tonic tension with long (2 sec) step depolarizations (Morad and Goldman, 1973). The tonic tension appears to be functionally dependent on the surface membrane as in the frog heart. However, the phasic tension appears to have developed as an outcome of the increased organization of the SR and the formation of T-tubules in the mammalian heart. With successive voltage clamp depolarizations or paired pulse stimulation, contractility increases for 6 to 8 beats in the mammalian heart.

The above differences between the frog and mammalian heart

support a hypothesis that the SR recycles a releasable quantity of activator calcium. This section reports the membrane control of contractility as studied by means of the single sucrose gap technique in right ventricular papillary muscles from neonatal and adult cats.

Methods

Preparation, muscle chamber and mounting of preparation.

Right ventricular papillary muscles from neonatal and adult cats were excised and mounted in the tissue chamber (figure IV-1) as described in Section III. A modification of the tissue chamber was made to form a sucrose gap. The lexan wall on the tissue chamber was used to form one end of the middle compartment. The other end of the middle compartment was formed by a rubber membrane (70 μ thick) which was attached to the ends of four arms that could be radially spread. A 0.4 mm hole was made in the center of the membrane by a heated copper needle. The diameter of the hole was varied by spreading the arms of the rubber stretcher. The rubber stretcher was mounted between the two blocks such that the center of the hole in the rubber membrane was aligned with the center of the two grooves and the lexan wall. A 1.5 mm thick disk with a 3 mm slot was mounted between the rubber membrane and the lexan wall to form the sucrose compartment.

The papillary muscle was pulled through the hole in the lexan wall and rubber membrane until the stub on the end of the muscle wedged in the hole of the lexan disk. The silk thread was attached

Figure IV-1. Modification of the tissue chamber used in Section III (figure III-1). A lexan disk and rubber membrane were inserted between the two end blocks of figure III-1 to form three compartments. See text for further explanation.

Figure IV-2. Diagram of the electronic system used for the simultaneous recording of tension, transmembrane potential (Vm), and transmembrane current (Im). Other abbreviations are: tension transducer (TT), feedback amplifier (Avc), current transducer amplifier (A), and microelectrode amplifier with a gain of 10 (E). See text for further explanation.

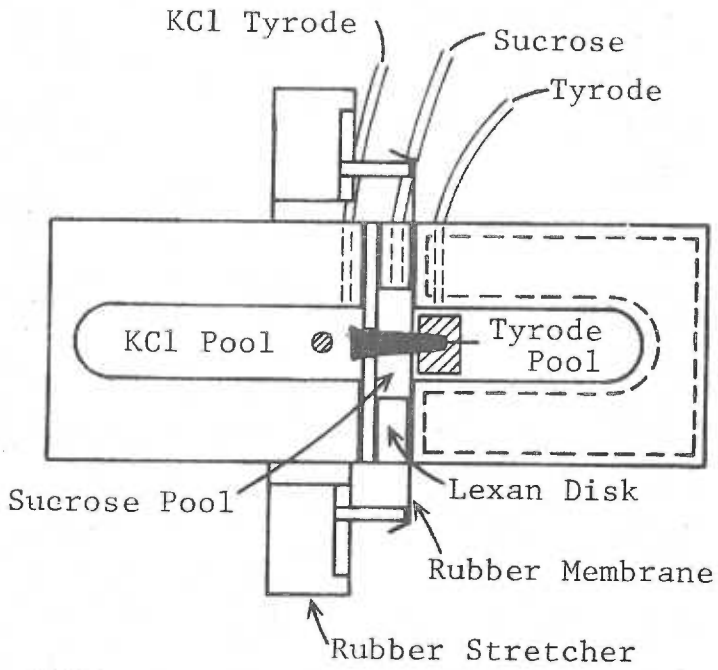
KCl Tyrode
Sucrose
Tyrode
KCl Pool
Tyrode
Pool
Sucrose Pool
Lexan Disk
Rubber Membrane
Rubber Stretcher

IV-1

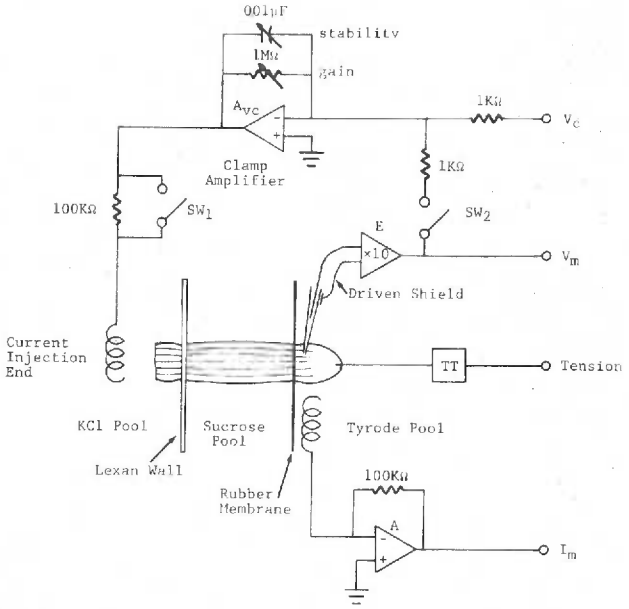
.001μF
stability
1MΩ
gain
A_{VC}
1KΩ
V_c
Clamp
Amplifier
1KΩ
100KΩ
SW_1
SW_2
E
×10
V_m
Driven Shield
Current
Injection
End
TT
Tension
KCl Pool
Sucrose
Pool
Tyrode Pool
Lexan Wall
Rubber
Membrane
100KΩ
A
I_m

IV-2

to a force-transducer (Section III) mounted on a micrometer. The muscle was slightly stretched until 0.4 to 0.6 mm of the muscle protruded through the rubber membrane. The rubber stretcher was released enough that the hole in the rubber membrane was reduced to fit the preparation snugly. The muscle was stimulated for 30 to 60 min as described in the Methods of Section III. Following recovery from damage sustained during dissection and handling, sucrose and KCl-Tyrode were perfused through the middle and left (current injection) compartments, respectively. Solutions ($37^{\circ}C$) were supplied to the compartments through thin polyethylene tubes. The effluent from the outside compartments were removed by cotton wicks and from the middle compartment by suction.

Solutions.

The compositions of the solutions are given in table IV-1. The Tyrode and KCl-Tyrode solutions were equilibrated with 98% O_2 and 2% CO_2. The pH was 7.4. The sucrose solution was made from analytical reagent sucrose and deionized distilled water. The osmolarity of the sucrose solution was 300 mosm as measured by freezing point depression (Advanced Osmometer). The sucrose solution was further deionized. $MnCl_2$ (0.01 mM/L final concentration) was added to the sucrose solution to prevent cell decoupling in the gap and thus maintain a low resistance intracellular pathway across the gap (New and Trautwein, 1972a). $MnCl_2$ was used instead of $CaCl_2$ to inhibit contractions in the gap region. The sucrose solution was equilibrated with 100% O_2.

TABLE IV-1

Composition of solutions (mM/L)

	NaCl	KCl	$MgCl_2$	$CaCl_2$	$NaHCO_3$	$NaHPO_4$	Glucose	Sucrose	$MnCl_2$
Tyrode	137	3	1	1.8 or 3.6	12	0.4	5	-	-
KCl-Tyrode	-	142	1	-	12	0.4	5	-	-
Sucrose	-	-	-	-	-	-	-	262	0.01

Experimental apparatus.

Figure IV-2 shows the electronic arrangement necessary to supply constant current or to control the membrane potential in the active end of the muscle. The silver-silver chloride electrode in the active side was held at ground potential by a high gain operational amplifier that measured the current through the sucrose gap (Im). The intracellular potential was lead off by a 3M-KCl filled glass microelectrode (15-30 MΩ resistance) and measured by an amplifier (E) that compensated for stray capacitance. A driven guard shield was used around the electrode and electrode cable to reduce shielding capacitance. The intracellular potential (Vm) was compared with the command signal (Vc) at the input of the clamp amplifier (Avc) which supplied the necessary current through the sucrose gap to clamp the intracellular potential. The clamp amplifier (Datel AM-302) had an output range of $\pm$140 V and $\pm$20 mA. The apparatus was a constant current amplifier when the two switches (SW_1 and SW_2) were open.

The intracellular potential (Vm), transgap current (Im) and tension signal were displayed on a Tektronix 5103 storage oscilloscope and photographed with a Polaroid camera. The signals were also recorded on paper by a Grass polygraph.

Criteria.

The segment of muscle in the sucrose compartment contracted vigorously in response to electrical stimulation when the sucrose was initially infused. Within ½ hour no visible contractions in the

sucrose compartment were observed. The segment in the KCl compartment was inactivated by the high KCl and no visible contractions were observed. The following criteria were met before continuation of the experiment:

1.) No visible contraction in the segment of the muscle in the sucrose compartment.

2.) Resting potentials of -70 to -90 mV, action potential duration 150 to 250 ms with a well maintained plateau in the active end (right compartment) of the muscle.

3.) Smooth current records during a voltage clamp with no sudden deflections.

Results

1. Electrical shortening of the action potential.

Repolarizing current pulses were injected through the sucrose gap at various times during the action potential plateau to prematurely terminate the action potential. Figure IV-3 shows three records of such an experiment on one adult papillary muscle. The left side of each record shows superimposed tracings of the control beat followed by 6 consecutive shortened beats. After the sixth shortened beat the beginning of the traces was shifted to the right to record the last steady state shortened beat followed by the first 6 beats of normal stimulation. The results are similar to those observed by Wood, Heppner and Weidmann (1969). Time to peak tension was reduced with the first shortened beat while the maximum rate of tension development

Figure IV-3. Premature termination of the action potential by repolarizing current injections in an adult right ventricular papillary muscle. Upper line of each record shows superimposed tracings of the membrane current during a normal and shortened action potential (inward current is an upward deflection in this figure). The left side of each record shows superimposed contractions associated with a control action potential (a) and with 6 to 8 shortened action potentials (b is the contraction of the first shortened action potential). The right side of each record shows the last contraction associated with the steady state shortened action potential (c) and the first 6 to 8 contractions of normal action potentials following those of the shortened action potentials (d is the contraction of the first normal action potential). Stimulation rate is 19 beats/min. The tension traces are delayed by 40 ms with respect to the current and voltage traces.

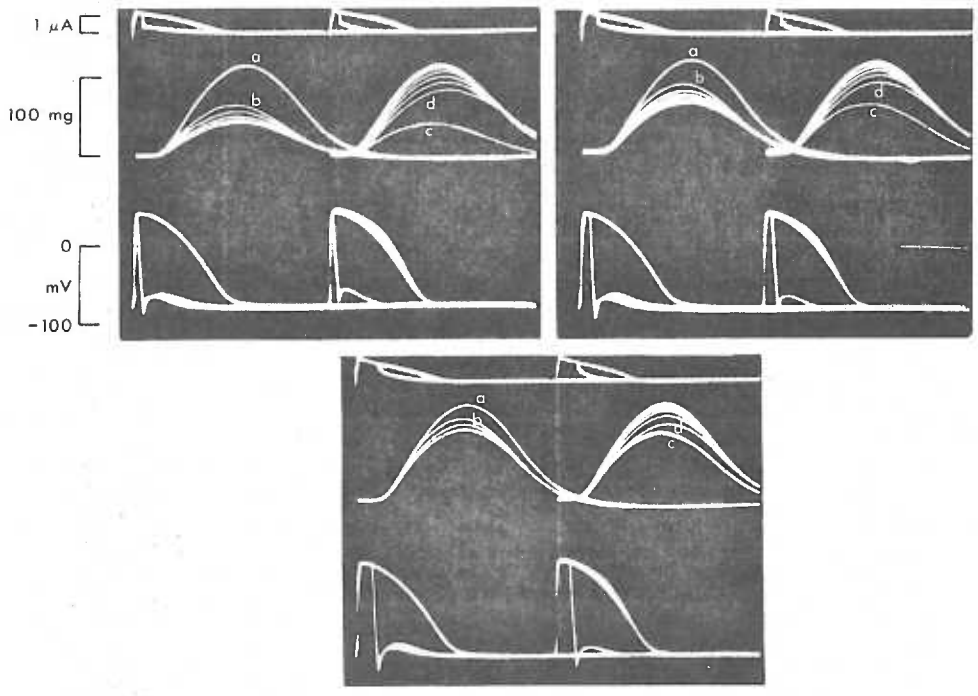
1 μA
100 mg
0
mV
-100
a
b
d
c
0.2 sec

(maximum derivative of tension=dT/dt_{max}) was unaffected, except for very short action potentials in which dT/dt_{max} was reduced on the first shortened beat. Subsequent shortened action potentials resulted in a continuous decrease in dT/dt_{max} while time to peak tension did not change further as peak tension continued to decline. Steady state tension was reached within 5 to 6 shortened action potentials. With the return to normal stimulation following the release of the repolarizing current pulses, tension gradually returned to control values within 5 to 6 beats (right side of figure IV-3). These results were also observed in 5 other adult cats on which the experiment was performed.

Figure IV-4 shows records of prematurely terminated action potentials in 4 neonatal cat hearts. Time to peak tension was reduced with the first shortened beat while dT/dt_{max} was unaffected, except in very short action potentials in which dT/dt_{max} was reduced on the first shortened beat. However, shortening of the action potential in neonatal cats for more than one beat consecutively was not associated with a prominent tension staircase as in the adult. The reduction in tension between the first and steady state shortened action potential was small if it existed at all. The contractions of the first 6 to 8 beats of normal stimulation following a series of shortened action potentials also was associated with only a negligible tension staircase (figure IV-4). These results were consistently observed in 8 neonatal cat hearts.

Figure IV-4. Premature termination of the action potential in right ventricular papillary muscles from 4 neonatal cats. The letters a, b, c, and d indicate the contractions of the control action potential, first shortened action potential, steady state shortened action potential and first normal action potential following the steady state shortened action potential (respectively). Upper two records show the action potentials (bottom trace) with the corresponding contractions (top trace). The lower records show the membrane currents (top trace, upward deflection is an inward current) and contractions (bottom trace). The stimulation rate is 19 beats/min. The tension traces are delayed by 40 ms.

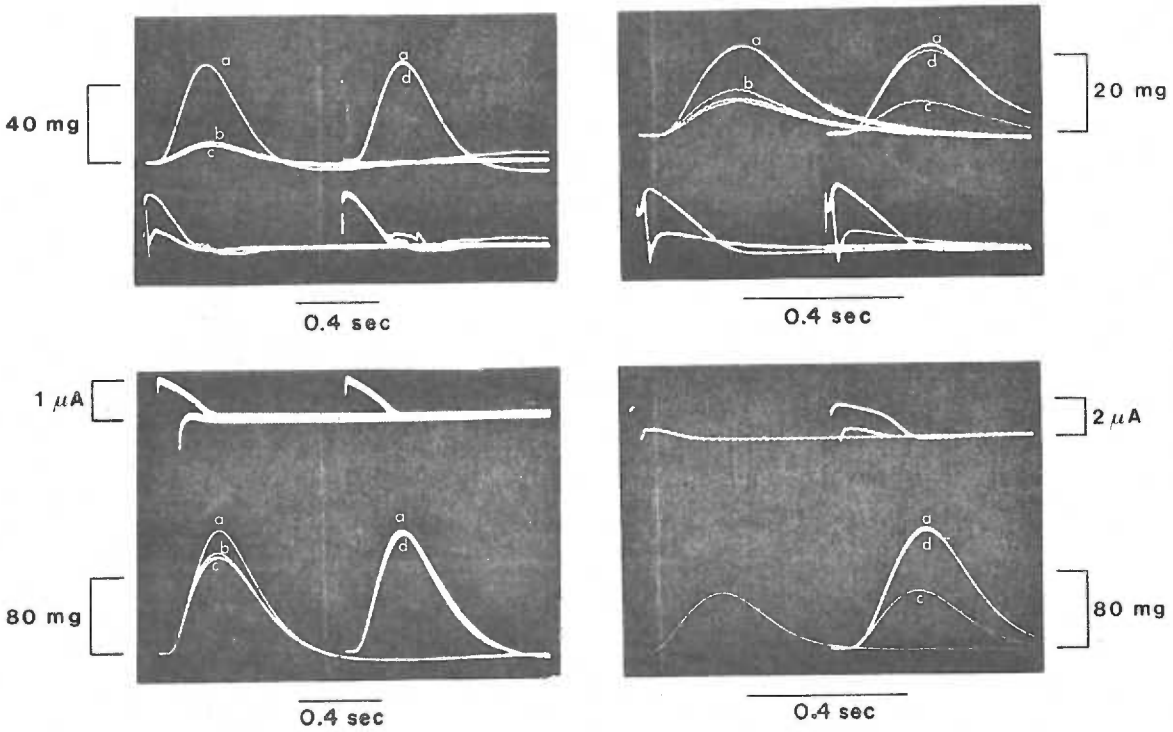
40 mg
a
b
c
d
0.4 sec
20 mg
0.4 sec
1 μA
80 mg
0.4 sec
2 μA
80 mg
0.4 sec

2. Development of tonic tension.

Sustained contractions (tonic tension) following an initial phasic contraction were observed with constant depolarizing currents in both neonatal and adult cat hearts (figure IV-5A and 5C). However, larger total currents were required to produce equivalent changes in tonic tension in the adult than in the neonate. In the adult, contractions were observed following the release of the depolarizing current pulses (figure IV-5C). These break contractions increased with increasing depolarizing currents. A break contraction was also observed following the voltage clamp pulse in figure IV-5D. Similar break contractions were observed by Wood, Heppner and Weidmann (1969) and Morad and Trautwein (1968). In the adult, peak tension and dT/dt_{max} of the initial phasic component of contraction declined while the tonic component of contraction increased with increasing currents (figure IV-5C). With currents greater than 60 μA the tonic component developed faster and dT/dt_{max} increased with increasing currents in the adult. Similar results were observed in 3 other adults. However, in the neonate a small increase in current resulted in a larger increase in tonic tension than in the adult and peak tension increased with no change in dT/dt_{max} as the constant depolarizing currents were increased. Similar results were observed in 6 other neonatal cats.

The relation between membrane potential and the development of tonic tension was not systematically studied. Records obtained in 2 adults and 4 neonates showed that the development of tonic tension with depolarizations to the same membrane potential was greater in the neonate than in the adult (figure IV-5B and 5D). Figure IV-5B is

Figure IV-5. Superimposed contractions elicited by a normal action potential (a is the control contraction) and increasing constant depolarizing currents (records A and C) or a constant membrane depolarization to +95 mV (records B and D). Inward current is recorded as an upward deflection in records A and C and as a downward deflection in records B and D. The letter 'b' identifies the contraction of the first voltage clamp depolarization. Tension is maintained (tonic tension) for the duration of depolarization in both neonatal and adult hearts. But the tonic tension develops so much faster in the neonate than in the adult that there is fusion of the initial phasic contraction with the tonic contraction in the neonate (records A and B). The phasic contraction is suppressed in the adult and unchanged or enhanced in the neonate with increasing depolarizing currents (records A and C). The stimulation rate is 19 beats/min. The tension traces are delayed by 40 ms.

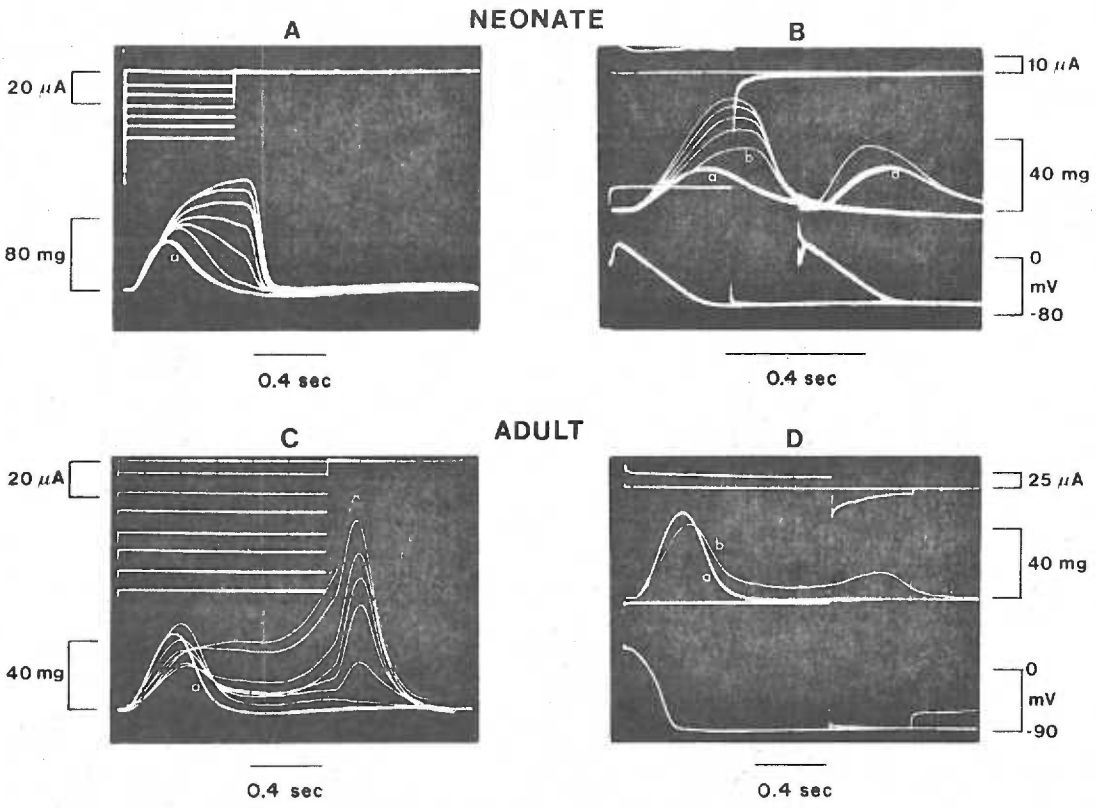
NEONATE
A
B
20 μA
80 mg
10 μA
40 mg
0
mV
-80
0.4 sec
0.4 sec
ADULT
C
D
20 μA
40 mg
25 μA
40 mg
0
mV
-90
0.4 sec
0.4 sec

a record of 5 consecutive voltage clamp depolarizations to membrane potentials of +95 mV in a neonatal cat. Tension of the first voltage clamp (b) in the neonate was maintained for the duration of depolarization and was 65% greater than control tension (a). A single voltage clamp depolarization to a membrane potential of +95 mV in the adult (figure IV-5D) resulted in suppression of the phasic tension below control tension and only a small tonic tension was maintained for the duration of depolarization. The direct control of contractility by the membrane potential appears to be greater in the neonate than in the adult.

3. Relation between membrane potential and tension in the adult cat.

The relation between contractility and membrane potential was studied by voltage clamping the membrane to different potentials for more than one beat following a series of stimulated control action potentials. Figure IV-6A shows records from an experiment on an adult cat heart in which the duration of depolarization was 170 ms (control action potential duration = 230 ms). The left side of each record shows superimposed tracings of a control beat generated by an action potential and 6 consecutive voltage clamp beats. The right side shows the last steady state voltage clamp beat followed by the first 6 beats of normal stimulation after the release of the clamp voltage. The change in tension was small when the muscle was voltage clamped for more than one beat successively. This is demonstrated in figure IV-6B, where peak tension (normalized by the control peak tension) of the contractions generated by the first and steady state

Figure IV-6. Relation between tension and membrane potential in the adult heart for voltage clamp durations of 170 ms. The left side of each record in 6A shows superimposed contractions evoked by a control action potential (a) and by 6 to 8 voltage clamp pulses (b and c are the contractions evoked by the first and steady state voltage clamp). The right side of the records in 6A are the first 6 to 8 contractions associated with normal action potentials following the release of the voltage clamp (d is the contraction of the first normal action potential). Inward current is recorded as a downward deflection in this and the following records. The stimulation rate is 19 beats/min. The tension traces are delayed by 40 ms. In 6B, peak tension of the contraction of the first (▲ = 1^{st} VC) and steady state (○ = SS VC) voltage clamp pulses (normalized by the peak tension of the control contraction) are plotted as a function of the membrane potential (abscissa). Normalized peak tension of the contraction of the first normal action potential (● = 1^{st} AP) after the release of the voltage clamp is plotted as a function of the membrane potential of the preceding steady state voltage clamp pulse.

Figure IV-7. Relation between tension and membrane potential in the same adult muscle used in figure IV-6 but studied with a voltage clamp duration of 480 ms. The results are plotted as described in the legend of figure IV-6. The stimulation rate is 19 beats/min. The tension traces are delayed by 40 ms.

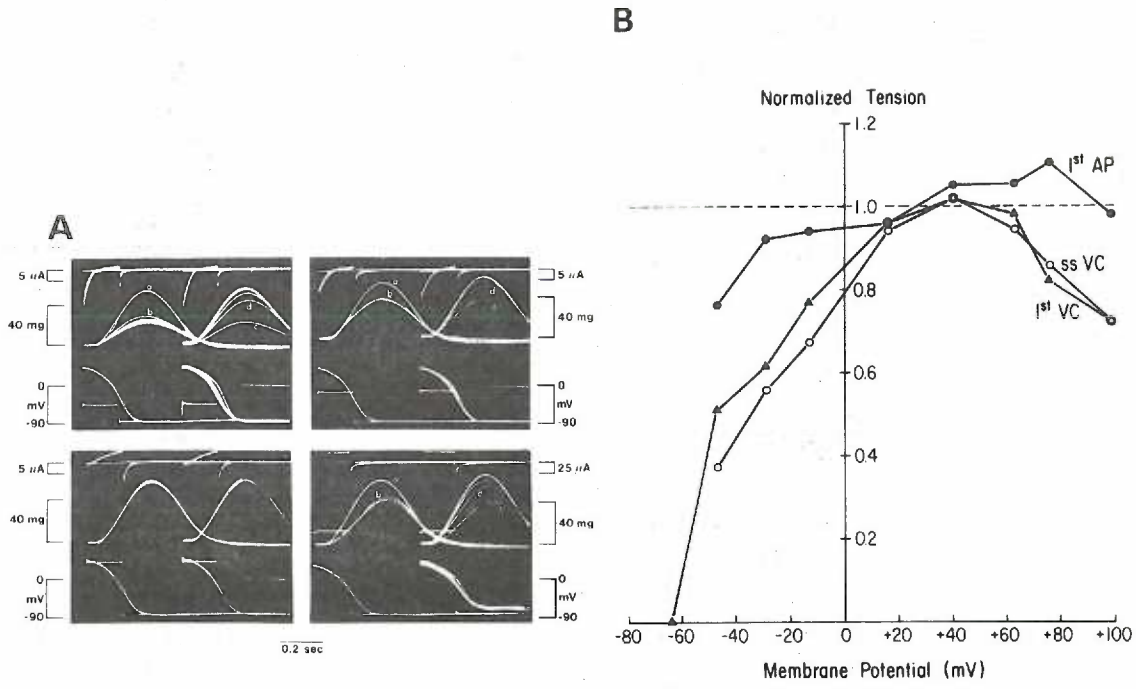
A
B
5 uA
40 mg
0
mV
-90
25 uA
0.2 sec
Normalized Tension
1.2
1.0
0.8
0.6
0.4
0.2
1st AP
ss VC
1st VC
-80 -60 -40 -20 0 +20 +40 +60 +80 +100
Membrane Potential (mV)

IV-6

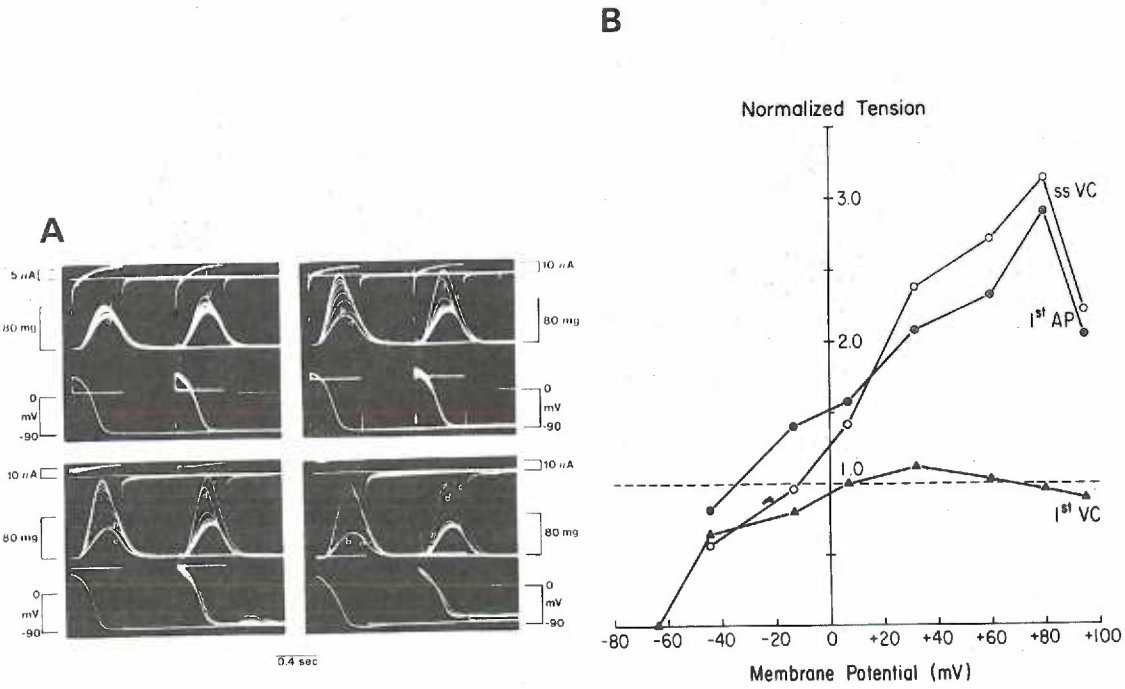
A
B
5 uA
10 uA
80 mg
0
mV
-90
0.4 sec
Normalized Tension
3.0
2.0
1.0
ss VC
1st AP
1st VC
-80 -60 -40 -20 0 +20 +40 +60 +80 +100
Membrane Potential (mV)

IV-7

voltage clamp pulse were plotted as a function of the membrane potential. The electrical threshold of contraction was between -65 and -55 mV. As the degree of depolarization was increased, tension of the first and steady state voltage clamp beat increased. Maximum peak tension was observed for membrane potentials between +30 and +40 mV. Depolarization to membrane potentials above +40 mV resulted in a decrease in tension of both the first and steady state voltage clamp beat (figure IV-6B). Peak tension of the contraction generated by the first action potential following the steady state voltage clamp beat, which reflects the influence on the storage of potentiation by the level of depolarization of the preceding voltage clamp beats, was not very different from control tension (figure IV-6B). Consequently an increase in the membrane potential greater than +40 mV (for pulse durations of 170 ms) affected the release of activator calcium with little influence on the storage of activator calcium in the adult. Similar results were observed in 2 other adult cats.

Figure IV-7A shows records from another experiment on the same muscle. In this case the relation between tension and membrane potential was studied with voltage clamp pulse durations of 480 ms. The tension-voltage relation of the first voltage clamp pulse for clamp durations of 480 ms in figure IV-7B and 170 ms in figure IV-6B are similar in that maximum peak tension was observed at depolarizations to membrane potentials between +30 and +40 mV. However, significant tension staircases between the first and steady state voltage clamp pulse were observed when the muscle was voltage clamped (480 ms) for more than one beat consecutively (figure IV-7A). Furthermore, this

potentiation was stored in the muscle as demonstrated by the increased contractility of the beat elicited by the first action potential generated after the steady state voltage clamp pulses (figure IV-7A). As shown in figure IV-7B tension generated by the steady state clamp pulse and tension generated by the first action potential increased with increasing depolarization and reached a maximum with depolarizations to a membrane potential of +70 mV. Depolarizations to membrane potentials in excess of +70 mV resulted in suppression of tension below the maximum tension observed at +70 mV. Similar results were observed in 3 other adult preparations of which 2 were studied with both short and long durations of depolarization. In the other 3 adult preparations studied with long pulse durations, tension generated by the first action potential following the steady state clamp pulse became greater than the decreasing tension generated by the steady state depolarization to membrane potentials greater than +80 mV (figure IV-8).

The tension-voltage relation of the steady state voltage clamp pulse for durations of 480 ms contrasted sharply with that obtained for clamp durations of 170 ms. Yet the tension-voltage relation of the first voltage clamp pulse for both durations were similar. Thus the pulse duration strongly affects what appears to be accumulation of calcium in the internal releasable stores.

4. Relation between membrane potential and tension in the newborn kitten.

Figures IV-9A and IV-10A show records of a voltage clamp experiment on a 1 day old neonate. The voltage clamp duration was 250 and 350 ms respectively. The results are plotted in figures IV-9B

Figure IV-8. Relation between tension and membrane potential in an adult papillary muscle. Voltage clamp pulse duration was 400 ms (normal action potential duration = 205 ms). Peak tension (normalized by the peak tension of the control contraction) is plotted on the ordinate versus the membrane potential of the voltage clamp pulse (abscissa). The stimulation rate was 19 beats/min.

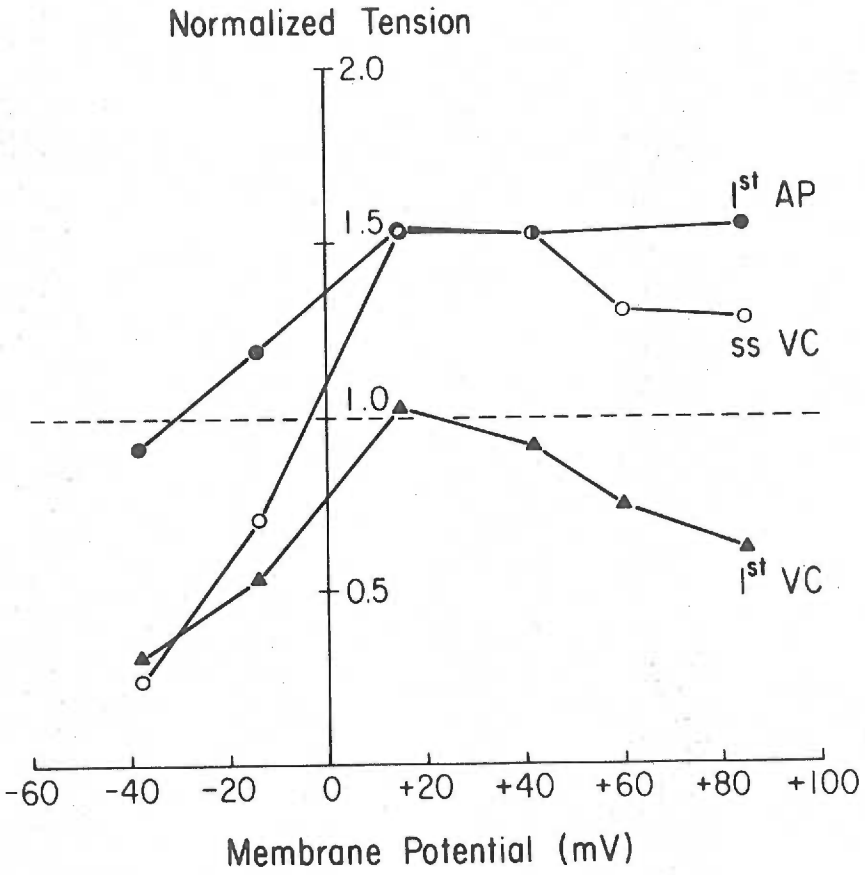
Normalized Tension
2.0
1.5
1.0
0.5
1st AP
ss VC
1st VC
-60
-40
-20
0
+20
+40
+60
+80
+100
Membrane Potential (mV)

Figure IV-9. Relation between tension and membrane potential in a 1 day old neonate with a voltage clamp duration of 248 ms. The results are plotted as described in the legend of figure IV-6. The stimulation rate is 19 beats/min. The tension traces are delayed by 40 ms.

Figure IV-10. Relation between tension and membrane potential in the same neonatal muscle used in figure IV-9 but studied with voltage clamp durations of 350 ms. The results are plotted as described in the legend of figure IV-6. The stimulation rate is 19 beats/min. The tension traces are delayed by 40 ms.

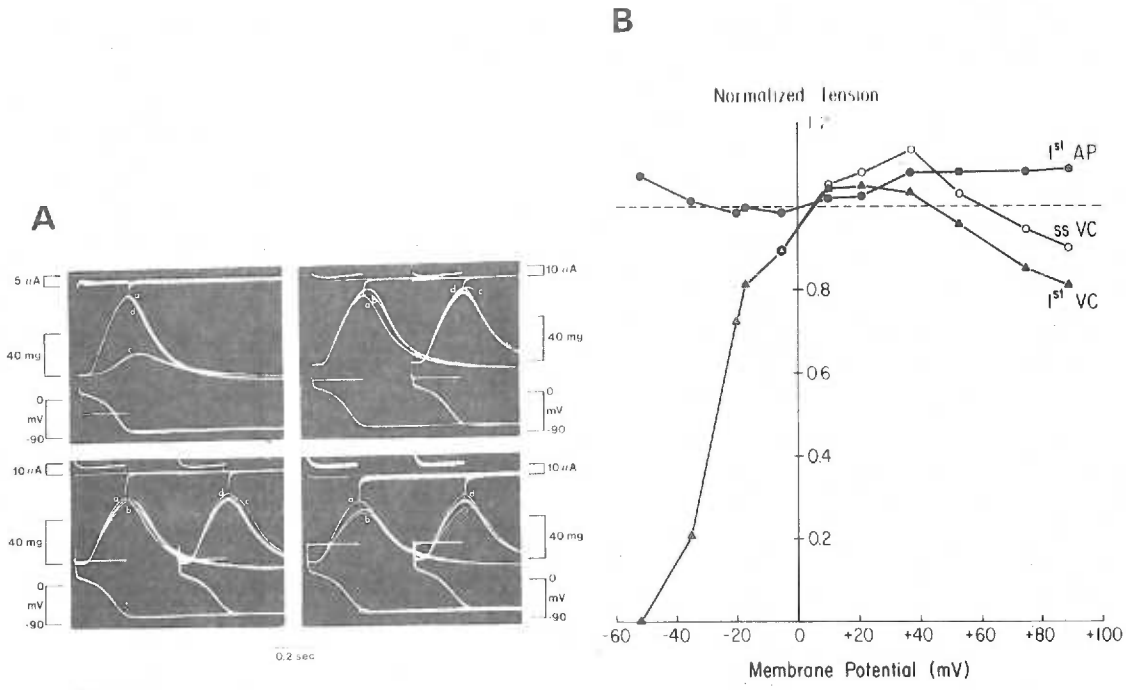
A
B
5 uA
40 mg
0
mV
-90
10 uA
40 mg
0
mV
-90
0.2 sec
Normalized Tension
1.0
0.8
0.6
0.4
0.2
1st AP
ss VC
1st VC
-60 -40 -20 0 +20 +40 +60 +80 +100
Membrane Potential (mV)

IV-9

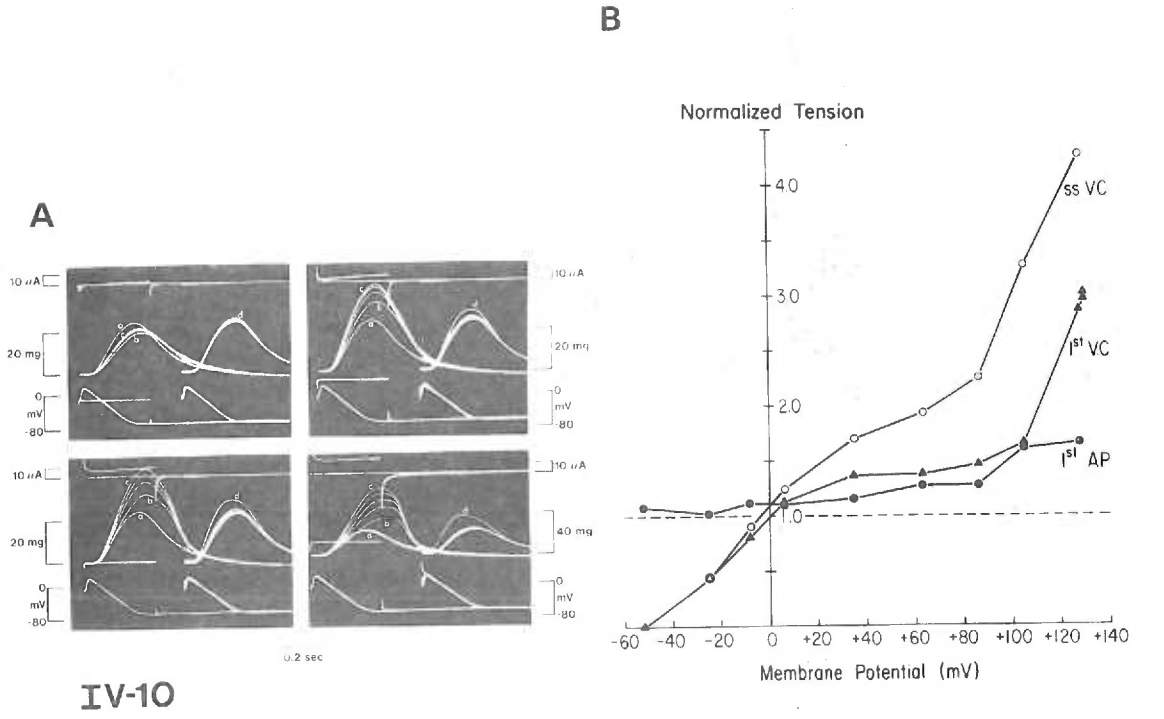
A
B
10 uA
20 mg
0
mV
-80
10 uA
20 mg
40 mg
0.2 sec
Normalized Tension
4.0
3.0
2.0
1.0
ss VC
1st VC
1st AP
-60 -40 -20 0 +20 +40 +60 +80 +100 +120 +140
Membrane Potential (mV)

IV-10

and IV-10B as previously described. The tension-voltage relations in the neonate for the short voltage clamp durations (250 ms, figure IV-9B) were similar to those observed in adult preparations with short voltage clamp durations (figure IV-6B). However, in the neonate a tension staircase was not observed for small depolarizations (membrane potentials between -50 and 0 mV) whereas the adult developed a small tension staircase in the same voltage range. When the neonate was depolarized to membrane potentials between -50 and -20 mV, the onset of activation was delayed and this time delay decreased with increasing depolarization (figure IV-9A). Similar results were observed in 2 other neonatal cat hearts.

Increasing the voltage clamp pulse duration to 350 ms resulted in a significant increase in the tension-voltage curves (figure IV-10B). Peak tension of the contraction generated by the first and steady state voltage clamp pulses increased and showed no tendency to decline with increasing depolarizations. The increase in tension of the first voltage clamp pulse with membrane potentials greater than +40 mV was not observed in the adult heart (figure IV-7B). Peak tension of the contraction generated by the first action potential following each steady state voltage clamp pulse increased with increasing depolarization (figure IV-10A). However the tension-voltage relation of the first action potential generated after discontinuation of the clamp was significantly lower than the steady state clamped tension-voltage relation (figure IV-10B). This suggests that the capacity of heart cells to store activator calcium from a previously potentiated beat is lower in the neonate than in the adult. The same conclusion is

apparent upon comparison of figures IV-10B and 7b for the difference between the tension-voltage curves of the first and steady state voltage clamp pulses. Furthermore, the membrane potential appears to have a more direct control on contractility in the neonate than in the adult. The same results were observed in 2 other 1 day old neonatal cats.

5. Beat dependent decay of potentiation following a voltage clamp.

Figure IV-7A shows that tension developed by the first action potential following a voltage clamp in the adult was greatly potentiated and this increased contractility decayed to control values in 6 to 8 beats. A single exponential curve was fitted to the decay of potentiation versus the beat number on data from 7 adults in which potentiation was produced either by constant depolarizing currents or a voltage clamp (figure IV-11). Similar calculations were performed on 8 neonates and plotted in figure IV-11. The decay of potentiation was significantly faster in the neonate than in the adult ($P << 0.01$). The beat constant for the decay of potentiation (mean $\pm$ S.E. of mean, $beats^{-1}$) was -0.604 ± 0.017 in the adult and -1.557 ± 0.023 in the neonate. In the adult the beat constant for the decay of potentiation following depolarizing currents was not significantly different from the beat constant for the decay of post-extrasystolic potentiation and frequency potentiation ($0.1 \leq P \leq 0.05$). However, in the neonate, decay of potentiation following depolarizing currents was significantly faster than the decay of potentiation following an extrasystole or rate inotropism ($P << 0.01$). The reason for this difference is not clear.

Figure IV-11. Beat dependent decay of potentiation after constant depolarizing current injections or constant membrane depolarizations in 8 neonatal and 7 adult cat hearts. Potentiation is plotted on the ordinate versus the beat number following the inotropic procedure on the abscissa. Regression analysis was performed on the ln of the percent potentiation versus the beat number. The solid curve represents the exponential least squares fit to the experimental points (+). The dotted curves are the 95% confidence limits of the means. Stimulation rate was 19 beats/min.

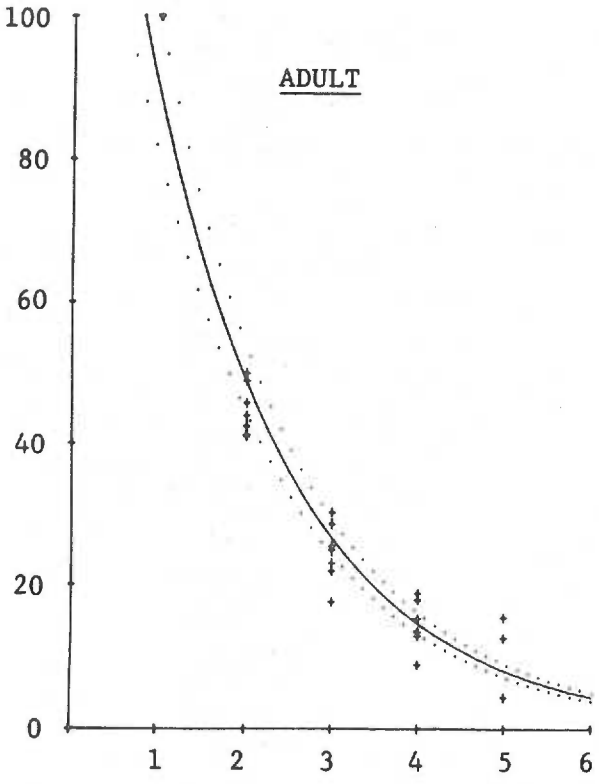
ADULT
100
80
60
40
20
0
1
2
3
4
5
6

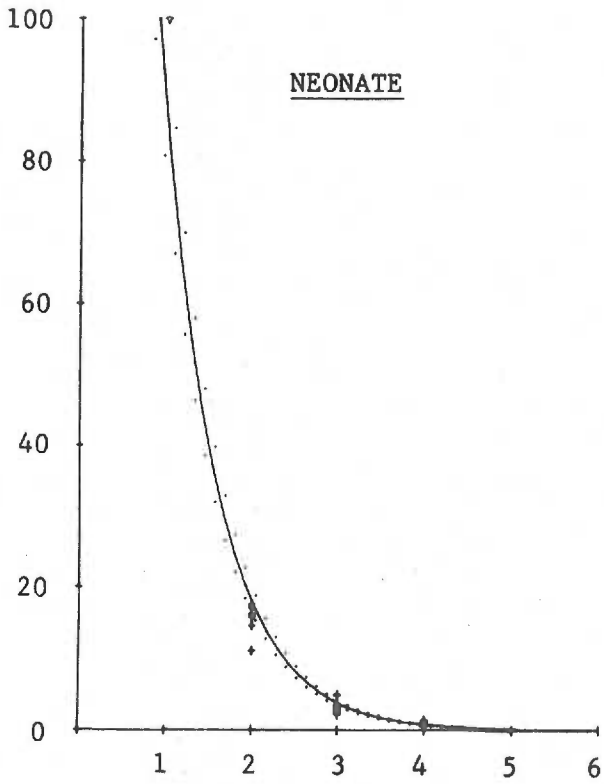
NEONATE
100
80
60
40
20
0
1
2
3
4
5
6

Discussion

The results obtained with the sucrose gap technique on adult preparations support the proposition that two functionally separate sources of activator calcium contribute to the production of tension, as suggested by Morad and Goldman (1973). One source of activator calcium appears to be a graded release of calcium from internal stores as a function of the membrane potential. The second source appears to be a continuous transmembrane inflow of calcium for the duration of depolarization, generated either by an action potential or by a voltage clamp, as demonstrated by the tonic tension obtained with 1 to 2 sec depolarizations (figure IV-5).

The skewed bell-shaped curve for the first voltage clamp beat in the adult heart (figures IV-6B and IV-7B) could represent the dependency of the release of activator calcium on the membrane potential in the adult heart. Similar tension-voltage curves for the first voltage clamp pulse have been obtained by Morad and Goldman (1973) on cat and dog ventricular fibers and by Gibbons and Fozzard (1975) on sheep cardiac Purkinje fibers.

The tension-voltage relations, with voltage clamps of short duration were qualitatively similar in the adult for the first and steady state voltage clamp pulses. Potentiation resulting from the voltage clamps of short duration was small as demonstrated by the tension-voltage relation of the first action potential generated after the steady state voltage clamp pulses. Consequently the amount of calcium stored in the internal stores was not greatly affected by

the short voltage clamp pulses in the adult.

However with long durations of depolarization (400-600 ms), a marked increase in the tension-voltage relation of the steady state voltage clamp pulse was observed in the adult. Presumably the increased duration of depolarization resulted in an increase in the duration of the transmembrane inflow of calcium which increased the filling of the internal calcium stores during each beat resulting in a tension staircase. The amount of calcium stored in the internal stores was greatly increased as further demonstrated by the increased contractility evoked by the first action potential generated after long membrane depolarizations. Furthermore, a decrease in filling of the internal stores can explain the negative tension staircase observed with premature termination of the action potential for more than one beat in adult preparations.

The tension-voltage relation of the first voltage clamp beat with long pulse durations was only slightly higher than the corresponding relation with short pulse durations in the adult. However, the increase in tension produced by the second voltage clamp pulse of long duration was much greater than the increase produced by the first voltage clamp pulse of the same duration (figure IV-7B). Consequently the extra calcium influx during the first voltage clamp with an increased duration of depolarization had a greater effect on the filling of the calcium stores than on the immediate production of tension. This suggests that contractility in the adult heart is strongly dependent on the intracellular stores and only indirectly dependent on extracellular calcium for the filling of the intracellular stores.

The results obtained with the sucrose gap technique on neonatal preparations show that contractility in the neonate is directly dependent on the membrane potential. The tension-voltage relation obtained with short pulse durations suggest that a voltage dependent release of calcium is occurring at low membrane depolarizations. However, step depolarizations with long pulse durations (350-400 ms) result in a continuous increase in tension of the first voltage clamp beat with increasing membrane depolarization. The tension staircase between the first and steady state voltage beat with long pulse durations is proportionately much smaller in the neonate than in the adult. Also storage of potentiation resulting from the voltage clamp in the neonate is significantly reduced as demonstrated by the contraction associated with the first action potential generated after the steady state voltage clamp pulse (figure IV-10). Thus the capacity of the internal stores is significantly lower in the neonate than in the adult. But the control of contractility by the sarcolemma is of greater importance in the neonate than in the adult. The lack of a significant tension staircase when the action potential is prematurely terminated for more than one beat further supports the decreased contribution of the internal stores in the neonate.

V. GENERAL DISCUSSION, SUMMARY AND CONCLUSION

The structural differences between the neonatal and adult myocardium are not absolute but gradual. Thus, it is not possible to correlate function and structure on an all or none basis. Rather, the structural and functional differences are differences of degree, differences, however, that correlate well with each other and with the presumed functions in the excitation-contraction coupling scheme of Morad and Goldman (1973). To avoid repetition, it is suggested that the reader consult page 39 for a brief review of the Morad and Goldman scheme.

To avoid frequent references to the earlier sections of this thesis, I will briefly restate the findings before passing on to a discussion of the consistency of the findings reported in each of the three experimental sections. All findings pertain to the cat unless otherwise stated.

Section II. -The neonatal heart has less longitudinal SR and fewer SR saccules than the adult heart.

-The neonatal cat heart is like the frog heart in that it does not have T-tubules (figure II-6, page 51).

-Neonatal heart cells have a much smaller diameter than adult heart cells (figures II-1 and II-5, pages 49 and 51).

-Unlike the cells of the frog heart, cells of the neonatal cat heart possess a well developed basement membrane (figures II-5, II-7 and II-8, pages 51 and 52).

Section III. -The fast components of the frequency staircases

(first 6 to 8 beats) are much more important in the adult heart than in the neonatal heart in comparison to the second, slow components of the frequency staircases (figure III-3, page 62).

-Post-extrasystolic potentiation is much more pronounced in the adult than in the neonatal heart (figure III-2, page 60).

-Post-extrasystolic potentiation superimposed on a frequency staircase decays back to the envelope of an undisturbed frequency staircase in both neonatal and adult cat hearts as if the two inotropisms are completely independent (figure III-4, page 65).

-The negative frequency staircase shows a decay in potentiation that consists of a fast and a slow component. In both neonatal and adult hearts, the beat constant of the fast component and the beat constant of the decay of post-extrasystolic potentiation are all the same (figure III-6, page 68).

-Recovery of contractility from a previous beat and the decay of contractility towards a "rest contraction" are much faster in the neonate than in the adult (figures III-7 and III-8, pages 72 and 73).

Section IV. -Forced premature termination of the action potential plateau results in a negative staircase over 6 to 8 beats in the adult heart but over only 1 to 2 beats in the neonatal heart (figures IV-3 and IV-4, pages 85 and 87).

-When the action potential plateau is experimentally prolonged by constant current injections, one sees an initial twitch-like contraction (phasic tension) followed by incomplete relaxation for the duration of depolarization (tonic tension) (figure IV-5, page 89).

-Tonic tension in the adult occurs late in the duration of the action potential and increases only with extreme depolarizations whereas the phasic tension decreases (figure IV-5, page 89).

-Tonic tension develops very early in the neonate and extreme depolarizations are not necessary to produce tonic tensions that are far greater than the phasic tensions (figure IV-5, page 89).

-The tension-voltage relations obtained with <u>short</u> forced depolarizations show that the force of contraction in both neonatal and adult hearts is only little potentiated regardless of the degree of depolarization and there is only a little staircase effect (figures IV-6 and IV-9, pages 91 and 95).

-Tension-voltage relations obtained with forced depolarizations of <u>long</u> duration show substantial potentiation in both neonatal and adult hearts. However, potentiation occurs after a delay of one beat in the adult whereas it occurs immediately in the neonate. There is a tremendous staircase effect in the adult and only a small staircase effect in the neonate. Likewise the first normal

beat after release of the clamp is still greatly potentiated in the adult but not in the neonate (figures IV-7 and IV-10, pages 91 and 95).

-In the adult heart tension developed in a steady state during a series of voltage clamp beats of extreme depolarization decreases whereas the first normal beat after release of the clamp is potentiated (figure IV-8, page 94).

-Tension of the first voltage clamped beat continues to increase in the neonate with increasing depolarization, with pulse durations slightly longer than the action potential duration, whereas in the adult tension of the first voltage clamped beat decreases when the depolarization is increased beyond +30 mV (figures IV-7 and IV-10, pages 91 and 95).

Items that support various parts of the Morad and Goldman hypothesis:

The presumed graded release of activator calcium from an internal store during the initial phase of the action potential is supported by the observed tension-voltage relations of the first voltage clamp beat of short pulse duration in both neonatal and adult hearts. This store is believed to be the same store that is involved in post-extrasystolic potentiation. The store is significantly less important in the neonatal heart than in the adult heart. Steady state potentiations from voltage clamp depolarizations with long pulse duration are lower in the neonatal heart than in the adult heart. The ultrastructural difference in the amounts of the SR cisternae in

the neonatal and adult hearts may well explain the differences in releasable calcium during the phasic part of the contraction and also the fact that no extra releasable calcium accumulates in the neonate after prolonged depolarizations.

In the neonatal heart, the tonic tension develops earlier than in the adult, so much so that it is fused with the phasic tension and may under normal conditions contribute to the force of contraction during a regular action potential. The extremely steep rise in the curve relating peak tonic tension as a function of the membrane potential at +130 mV (figure IV-9, page 95) supports the assumption that the source of this activator calcium is not an independent ionic calcium channel. (The reversal potential for such a channel in 3.6 mM $CaCl_2$, assuming 50% activation (figure I-3, page 6), would be about +110 mV.) However, since the K^+ reversal potential is around -80 mV the electrochemical gradient for K^+ continues to increase with increasing membrane potentials positive to -80 mV suggesting that a simple K^+ - Ca^{2+} exchange carrier might mediate the calcium influx and the tonic tension during the later part of the action potential as proposed by Morad and Goldman (1973).

The extreme depolarizations necessary to maintain the tonic tension and the slower development of the tonic tension in the adult heart in comparison with the neonatal heart support the assumption that the longitudinal SR sequesters calcium and thus effectively competes with the actomyosin for the calcium flowing in during the later part of the action potential. The ultrastructural studies show far less longitudinal SR in the neonate than in the adult supporting

the view that this sequestration is a function of the SR which is unable to prevent the tonic tension in the neonate.

Additional findings that add new information to the Morad and Goldman scheme:

The paradoxical effects of extreme depolarizations in the adult heart consisting of a decrease in the phasic tension with an increase in the tonic tension support that two separate sources of activator calcium are present. Thus, the replenishment of the phasic source with calcium from a second source (possibly K^+ - Ca^{2+} exchange) increases with extreme membrane depolarizations yet the graded release of activator calcium from the phasic source decreases with extreme membrane depolarizations. The fact that calcium release from these two sources is affected in opposite directions by extreme depolarizations explains the decrease in steady state tension during a sequence of extreme voltage clamps and an increase in potentiation of the first beat afterwards in the adult heart muscle.

The presence of a basement membrane surrounding the neonatal and adult heart cells suggests that the basement membrane is not an important storage site for activator calcium for the phasic tension, contrary to the proposal of Langer (1973). Also, the basement membrane appears not to be important in the regulation of the tonic tension, for in the frog heart, which develops only a tonic tension, no basement membrane surrounds the individual cardiac cells.

A more important new finding is that the rate inotropism, formerly thought to be a single mechanism, consists of two functionally separate components. The fast component is most likely dependent on

the "phasic" store, consequently the fast component is associated with the SR saccules as previously argued. However, the slow component of the rate inotropism must be due to a different and independent mechanism. The source of this mechanism may be a Na^+-pump lag (see pages 75 to 76).

In summary this study shows that the neonatal heart is far less sensitive to fast inotropic procedures such as post-extrasystolic potentiation in comparison to the adult heart. A second source of activator calcium which sets the basal rate of replenishment of the phasic store, possibly by some sort of a $K^+ - Ca^{2+}$ exchange, is relatively more important in the neonatal heart than in the adult heart. This source may also be responsible for the tonic tension that is observed in the neonatal and adult heart with artificially maintained depolarizations. One would predict therefore that contractility in the neonatal heart would be more sensitive to alterations of the external ionic concentrations (Na^+, K^+, and Ca^{2+}) which would affect the $K^+ - Ca^{2+}$ and the $2Na^+ - Ca^{2+}$ systems. It would appear that of the two calcium activating mechanisms, the frog uses the one associated with the "tonic" tension whereas the adult cat heart uses the one associated with the "phasic" tension. The neonatal cat heart is heavily dependent on both and will at some later time drop the phylogenetically older mechanism in favor of the newer one.

VI. BIBLIOGRAPHY

1. Antoni, H., Jacob, R., & Kaufman, R. Mechanische Reaktionen des Frosch und Säugtiermyokards bei Veränderung der Aktionspotential-Dauer durch konstante Gleichstromimpulse. Pflügers Arch., 1969. 306, 33-57.

2. Bass, B.G. Enhanced contractility during relaxation of cat papillary muscle. Am. J. Physiol., 1975a. 228, 1708-1716.

3. Bass, B.G. Restitution of the action potential in cat papillary muscle. Am. J. Physiol., 1975b. 228, 1717-1724.

4. Bassingthwaighte, J.B., Beeler, G.W., Sidell, P.M., Reuter, H., & Safford, R.E. A model for calcium movements and excitation-contraction coupling in cardiac cells. In A.S. Iberall and A.C. Guyton (Ed.) Regulation and control in physiological systems. Pittsburgh, Pa.: Instrument Society of America, 1973. pp. 36-38.

5. Bassingthwaighte, J.B., & Reuter, H. Calcium movements and excitation-contraction coupling in cardiac cells. In W.C. DeMello (Ed.) Electrical phenomena in the heart. New York, N.Y.: Academic Press, 1972. pp. 353-395.

6. Beeler, G.W., & Reuter, H. Membrane calcium current in ventricular myocardial fibers. J. Physiol. (Lond), 1970a. 207, 191-209.

7. Beeler, G.W., & Reuter, H. The relation between membrane potential, membrane currents and activation of contraction in ventricular myocardial fibers. J. Physiol. (Lond), 1970b. 207, 211-229.

8. Blinks, J.R., & Koch-Weser, J. Analysis of the effects of changes in rate and rhythm upon myocardial contractility. J. Pharmacol. Exp. Ther., 1961. 134, 373-389.

9. Bowditch, H.P. Über die Eigenthümlichkeiten der Reizbarkeitt, welche die Muskelfasern des Herzens zeigen. Ber. Sachs. Ges.(Akad.) Wiss., 1871. 652-689.

10. Chapman, R.A., & Niedergerke, R. Interaction between heart rate and calcium concentration in the control of contractile strength of the frog heart. J. Physiol. (Lond), 1970. 211, 423-443.

11. Connor, J., Barr, L., & Jakobsson, E. Electrical characteristics of frog atrial trabeculae in the double sucrose gap. Biophys. J., 1975. 15, 1047-1067.

12. Ebashi, S. Excitation-contraction coupling. Annu. Rev. Physiol., 1976. 38, 293-313.

13. Edman, K.A.P., & Johannsson, M. The contractile state of rabbit papillary muscle in relation to stimulation frequency. J. Physiol. (Lond), 1976. 254, 565-581.

14. Edmands, R.E., Greenspan, K., & Fisch, C. Electrophysiological correlates of contractile change in mammalian and amphibian myocardium. Cir. Res., 1968. 3, 252-260.

15. Einwächter, H.M., Haas, H.G., & Kern, R. Membrane current and contraction in frog atrial fibers. J. Physiol. (Lond), 1972. 227, 141-171.

16. Fabiato, A., & Fabiato, F. Contractions induced by a calcium-triggered release of calcium from the sarcoplasmic reticulum of single skinned cardiac cells. J. Physiol. (Lond), 1975. 249, 469-495.

17. Fawcett, D.W., & McNutt, N.S. The ultrastructure of the cat myocardium. J. Cell. Biol., 1969. 42, 1-45.

18. Forssmann, W.G., & Girardier, L. A study of the T-system in rat heart. J. Cell. Biol., 1970. 44, 1-17.

19. Fuchs, F. Striated muscle. Annu. Rev. Physiol., 1974. 36, 461-502.

20. Gettes, L.S., & Reuter, H. Slow recovery from inactivation of inward currents in mammalian myocardial fibers. J. Physiol. (Lond), 1974. 240, 703-724.

21. Gibbons, W.R., & Fozzard, H.A. Relationships between voltage and tension in sheep cardiac Purkinje fibers. J. Gen. Physiol., 1975. 65, 345-365.

22. Gibbs, C.L., Johnson, E.A., & Tille, J. A quantitative description of the relationship between the area of rabbit ventricular action potentials and the pattern of stimulation. Biophys. J., 1963. 3, 433-458.

23. Glitsch, H.G., Reuter, H., & Scholz, H. Effect of internal sodium concentration of calcium fluxes in isolated guinea-pig auricles. J. Physiol. (Lond), 1970. 209, 25-43.

24. Graham, R.C., & Karnovsky, M.J. The early stages of absorption of injected horseradish peroxidase in the proximal tubules of mouse kidney: ultrastructural cytochemistry by a new technique. J. Histochem. Cytochem., 1966. 14, 291-301.

25. Langer, G.A. Ion fluxes in cardiac excitation-contraction and their relation to myocardial contraction. Physiol. Rev., 1968. 48, 708-757.

26. Langer, G.A. Heart: excitation-contraction coupling. Annu. Rev. Physiol., 1973. 35, 55-86.

27. Langer, G.A. Ionic movements and the control of contraction. In G.A. Langer and A.J. Brady (Ed.) The mammalian myocardium. New York, N.Y.; John Wiley & Sons, 1974. pp. 193-217.

28. Langer, G.A., & Frank, J.S. Lanthanum in heart cell culture: effect on calcium exchange correlated with its localization. J. Cell. Biol., 1972. 54, 441-455.

29. Legato, M.L. Ultrastructural changes during normal growth in the dog and rat ventricular myofiber. In M. Lieberman and T. Sano (Ed.) Developmental and physiological correlates of cardiac muscle. New York, N.Y.: Raven Press, 1976. pp. 249-274.

30. Lèoty, C. Membrane currents and activation of contraction in rat ventricular fibers. J. Physiol. (Lond), 1974. 239, 237-249.

31. Lèoty, C., & Raymond, G. Mechanical activity and ionic currents in frog trabeculae. Pflügers Arch., 1972. 334, 114-128.

32. McDonald, T.F., Nawrath, H., & Trautwein, W. Membrane currents and tension in cat ventricular muscle treated with cardiac glycosides. Cir. Res., 1975. 37, 674-682.

33. McWilliam, J.A. On the rhythm of the mammalian heart. J. Physiol. (Lond), 1888. 9, 167-198.

34. Marriott, H.J.L. Practical electrocardiography. Baltimore, Md.: The Williams & Wilkins Co., 1972.

35. Morad, M., & Goldman, Y. Excitation-contraction coupling in heart muscle: membrane control of development of tension. Prog. Biophys. Mol. Biol., 1973. 27, 257-313.

36. Morad, M., Mascher, D., & Brady, A.J. Membrane potential and development of tension in mammalian myocardium. Fed. Proc., 1968. 27, 2702. (Abstract).

37. Morad, M., & Orkand, R.K. Excitation-contraction coupling in frog ventricle: evidence from voltage clamp studies. J. Physiol. (Lond), 1971. 219, 167-189.

38. Morad, M., & Trautwein, W. The effect of the duration of the action potential on contraction in the mammalian heart tissue. Pflüger Arch., 1968. 299, 66-82.

39. Murray, J.M., & Weber, A. The cooperative action of muscle proteins. Sci. Am., 1974. 230, 59-71.

40. New, W., & Trautwein, W. Inward membrane current in mammalian myocardium. Pflügers Arch., 1972a. 334, 1-23.

41. New, W., & Trautwein, W. The ionic nature of the slow inward current and its relation to contraction. Pflügers Arch., 1972b. 334, 24-38.

42. Niedergerke, R., & Orkand, R.K. The dual effect of calcium on the action potential of the frog's heart. J. Physiol. (Lond), 1966a. 184, 291-311.

43. Niedergerke, R., & Orkand, R.K. The dependence of the action potential of the frog's heart on the external and intracellular sodium concentration. J. Physiol. (Lond), 1966b. 184, 312-334.

44. Orkand, P. Light and electron microscopical studies of skeletal and cardiac muscle in the normal state and in drug induced myopathies in the cat. Doctor's dissertations, Univ. London, 1964.

45. Page, A.A.W., Manring, A., Sommer, J., & Johnson, E.A. Cardiac muscle: an attempt to relate structure to function. J. Mol. Cell. Cardiol., 1976. 8, 123-143.

46. Page, E., McCallister, L.P., & Power, B. Stereological measurements of cardiac ultrastructures implicated in excitation-contraction coupling. Proc. Nat. Acad. Sci., 1971. 68, 1465-1466.

47. Page, S.G., & Niedergerke, R. Structures of physiological interest in the frog heart ventricle. J. Cell. Biol., 1972. II, 179-203.

48. Reuter, H. Divalent cations as charge carriers in excitable membranes. Prog. Biophys. Mol. Biol., 1973. 26, 1-43.

49. Reuter, H. Exchange of calcium ions in the mammalian myocardium. Cir. Res., 1974. 34, 599-605.

50. Reuter, H., & Seitz, N. Dependence of calcium efflux from cardiac muscle on temperature and external ion composition. J. Physiol. (Lond), 1968. 195, 451-470.

51. Sanborn, W.G., & Langer, G.A. Specific uncoupling of excitation and contraction in mammalian cardiac tissue by lanthanum. J. Gen. Physiol., 1970. 56, 191-217.

52. Sandow, A. Excitation-contraction coupling in muscular response. Yale J. Biol. Med., 1952. 25, 176-201.

53. Schiebler, T.H., & Wolff, H.H. Elektronen microskopische untersuchungen am herzmuskel der ratte während der entwicklung. Z. Zellforsh. Mikrosk. Anat., 1966. 69, 22-44.

54. Sopis, J.A., & Langer, G.A. Calcium kinetics in frog heart. J. Mol. Cell. Cardiol., 1970. 1, 291-305.

55. Spurr, A.J. A low-viscosity epoxy resin embedding medium for electron microscopy. J. Ultrastruct. Res., 1969. 26, 31-43.

56. Staley, N.A., & Benson, E.S. The ultrastructure of frog ventricular cardiac muscle and its relationship to mechanisms of excitation-contraction coupling. J. Cell. Biol., 1968. 38, 99-114.

57. Tarr, M. Two inward currents in frog atrial muscle. J. Gen. Physiol., 1971. 58, 523-543.

58. Tarr, M., & Trank, J.W. An assessment of the double sucrose-gap voltage clamp technique as applied to frog atrial muscle. Biophys. J., 1974. 14, 627- 643.

59. Trautwein, W. Membrane currents in cardiac muscle fibers. Physiol. Rev., 1973. 53, 793-835.

60. Vassort, G. Influence of sodium ions on the regulation of frog myocardial contractility. Pflügers Arch., 1973. 339, 225-240.

61. Vassort, G., & Rougier, O. Membrane potential and slow inward current dependence of frog cardiac mechanical activity. Pflügers Arch., 1972. 331, 191-203.

62. Venable, J.H., & Coggeshall, R. A simplified lead citrate stain for use in electron microscopy. J. Cell. Biol., 1965. 25, 407-408.

63. Watson, P.T., & Winegrad, S. A possible sodium-calcium exchange in skeletal muscle. Fed. Proc., 1973. 32, 374. (Abstract).

64. Weiss, G.B. On the site of action of lanthanum in frog sartorius muscle. J. Pharmacol. Exp. Ther., 1970. 174, 517-526.

65. Winegrad, S. Studies of cardiac muscle with a high permeability to calcium produced by treatment with ethylenediaminetetraacetic acid. J. Gen. Physiol., 1971. 58, 71-93.

66. Wood, E.H., Heppner, R.L., & Weidmann, S. Inotropic effects of electric currents. Cir. Res., 1969. 24, 409-445.

67. Woodworth, R.S. Maximal contraction, "staircase" contraction, refractory period, and compensatory pause, of the heart. Am. J. Physiol., 1902. 8, 213-249.